

Doctoral Thesis for the Doctoral Degree  
at the Julius-Maximilians-Universität Würzburg



**The Role of FGF Receptor 2  
in GDF5 mediated Signal Transduction**

**Die Rolle des FGF Rezeptors 2  
in GDF5-vermittelter Signaltransduktion**

submitted by

Anna Theresa Schliermann

born Anna Theresa Stratmann in 59457 Werl

Würzburg 2018



Submitted on: .....

**Members of the Committee**

Chairperson: .....

Primary Supervisor: Prof. Dr. Heike Walles

Supervisor (Second): Prof. Dr. Thomas Müller

Date of Public Defense: .....

Date of Receipt of Certificates: .....

# Affidavit

I hereby declare that my thesis entitled “The Role of FGF Receptor 2 in GDF5 Mediated Signal Transduction” is the result of my own work. I did not receive any help or support from commercial consultants. All sources and / or materials applied are listed and specified in the thesis.

Furthermore, I verify that the thesis has not been submitted as part of another examination process neither in identical nor in similar form.

Besides, I declare that if I do not hold the copyright for figures and paragraphs, I obtained it from the rights holder, and that paragraphs and figures have been marked according to law, or for figures taken from the internet the hyperlink has been added accordingly.

# Eidesstattliche Erklärung

Hiermit erkläre ich an Eides statt, die Dissertation “Die Rolle des FGF Rezeptors 2 in der GDF5-vermittelten Signaltransduktion” eigenständig, d.h. insbesondere selbständig und ohne Hilfe eines kommerziellen Promotionsberaters, angefertigt und keine anderen als die von mir angegebenen Quellen und Hilfsmittel verwendet zu haben.

Ich erkläre außerdem, dass die Dissertation weder in gleicher noch in ähnlicher Form bereits in einem anderen Prüfungsverfahren vorgelegen hat.

Weiterhin erkläre ich, dass bei allen Abbildungen und Texten, bei denen die Verwertungsrechte (Copyright) nicht bei mir liegen, diese von den Rechtsinhabern eingeholt wurden und die Textstellen bzw. Abbildungen entsprechend den rechtlichen Vorgaben gekennzeichnet sind sowie bei Abbildungen, die dem Internet entnommen wurden, der entsprechende Hypertextlink angegeben wurde.

Ort, Datum

Unterschrift

# Acknowledgments

I want to thank Prof. Dr. Heike Walles for the opportunity to conduct my PhD work at the Chair of Tissue Engineering and Regenerative Medicine. I also want to thank her for her continuous support, especially after I started my family, and for being the first examiner for my thesis.

I want to thank Prof. Dr. Thomas Müller for being the second examiner of my thesis. I also want to thank him for the inspiring discussions about my results, and I want to thank him for conducting the SPR measurements and providing these data for my thesis, as well as providing FGFR2 ectodomain and FGF ligands.

My deepest gratitude goes to my supervisor Dr. Joachim Nickel. Thank you for being my mentor and for teaching me how to be a better scientist. Thank you for trusting me in my work, and for always having an open door whenever I needed help or input. Thank you for always being supportive, and for your candor. I want to keep learning from you for as long as possible!

I want to thank all the members of the chair for providing an open and friendly atmosphere. My gratitude goes to the ladies in the secretary, and to everyone in the lab who supported me in the conduction of my experiments. Special thanks goes to Viktoria Sokolowski for supplementing my data with her own, to Sabine Graiff and Sebastian Kress for their support in maintaining my cells, to Sabine Wilhelm for her support in Western Blotting and cloning, to Fabian Prenzlau for the preparation of *Fgfr2* splice variant plasmids, and to Dr. Markus Mühlemann for his kind support in lentiviral transduction.

I want to especially thank Dr. Claudia Siverino for being a great colleague and friend. You helped me all around the protein chemistry lab, and the cell culture lab, and you always had my back. I could not have asked for a better fellow PhD in our group!

I also want to thank all current and former residents of office 009. You were there to laugh, to brain-storm over a problem, to comfort, or to chit-chat – whatever the situation called for. I loved sharing my working space with you.

Finally, I want to thank my parents, my family and my friends for their unconditional and full support. To my long-suffering husband, thank you so much for your understanding, and for always being there. I love you!

## Related Publications

This work is associated with three publications.

The preliminary data preceding this thesis were published in BMC Biology (2015) under the title „*GDF-5 can act as a context-dependent BMP-2 antagonist*“. Findings from this work are detailed in the introduction, as they serve as the starting point for this thesis, and referenced accordingly.

Major parts of the literature research conducted for this thesis have been published as a review article entitled “*Unraveling the Connection between Fibroblast Growth Factor and Bone Morphogenetic Protein Signaling*”, published in the International Journal of Molecular Sciences (2018). Excerpts from this article are incorporated into the introduction and discussion of this thesis, and are referenced accordingly.

A subset of the experimental findings presented in this thesis were submitted for publication under the working title “*A Receptor with Identity Crisis: Fibroblast Growth Factor Receptor 2 Directly Binds BMPs to Modulate their Signaling Outcome*” to PNAS on 6 Dec, 2018.

The graphical depiction of data included in this manuscript are part of the results of this thesis, and referenced accordingly.

# Abstract

Bone morphogenetic proteins (BMPs) are involved in various aspects of cell-cell communication in complex life forms. They act as morphogens, help differentiate different cell types from different progenitor cells in development, and are involved in many instances of intercellular communication, from forming a body axis to healing bone fractures, from sugar metabolism to angiogenesis. If the same protein or protein family carries out many functions, there is a demand to regulate and fine-tune their biological activities, and BMPs are highly regulated to generate cell- and context-dependent outcomes.

Not all such instances can be explained yet. Growth/differentiation factor (GDF)5 (or BMP14) synergizes with BMP2 on chondrogenic ATDC5 cells, but antagonizes BMP2 on myoblastic C2C12 cells. Known regulators of BMP2/GDF5 signal transduction failed to explain this context-dependent difference, so a microarray was performed to identify new, cell-specific regulatory components. One identified candidate, the fibroblast growth factor receptor (FGFR)2, was analyzed as a potential new co-receptor to BMP ligands such as GDF5: It was shown that FGFR2 directly binds BMP2, GDF5, and other BMP ligands *in vitro*, and FGFR2 was able to positively influence BMP2/GDF5-mediated signaling outcome in cell-based assays. This effect was independent of FGFR2's kinase activity, and independent of the downstream mediators SMAD1/5/8, p42/p44, Akt, and p38. The elevated colocalization of BMP receptor type IA and FGFR2 in the presence of BMP2 or GDF5 suggests a signaling complex containing both receptors, akin to other known co-receptors of BMP ligands such as repulsive guidance molecules.

This unexpected direct interaction between an FGF receptor and BMP ligands potentially opens a new category of BMP signal transduction regulation, as FGFR2 is the second receptor tyrosine kinase to be identified as BMP co-receptor, and more may follow. The integration of cell surface interactions between members of the FGF and BMP family especially may widen the knowledge of such cellular communication mechanisms which involve both growth factor families, including morphogen gradients and osteogenesis, and may in consequence help to improve treatment options in osteochondral diseases.

# Zusammenfassung

Bone morphogenetic proteins (BMPs) sind oft an interzellulärer Kommunikation beteiligt. Sie sind Morphogene, spielen eine Rolle in der Differenzierung von zahlreichen Zelltypen aus verschiedenen Vorgängerzellen während der Entwicklung, und sind an vielen weiteren Beispielen der Zell-Zell-Kommunikation beteiligt: von der Formation einer Körperachse bis hin zur Heilung von Knochenbrüchen, vom Zuckermetabolismus bis zur Angiogenese. Wann immer dasselbe Protein oder dieselbe Proteinfamilie so viele Funktionen erfüllt, bedarf es der Regulation und Feinabstimmung ihrer diversen biologischen Aktivitäten, und BMPs sind zu dem Erzielen zell- und kontextspezifischer Effekte in ihrer Wirkung entsprechend stark reguliert.

Nicht in allen Fällen sind die Mechanismen solcher Regulation bisher bekannt. Growth/differentiation factor (GDF)5 (oder BMP14) agiert mit BMP2 auf den chondrogenen ATDC5 Zellen synergistisch, aber antagonisiert BMP2 auf den myoblastischen C2C12 Zellen. Diese kontextabhängige Diskrepanz konnte mithilfe der bekannten Regulatoren von BMP2/GDF5-medierte Signalen nicht erklärt werden. Daher wurde ein Microarray durchgeführt, um neue, zellspezifische regulatorische Proteine zu identifizieren. Einer der identifizierten Kandidaten, fibroblast growth factor receptor (FGFR)2, wurde auf eine potentielle Funktion als neuer Korezeptor für BMP Liganden wie GDF5 analysiert: Es konnte gezeigt werden, dass FGFR2 BMP2, GDF5 und andere BMP Liganden *in vitro* direkt binden und die biologische Aktivität von BMP2 und GDF5 in Zellkultursystemen positiv beeinflussen konnte. Diese Beobachtungen waren unabhängig von der Kinaseaktivität des FGFR2, und unabhängig von den intrazellulären Mediatoren SMAD1/5/8, p42/p44, Akt und p38. Die erhöhte Kolo-kalisation von FGFR2 mit dem BMP Rezeptor IA in der Präsenz von BMP2 oder GDF5 weist darauf hin, dass der entsprechende Signalkomplex möglicherweise beide Rezeptoren gleichzeitig enthält; ähnlich, wie das für andere bekannte Korezeptoren von BMP Liganden wie etwa den repulsive guidance molecules der Fall ist.

Die unerwartete direkte Interaktion von einem FGF Rezeptor mit BMP-Liganden ist möglicherweise nur ein Beispiel für einen generelleren Mechanismus. Tatsächlich ist FGFR2 bereits die zweite Rezeptortyrosinkinase, die als BMP-Korezeptor identifiziert wurde, und es ist

möglich, dass es noch mehr gibt. Speziell im Bezug auf die FGF-BMP Interaktion bergen die hier dargestellten Ergebnisse Potential zu neuen Erkenntnissen. Die Proteinfamilien dieser beiden Wachstumsfaktoren sind häufiger an demselben zellulären Mechanismen beteiligt; etwa an der Entstehung von Morphogengradienten in der Entwicklung oder an der Osteogenese. Die Interaktion der FGF und BMP Proteinfamilien auf der Zelloberfläche könnte eine wertvolle Ergänzung zu der Untersuchung ihres Zusammenspiels im Zellinneren sein, und könnte in diesem Zusammenhang sogar langfristig die Behandlungsmöglichkeiten von osteochondralen Erkrankungen erweitern.



# Content

<b>1. Introduction.....</b>	<b>12</b>
<b>1.1. Bone Morphogenetic Proteins (BMPs).....</b>	<b>12</b>
1.1.1.What BMPs are and how they work.....	12
1.1.2.Receptor promiscuity is met by a tight network of regulatory mechanisms.....	16
<b>1.2. Fibroblast Growth Factors (FGFs).....</b>	<b>18</b>
1.2.1.What FGFs are and how they work.....	18
1.2.2.Regulating FGF signals.....	21
1.2.3.The many faces of FGFR2 .....	22
<b>1.3. Signaling Cross-Talk.....</b>	<b>23</b>
1.3.1.Molecular connections between TGF $\beta$ /BMPs, FGFs, and others.....	23
1.3.2.BMPs and FGFs in cartilage and bone.....	25
1.3.3.BMPs and FGFs in other tissues .....	29
1.3.4.Unanswered questions .....	30
<b>1.4. Getting Started: The Findings That Preceded This Work.....</b>	<b>31</b>
1.4.1.The co-receptor concept .....	31
1.4.2.The ATDC5 / C2C12 discrepancy.....	32
<b>2. Aim of Work.....</b>	<b>34</b>
<b>3. Methods.....</b>	<b>35</b>
<b>3.1. Addressing Questions of Protein-Protein Interaction and Signal Transduction.....</b>	<b>35</b>
<b>3.2. Cell Culture Methods.....</b>	<b>37</b>
3.2.1.Transient transfection.....	37
3.2.2.Lentiviral transduction.....	37
3.2.3.Crystal violet assay.....	38
3.2.4.Alkaline phosphatase assay.....	38

<b>3.3. Immunohistochemistry.....</b>	<b>39</b>
3.3.1.Colocalization staining.....	39
<b>3.4. Molecular Methods.....</b>	<b>40</b>
3.4.1.RNA isolation .....	40
3.4.2.cDNA synthesis.....	40
3.4.3.Quantitative real-time PCR .....	40
<b>3.5. Cloning .....</b>	<b>41</b>
3.5.1.Primer Design.....	41
3.5.2.Generation of the DNA insert by PCR.....	43
3.5.3.DNA digestion.....	45
3.5.4.Gel extration of DNA plasmids.....	45
3.5.5.DNA ligation.....	45
3.5.6.Bacterial transformation.....	46
3.5.7.Plasmid preparation.....	46
<b>3.6. Biochemical Methods .....</b>	<b>47</b>
3.6.1.Protein isolation .....	47
3.6.2.Determination of total protein concentration.....	47
3.6.3.Western blotting.....	47
<b>3.7. Statistical Analysis.....</b>	<b>48</b>
<b>4. Results.....</b>	<b>49</b>
<b>4.1. Testing the Tenability of FGFR2 as Co-Receptor Candidate.....</b>	<b>49</b>
4.1.1.FGFR2IIIc extracellular domain binds BMP ligands GDF5 and BMP2 in vitro.....	49
4.1.2.FGFR2 shRNA specifically inhibits GDF5-induced ALP expression in ATDC5 cells .....	52
4.1.3.Fgfr2IIIc cDNA boosts BMP ligand-induced ALP expression in C2C12 cells .....	54
<b>4.2. Investigating the Mechanism Underlying FGFR2 Mediated GDF5 Responsiveness.....</b>	<b>57</b>
4.2.1.Western blotting does not show synergistic downstream signaling.....	58
4.2.2.Erk inhibition does not compromise BMP ligand-mediated ALP expression.....	61
<b>4.3. Exploring the Possibility of FGFR2IIIc as Part of the BMP Ligand-Receptor-Complex... </b>	<b>66</b>
4.3.1.Competition behavior of FGFR2IIIc and BMPRIA extracellular domains indicate a common receptor binding site within ligands .....	66
4.3.2.FGFR2IIIc and BMPRIA colocalize when overexpressed in HEK293AD cells .....	71
4.3.3.Manipulating signaling outcome by changing receptor-ligand interaction parameters .....	72
<b>5. Discussion.....</b>	<b>76</b>
<b>5.1. Testing the Tenability of FGFR2 as Co-Receptor Candidate.....</b>	<b>76</b>
<b>5.2. Investigating the Mechanism Underlying FGFR2 Mediated GDF5 Responsiveness.....</b>	<b>83</b>

<b>5.3. Exploring the Possibility of FGFR2 as Part of the BMP Ligand-Receptor-Complex.....</b>	<b>87</b>
<b>5.4. Drawing Conclusions.....</b>	<b>92</b>
<b>6. Outlook.....</b>	<b>98</b>
<b>7. Index.....</b>	<b>100</b>
<b>7.1. Table of Abbreviations.....</b>	<b>100</b>
<b>7.2. List of Figures.....</b>	<b>103</b>
<b>7.3. List of Tables.....</b>	<b>104</b>
<b>8. Literature.....</b>	<b>105</b>
<b>9. Appendix.....</b>	<b>116</b>
<b>9.1. Additional Figures and Overviews.....</b>	<b>116</b>
9.1.1.The 100 most differentially expressed membrane-associated genes in ATDC5 vs C2C12 cells.....	116
9.1.2.Overview of receptor-ligand pairings in the TGF $\beta$ growth factor family.....	120
9.1.3.Overview of receptor-ligand pairings in the FGF growth factor family .....	121
9.1.4.Overview of developmental stages and regulatory components of the cranial and appendicular skeleton.....	122
9.1.5.Examples of BMP-FGF interactions in development .....	124
<b>9.2. Materials.....</b>	<b>125</b>
9.2.1.Equipment.....	125
9.2.2.Laboratory material and consumables.....	126
9.2.3.Chemicals.....	127
9.2.4.Solutions.....	129
9.2.5.Cell lines.....	132
9.2.6.Enzymes and other proteins.....	132
9.2.7.Antibodies.....	133
9.2.8.Plasmids.....	134
9.2.9.Kits.....	134
9.2.10.Software.....	135
<b>9.3. Figure References to the Laboratory Notebook.....</b>	<b>137</b>
<b>9.4. Supplemental References.....</b>	<b>139</b>

# 1. Introduction

Many organisms gained complexity over time in the course of evolution. Entangled with growing complexity is an increasing amount of specialized cell types and tissues; and with this comes the need for regulatory processes to adapt and extend as well. Hence, both genome and proteome tend to grow along the path of evolution, although notably, their size does not directly correlate with the complexity<sup>a</sup> of a given organism. Some protein families did not really expand at all, such as those involved in DNA replication and protein biosynthesis for example – their functions are universal to different cells and organisms. Those protein families whose size does highly correlate with complexity are those which „are likely to have enabled the emergence of novel cell types and the communication between these cells“ [3]. They are the ones that enable cell differentiation into more lineages, the specialization of cell types, the division in cellular functions, and they are the ones that conduct the signal orchestra that allows all of these specialized cell types to work together. And among them: cellular translators and messengers, growth factors like BMPs and FGFs.

## 1.1. Bone Morphogenetic Proteins (BMPs)

### 1.1.1. What BMPs are and how they work

Bone morphogenetic proteins (BMPs), together with growth/differentiation factors (GDFs), are a subgroup of the transforming growth factor (TGF) $\beta$  family. Other family members include activins, inhibins, Nodal, and – naturally – the TGF $\beta$ s themselves. TGF $\beta$  family members cover a broad variety of functions in development and in adult tissues, from early developmental patterning to tissue homeostasis in the adult organism, and are important in many organs, from the brain to the eye and kidney to most of the musculoskeletal system [4]. To date, there are more than 30 TGF $\beta$  family members described, of which over 15 are BMPs and GDFs, 5 are

---

a.) Vogel et al. define the complexity of an organism by the number of their different specialized cell types [3].

activins/inhibins, and only 3 are „true“ TGF $\beta$ s [4]. As „TGF $\beta$ s“ can refer to either all family members or to just the subgroup of ligands TGF $\beta$ 1-3, the protein family as a whole will be referred to with the term „TGF $\beta$ /BMPs“ , and the ligand subgroup will be referred to as “TGF $\beta$ s“. All TGF $\beta$ /BMPs have a pro-domain and a mature part, and the mature parts dimerize covalently with a disulfate bond at their C-terminal ends. Hence, the shape of mature TGF $\beta$ /BMP ligands resembles a butterfly, or two hands that are joint at the palms. Consequently, the receptor binding epitopes in BMPs and activins are sometimes referred to as „wrist“ (type I receptors), and „knuckle“ (type II receptors) [4].

The receptors for all TGF $\beta$ /BMPs are serine-/threonine kinases with a single transmembranic domain and an intracellular kinase. They can be subdivided into seven type I receptors and five type II receptors. Only type I receptors carry an intracellular GS domain (a glycine-/serine-rich phosphorylation site upstream of the kinase domain), so intracellular signaling components anchor at the type I receptors of the signaling complex [4].

Each dimeric ligand can theoretically recruit two type I and two type II receptors into the signaling complex. The mechanisms to form a complex can vary. For TGF $\beta$ s, the type I receptor T $\beta$ RI and the type II receptor T $\beta$ RII form direct contacts within the complex, and the presence of T $\beta$ RII seems to be necessary to recruit T $\beta$ RI. Hence, TGF $\beta$  signaling complexes form sequentially, type II receptors first, and type I receptors second. For BMPs, the opposite may be presumed, if there is a sequence to it at all. BMPs recruit type I and type II receptors individually, so the assembly of multiple receptors is non-cooperative. For most BMPs, type I receptors are simply more likely to be bound first, because affinities to BMP type I receptors are usually higher and off-rates are usually lower than those to BMP type II receptors, although BMPs 6 and 7 are an exception to this. Apart from the order of binding, the modality of complex formation is likewise heterogeneous. Some receptors like BMPRII or ActRII for example go through little conformational changes upon ligand binding, whereas BMPRIA exhibits an induced fit mechanism upon BMP2 binding [4-6] .

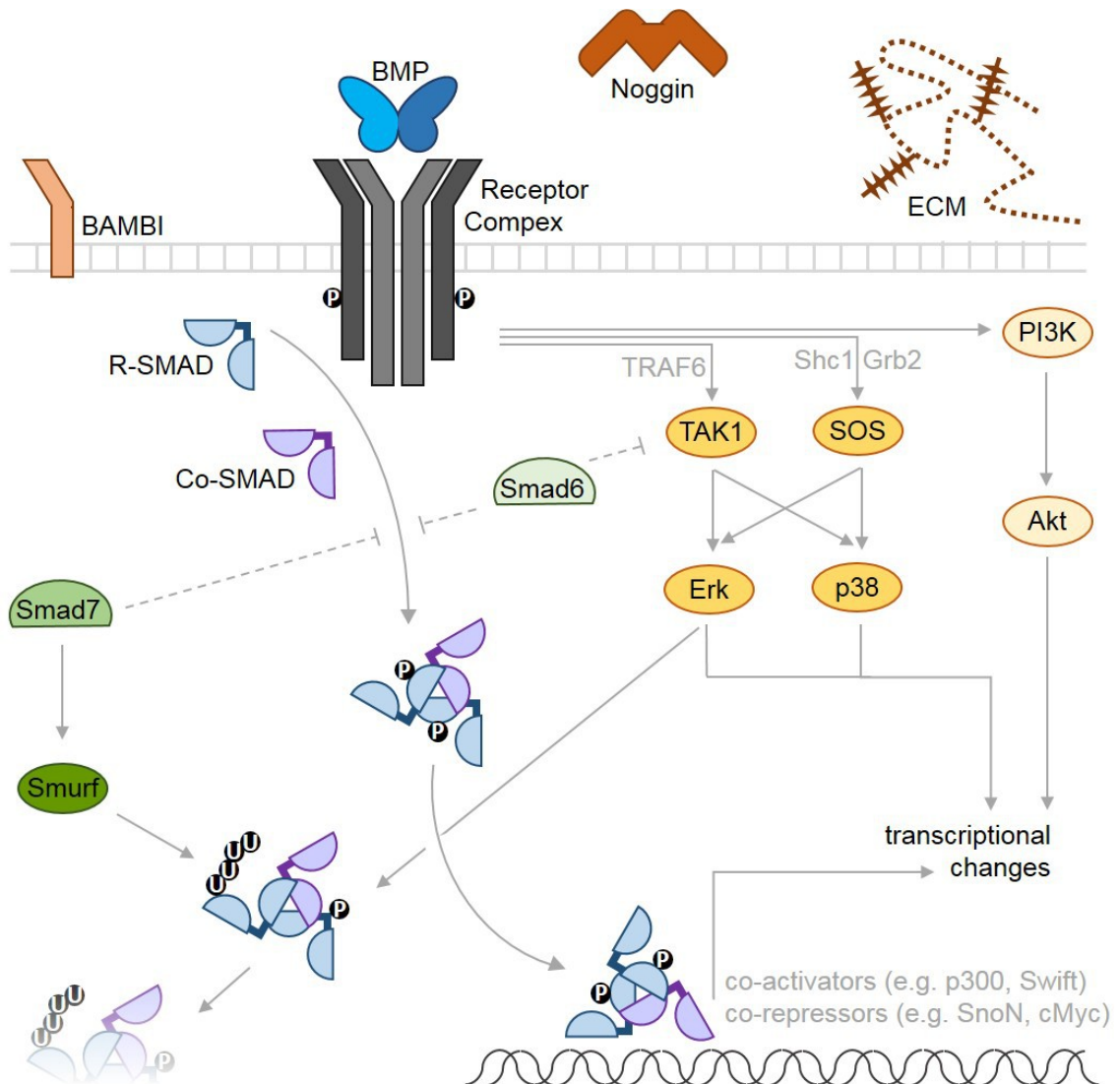


**Figure 1: BMP Signal Transduction**

BMP ligands recruit heterotetrameric receptor complexes to induce canonical signaling via SMAD proteins. Non-canonical signaling may involve kinases Erk, p38, or Akt. Regulatory components of BMP signal transduction include the ECM, extracellular inhibitors such as Noggin or BAMBI, and intracellular inhibitors such as SMADs 6 or 7. Abbreviations: BMP—bone morphogenetic protein; Co-SMAD—common mediator SMAD; ECM—extracellular matrix; Grb2 – growth factor receptor-bound protein 2; p300 – histone acetyltransferase p300; PI3K—phosphoinositide 3-kinase; R-SMAD—receptor-regulated SMAD; Shc1 – Src homology 2 domain containing transforming protein 1; Smurf—SMAD specific E3 ubiquitination regulatory factor; SnoN – SKI-like protein; SOS—Son of sevenless; TAK1 – TGF $\beta$ -activated kinase 1; TRAF6 – TNF receptor-associated factor 6.

A variation of this figure has been published in [1].

After the signaling complex is formed, the type II receptor phosphorylates the type I receptor, and the type I receptor binds and activates receptor-regulated (R-)SMAD proteins, which are the main cytoplasmic signaling proteins in canonical TGF $\beta$ /BMP signaling and function as transcription factors. R-SMADs belong to one of two groups, and type I receptors usually only activate one of them: most BMP/GDF receptors phosphorylate SMADs 1, 5 and 8, whereas TGF $\beta$  receptors phosphorylate SMADs 2 and 3. All R-SMADs consist of two globular domains connected by a linker region. The N-terminal domain (MH1) binds DNA (except in SMAD2), while the C-terminal domain (MH2) interacts with other proteins, including the receptor, DNA-binding co-factors, or other SMADs. Activated R-SMADs form heterotrimers with one SMAD4 protein (the common mediator or Co-SMAD), and translocate into the nucleus to influence gene expression with the help of co-factors and histone modifying enzymes. Apart from this canonical pathway, BMP and TGF $\beta$  receptors have also been shown to activate other signaling proteins, including mitogen-activated protein kinases (MAPKs) such as p38 and Erk, as well as phosphoinositide 3-kinase (PI3K)[4, 7, 8]. Some of these non-canonical pathways have been described only for certain receptors. For example, BMPRII is linked to activating CDC42, a Rho GTPase that activates the kinases LIM domain kinase (LIMK) and c-Jun N-terminal kinase (JNK). T $\beta$ RII can activate JNK and p38 via MAP2K4/7 and death associated protein 6 (Daxx). Both the TGF $\beta$  and the BMP branch may activate Akt via PI3K; and both can activate the MAP3K TAK1 (TGF $\beta$  activated kinase) via TNF receptor-associated factor 6 (TRAF6), which can activate MAPK signaling including Erk and p38, and has even been implicated to amplify SMAD1 phosphorylation. MAP kinases like Erk and p38 may also be activated via the association of SHC-transforming protein 1 (Shc1), growth factor receptor bound 2 (Grb2) and son of sevenless (SOS) to the receptor complex, facilitated by proto-oncogene tyrosine-protein kinase Src [9-11].

Non-canonical signaling seems to be quite context-dependent. For example, Akt has been described both as being activated by and thus synergistic to SMAD1/5/8-inducing BMP4 [12], as well as antagonistic to Smad2/3-inducing GDF15 by sequestering SMAD3 [13]. The activation of JNK may both stabilize SMAD3 activation and inhibit SMAD2 signaling. TGF $\beta$ s are apparently able to both activate and inactivate RhoA [10], possibly depending on the mediator available. p38 and Erk activation have been described in response to BMP receptor activation [14], but have likewise been strongly linked to BMP signaling inhibition [15]; and in our hands, we can

confirm neither Erk nor p38 phosphorylation in response to BMP2 or GDF5 in our cell culture system [2]. Thus, while non-SMAD signaling events are a widespread part of BMP/TGF $\beta$  signaling and may carry importance under certain conditions, they mainly seem to fine-tune the signal, enhancing context-specific effects and functions, rather than to be the primary translator of the signal.

#### **1.1.2. Receptor promiscuity is met by a tight network of regulatory mechanisms**

A signaling system with high receptor promiscuity and limited downstream pathways like this one can only generate as many distinct functions as it does if it is extensively regulated. Regulatory elements may interfere with signal generation and signal transduction at multiple levels.

For example, a signal can only be successfully induced if the ligand and the receptors match. A complex may not form if the available ligand is not able to bind to that cell's particular receptor set. If in turn multiple receptors and ligands are available, different ligands have to compete for the available receptors, and it is possible that more than one combination can form. Which combination does form, and whether the resulting complex contains more than two different types of receptor chains, may likewise influence the cell's response [4, 16, 17].

BMPs may be deflected from binding their receptors by other interaction partners, e.g. by extracellular matrix (ECM) components like heparins. On the one hand, this restricts ligand diffusion, leading to higher local concentrations; on the other hand, it also limits ligand availability in the extracellular space [18]. Other extracellular “deflectors” include inhibitory proteins that mask receptor binding epitopes on the ligand. Noggin is a prominent member of this group, and it strongly inhibits the function of BMPs (including BMPs 2, 4, 6, 7, and GDF5). Noggin shows an affinity to its substrate far higher than the substrate's affinity to its receptors [19], effectively neutralizing any ligand it binds. Other members include Sclerostin, a DAN family member that can both bind and hence inactivate BMPs and Noggin; or Follistatin, which only binds BMPs with low and activins with high affinities, as well as Chordin, Cerberus 1, Gremlin 1/2, among others [11, 20]. Finally, the cell itself might deflect the ligand by expressing pseudo-receptors: BAMBI is a transmembrane protein with a BMP ligand-binding extracellular domain, but without intracellular kinase domain. It associates with type I and type II receptors and



competes with genuine receptors for the ligands available, but is unable to transduce a canonical signal [4].

Once receptor-ligand complex assembly has been successful, and downstream signaling has been initialized, signal transduction can be regulated and/or terminated by intracellular interaction partners. The linker region of R-SMADs for example can be phosphorylated to either enhance or inhibit SMAD performance: while cyclin-dependent kinases (CDK) 8 and 9 boost their transcriptional activity, and sumoylation of SMAD4 stabilizes it, glycogen synthase kinase 3 (GSK3) prepares SMADs for ubiquitination, e.g. by Smurfs (SMAD-specific E3 ubiquitin protein ligase), and hence cause their subsequent degradation. While Smurf1 primarily targets SMADs 1 and 5, Smurf2 may interact with all R-SMADs. Inhibitory SMADs 6 and 7 likewise limit the signal transduction. They usually reside in the nucleus and get transported to the cytosol after receptor activation. Both compete with R-SMADs for receptor binding. Additionally, SMAD6 competes with them for the binding of SMAD4, and SMAD7 recruits Smurfs to the receptors [5, 7, 10, 21].

Other regulators may limit signal transduction in other ways. Receptors may be internalized and degraded, mediated e.g. by Smurf2 [11]. Phosphatases may interrupt the cascade by inactivating cascade members. For example, pyruvate dehydrogenase phosphatase (PDP) and  $Mg^{2+}/Mn^{2+}$  dependent protein phosphatase 1A (PPM1A) constantly de-phosphorylate R-SMADs, so an active SMAD signal may only be maintained as long as the receptors remain active. Proteins like inner nuclear membrane protein (MAN1) may limit or completely inhibit the entry of the activated SMAD complex into the nucleus. Ultimately, once an active SMAD complex has achieved translocation into the nucleus, it is dependent of as well as limited in its ability to alter gene expression by co-factors and/or co-repressors, such as CREB-binding protein (CBP) or (histone acetyltransferase) p300. Partly, this is due to the low affinity of the SMAD-binding element (SBE) to SMADs, requiring other DNA-binding factors for efficient interaction. Such a necessity for accessory proteins in the nucleus highly contributes to cell type specific functions of TGF $\beta$ /BMP signaling, as the differentiation status and identity of the cell will determine which co-factors are available, and hence which genes can be targeted [5, 8, 21].

Finally, TGF $\beta$ /BMP signal specificity is also orchestrated by defined spatiotemporal expression patterns. For example, GDF8 and GDF11 are structurally very similar proteins, but while both

can inhibit muscle growth/differentiation *in vitro*, only GDF8 deletion leads to deregulated muscle growth *in vivo*, simply because GDF11 is not naturally expressed in muscle tissue and hence, its absence does not cause symptoms there [4]. BMP2 and BMP4 are likewise highly homologous in their amino acid sequence, but associated diseases are distinctly different. Gene knock-outs of either BMP in mice are embryonically lethal, but for different reasons. Still, heterozygous knock-outs show less severe phenotypes alone than in combination [22, 23]. These observations show that despite some functional overlap, BMP2 and BMP4 have individual and important roles in development; and this is to some extent reflected in their partially overlapping, partially distinct expression patterns during organogenesis [24]. In many *in vitro* assays however, the mature proteins seem to be hard to distinguish [22].

Trying to understand how structurally similar ligands execute diverging effects if applied to the same cell or expressed in the same tissue is a good way to learn more about the fine-tuning of TGF $\beta$ /BMP signaling regulation.

## **1.2. Fibroblast Growth Factors (FGFs)**

### **1.2.1. What FGFs are and how they work**

Fibroblast growth factors (FGFs) are almost ubiquitously expressed. In development, they are necessary for patterning, growth and differentiation. In the adult organism, they orchestrate homeostasis by influencing cell proliferation and metabolism, as well as tissue regeneration [25].

Like BMPs, FGF ligands vastly outnumber their receptors. Unlike BMPs, the ligands are monomeric, and the receptors are heavily alternatively spliced. To date, 18 secreted (and four intracellular) FGF ligands have been described. Of the secreted ligands, 15 are considered paracrine [25, 26] and three act as endocrine factors. The latter signal through the same receptors influencing similar processes as their paracrine counterparts, but they also fulfill systemic functions, such as the regulation of phosphate, bile acid and carbohydrate [25].

The paracrine canonical FGFs rely on heparin/heparan sulfate as compulsory cofactors to signal, partially because they counter-balance the charges of receptor and ligand [26]. Heparan sulfates (HS) are a heterogeneous group of sulfated disaccharide chains, anchored to the cell membrane or the extracellular matrix (ECM) via HS proteoglycans (HSPGs). As the non-canonical endocrine FGFs have lost their affinity to heparan sulfates, they need alternative cofactors. Their signaling

requires members of the Klotho family, namely  $\alpha$ Klotho,  $\beta$ Klotho, or Klotho-LPH related protein (KLPH), sometimes referred to as  $\gamma$ Klotho. These proteins are anchored to the plasma membrane by a single transmembrane domain, and they differ from each other in their sites of expression [25].

There are four genuine FGF receptors, FGFR1 – 4. FGFRs are single-pass transmembrane receptor tyrosine kinases. Extracellularly, each receptor has up to three immunoglobulin-like domains (IgI - IgIII), a contingent acidic box, and a heparin-binding site. Intracellularly, each receptor has a tyrosine kinase domain. The ligand binds to IgII and IgIII, as well as to the linker region between them. [25]. A fifth receptor, FGFR5 or FGFR-like 1 (FGFRL1), shares the extracellular and transmembrane domain functions, but has no intracellular kinase domain, and hence might serve as a decoy receptor [27].

Once two receptor chains, two FGF ligands, and heparan sulfate come together, the receptors cross-phosphorylate and the ligand-receptor complex is activated [28]. Phosphorylated residues in the receptor kinase domain function as docking sites for various adaptor proteins, mediating the transduction of the signal from the receptor to effector kinases and transcription factors. Unlike other receptor tyrosine kinases (RTKs), FGFRs lack the canonical binding motif for the adapter protein Grb2, but instead mediate Grb2-dependent signaling through phosphorylation of FGFR substrate (FRS)2 $\alpha$  and - $\beta$  [25, 29]. FRS2 $\alpha$ , aided by the adapter molecule Crk-like protein (CRKL), then recruits Grb2 and the tyrosine phosphatase SHP2. Grb2 in turn activates Ras-MAPK signaling via SOS, which entails the phosphorylation of transcription factors and the alteration of gene expression. MAP kinases that become activated include p42 and p44 (also referred to as Erk 1 and 2), p38, and JNKs. Grb2 also activates PI3K-Akt signaling via the protein Grb2-associated binding protein 1 (Gab1), which promotes FGF signaling outcome by inhibiting anti-proliferatory and promoting pro-proliferatory factors in the cytosol [25, 27].

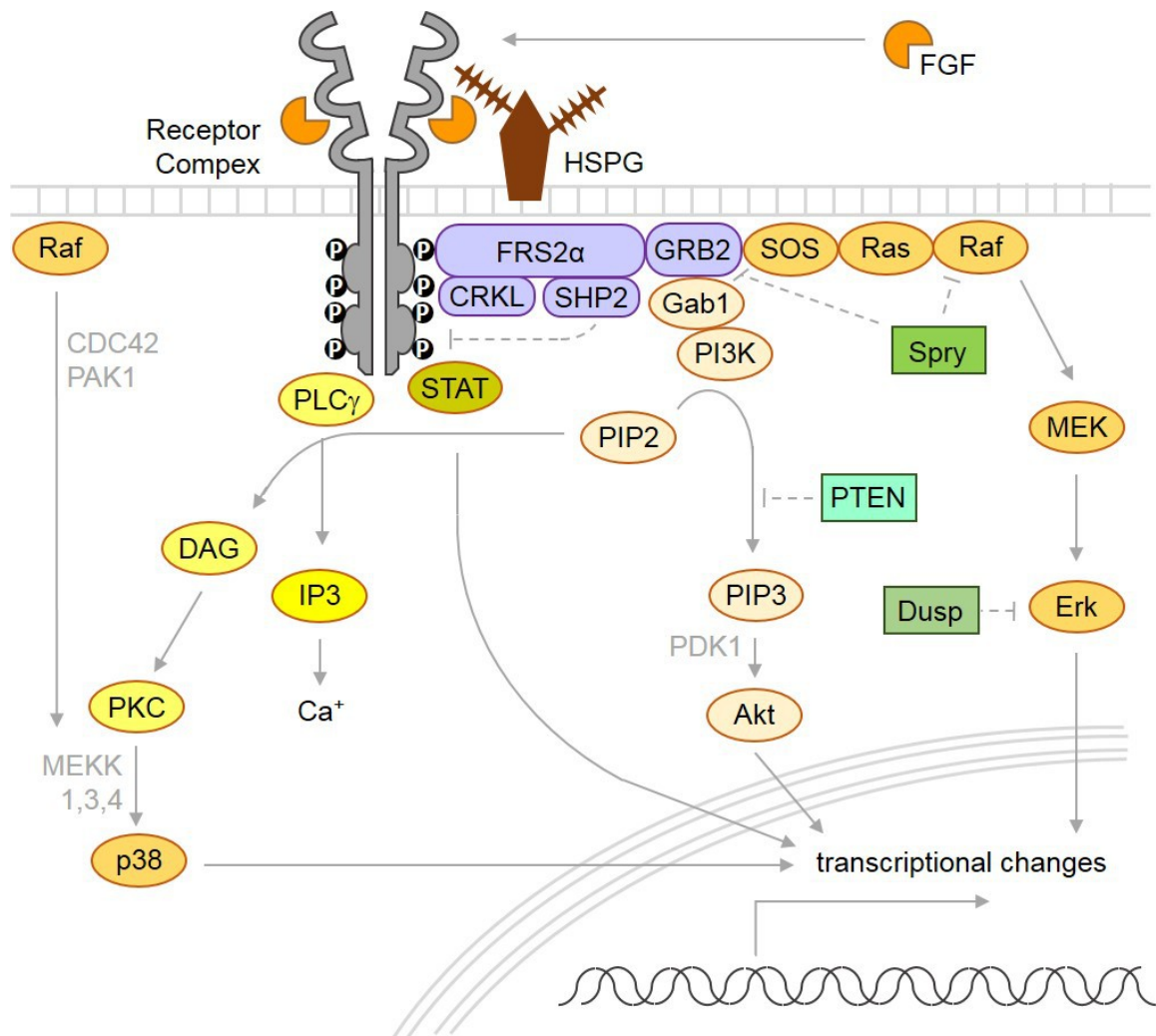


**Figure 2: FGF Signal Transduction**

FGF ligands recruit dimeric receptor complexes and HSPGs to induce signaling via Ras/Raf, PI3K/Akt, STAT, or PKC/p38. Regulatory components of FGF signaling include intracellular inhibitors such as Spry, Dusp, or PTEN. Abbreviations: CDC42 – cell division control protein 42 homolog; CRKL—Crk-like protein; DAG—diacylglycerol; Dusp—dual specificity phosphatase; FGF—fibroblast growth factor; FRS2 $\alpha$ —FGFR substrate 2 $\alpha$ ; Gab1—GRB2-associated-binding protein 1; GRB2—growth factor receptor-bound protein 2; HSPG—heparan sulfate proteoglycan; IP3—inositol triphosphate; MAPK—mitogen-activated kinase; MEK—MAPK kinase; PDK1—pyruvate dehydrogenase lipoamide kinase isozyme 1; PI3K—phosphoinositide 3-kinase; PKC—protein kinase C; PIP2— phosphatidylinositol 4,5-biphosphate; PIP3—phosphatidylinositol 3,4,5-trisphosphate; PLC $\gamma$  —phospholipase C $\gamma$ ; PTEN—phosphatase and tensin homolog; SHP2 – Src homology region 2-containing protein tyrosine phosphatase 2; SOS – sons of sevenless; Spry – Spouty. A variation of this figure has been published in [1].

The two other major pathways activated by FGFRs, signal transducer and activator of

transcription (STAT) and phospholipase C $\gamma$  (PLC $\gamma$ ), do not rely on adaptor proteins. STATs 1, 3, and 5 directly bind and get phosphorylated by the FGFR kinase domain, and go on to alter gene expression. PLC $\gamma$  likewise directly interacts with the FGFR kinase domain at the C-terminal p-tyrosine Y766 (FGFR1), or Y769 (FGFR2), respectively. Its effectors inositol triphosphate (IP $_3$ ) and diacylglycerol (DAG) stay in the cytosol, modulating calcium ion levels and activating protein kinase C (PKC), which stabilizes MAP signaling [25, 27, 30].

### 1.2.2. Regulating FGF signals

Just like BMP/TGF $\beta$ s, FGFs are promiscuous to their receptors, and their regulation is extensive. One mode of regulation is the short half-life of FGF ligands, which are quickly oxidized at their free cysteines [31, 32]. Another are cell- or tissue-specific expression patterns, as the formation of a signaling complex is dependent on whether the receptor type(s) presented can bind to the ligand(s) available. If FGF ligands are bound by decoys such as FGFR1, or trapped in the ECM, they do not reach their receptors to signal. Hence, proteases such as heparinases are necessary accomplices to FGF signaling to allow their release from the ECM. Alternative splicing of the extracellular domain then modulates ligand binding capacity and ligand sensitivity, as seen with switches in the Ig-like domains, or with the presence or absence of autoinhibitory parts of the extracellular domain [30](see 1.2.3.). Signaling complex formation can further be influenced by the HSPGs available [25, 26].

Once FGFRs are activated, the subsequent pathways, especially Ras-MAPK, contain multiple steps of kinase phosphorylation, amplifying and stabilizing the signal. To avoid persisting activation, self-regulatory or self-limiting mechanisms are intrinsic to any FGF signal: Receptors are usually internalized and degraded after ligand binding to limit the receptors available on the cell surface. MAPKs p42/44 are known to phosphorylate FRS2 $\alpha$  at threonine residues that interfere with Grb2 binding, terminating their own (tyrosine-phosphorylation dependent) activation [27, 30]. Grb2 is also inhibited by Sprouty (Spry) and by SHP2, negatively regulating the Ras-MAPK and PI3K-Akt pathways. Specific inhibitors can counteract single pathways as well, such as Sef or dual specificity phosphatase 6 (Dusp6) for p42/44 signaling, while the E3 ubiquitin ligase CBL acts as broad inhibitor by inducing the degradation of FRS2 $\alpha$ , of the receptor, and of PI3K [25, 30].

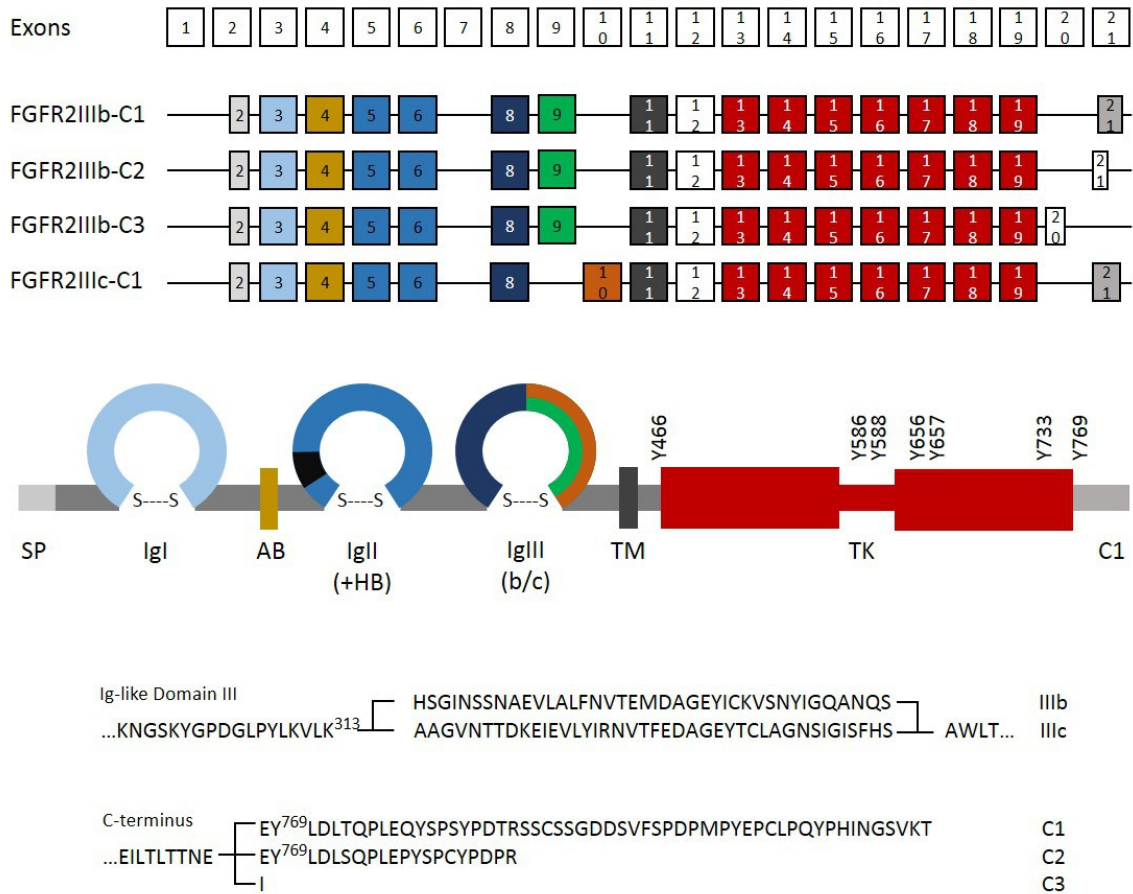


**Figure 3: FGFR2 Splice Variants**

FGFR2 is a single-pass type I membrane protein. At the N-terminus, it contains a signal peptide (SP) that is cleaved off in post-translation. The extracellular and intracellular domains are separated by a single transmembranic domain (TM). Within the extracellular domain, FGFR2 holds immunoglobuline-like domains (IgI – IgIII), an acidic box (AB), and a heparin binding site (HB). Intracellularly, the FGFR2 contains a tyrosine kinase domain (TK). The most common splicing events differ in the composition of IgIII (IIIb in green or IIIc in orange), number of Ig domains (isoform  $\alpha$  contains all three Ig domains, isoform  $\beta$  contains IgII and IgIII), or the length of the C-terminus (C1-C3).

Depicted are human FGFR2 splice variants. Murine FGFR2 has 20 exons, but is otherwise highly homogeneous. According to the Universal Protein Resource database, the murine FGFR2 consensus protein is FGFR2 $\alpha$ IIIc-C1 (<http://www.uniprot.org/uniprot/P21803>).

### 1.2.3. The many faces of FGFR2

In terms of FGF signaling, the focus of this work clearly lies on FGFR2. All FGF receptors are subject to heavy alternative splicing, and FGFR2 is no exception: there are more than 20 isoforms described [33]. Most prominently, the alternative splicing of the third immunoglobuline-like domain (IgIII) creates either the epithelial variant IIIb or the mesenchymal variant IIIc. While

FGFR2IIIb and FGFR2IIIc show overlapping ligand binding properties, for example for FGF1, they are mutually exclusive in binding others, for example FGF2 and FGF18 (FGFR2IIIc only) as well as FGF7 and FGF10 (FGFR2IIIb only). In addition to alternative splicing of the IgIII coding sequence, there are full-length isoforms, isoforms without the first Ig-like domain and/or the acidic box, isoforms without transmembranic and intracellular domains that are soluble as a consequence, isoforms with different carboxyl-termini, dubbed C1, C2 and C3, combinations of these, and others. C1 and C2 are translations from the same exon with different splice acceptor sites, while the third splice variant C3 is expressed by a different exon. C2 is 34 amino acids shorter, and C3 is 53 amino acids shorter than C1, but only C3 misses the sole c-terminal tyrosine known to be phosphorylated, Y769. This tyrosine is characterized as a binding site for phospholipase C- $\gamma$  (PLC- $\gamma$ ) and the Shb adapter protein [30, 34]. Many alternative gene names for FGFR2 refer to single splicing variants that were originally discovered and named as distinct genes, such as *Kgfr*, *K-sam I*, *K-sam II*, or *Bek*. With regard to terminology, KGFR is equivalent with full-length FGFR2IIIb-C1, or K-sam II C1; and BEK is the same as full-length FGFR2IIIc-C1, or K-sam I C1 [34-36]. For FGFR1 as well as in specifications of FGFR2-related commercial products, isoforms containing all three Ig-like domains are referred to as  $\alpha$  isoforms, whereas those containing only IgII and IgIII are referred to as isoform  $\beta$  [37].

### 1.3. Signaling Cross-Talk

The interaction of BMP and FGF signaling has also been detailed in [1], a review that originated from the work for this thesis.

#### 1.3.1. Molecular connections between TGF $\beta$ /BMPs, FGFs, and others

TGF $\beta$ /BMPs have been well described to cross-talk with other signaling pathways, although none of the interactions are strictly synergistic or antagonistic. This dualism is feasible, considering that some TGF $\beta$ /BMP may induce overlapping downstream components such as MAPKs themselves (see above, also [38]). TGF $\beta$ s especially have been referred to as a molecular Jekyll and Hyde in cancer [39], which at least in part has been attributed to their ability to non-canonically induce MAPKs and Akt [40]. In terms of SMAD1/5/8-inducing BMPs, MAPK signaling can more generally be considered antagonistic [38, 41]. p42/44, as well as other MAP kinases, are quite known to phosphorylate SMAD1/5 proteins in their linker region, hindering their

translocation into the nucleus and promoting their degradation. JNK and p38 may cause proteosomal degradation of SMAD4 [11, 15], and MAPK-inducing growth factor EGF has been observed to induce SMAD7 expression, subduing R-SMAD signaling [21]. During the patterning of the dorsoventral axis in early development, FGFs downstream of Wnt signaling antagonize ventralizing BMP signaling on several levels: by the down-regulation of BMP expression, by the up-regulation of Chordin and Noggin, and by SMAD-phosphorylation via p42/44 [42, 43]. In other cellular contexts, Wnt and BMP signaling can be synergistic: Wnt induces  $\beta$ -catenin, which can form one transcription factor complex with SMAD4 to regulate shared target genes [38].

Like MAP kinases, Akt has also been described as a downstream effector of BMP receptors [12]. However, it has likewise been stated that some TGF $\beta$ /BMP ligands may actively inhibit Akt signaling, for example via PTEN stabilization by BMPs, or via SHIP expression increase by TGF $\beta$ s. Both PTEN and SHIP are phosphatases that dephosphorylate PIP<sub>3</sub> (phosphatidylinositol 3,4,5-trisphosphate), which is an upstream activator of Akt [38, 40].

Like Wnts, the mammalian hedgehog proteins sonic (Shh), desert (Dhh) and Indian (Ihh) are morphogens that mostly interact with TGF $\beta$ /BMPs during development. Their downstream effectors, the Gli proteins, can bind to promoter binding sites of some TGF $\beta$ /BMP ligands, and are able to regulate them up or down, depending on the co-factors expressed by the cell (although up-regulation seems to be the more common interaction). Likewise, TGF $\beta$ /BMP members may up- or down-regulate hedgehogs depending on context [38].

Further examples of signaling molecules interacting with TGF $\beta$ /BMPs include Notch, NF $\kappa$ B, or other mediators of inflammation, e.g. IFN $\gamma$  and interleukins.

As stated above, it seems that agonism and antagonism usually co-exist, depending on the environment, or on the particular functions that the two cross-talking signals hold in a given cellular context. Therefore, it is not surprising that most cross-talk happens on the level of transcription, where gene accessibility, expression of co-factors, ligand concentration, or duration of receptor activation can be translated into distinct cellular responses. More direct ways of cross-talking seem to be more scarce, and to usually not involve the receptor-ligand interaction, but downstream effectors such as p42/44 vs. SMAD, or phosphatases. An example for this has been described by Srinivasan et. al., who have analyzed the formation of the tissue border between the dorsal midline and the cerebral cortex in the developing brain driven by



BMP-FGF antagonism. Based on their observations, they bioinformatically modeled an intracellular cross-inhibitory feedback as most likely underlying mechanism, meaning that downstream agents of both signaling pathways antagonize each other to create a sharp tissue border [44].

### **1.3.2. BMPs and FGFs in cartilage and bone**

A very prominent example for BMP-FGF interaction is the osteochondral development, most extensively studied in the context of the appendicular skeleton. Limb formation starts with the appearance of limb buds in the lateral plate mesoderm, and their outgrowth is driven by FGFs (mainly FGF8) and BMP inhibitor Gremlin-1. Distally, BMPs limit FGF signaling and hence limb bud outgrowth [45-48].

Histologically, limb bones are formed by endochondral ossification in a number of steps: (1) mesenchymal cell condensation, (2) chondrocyte proliferation, (3) column formation (pre-hypertrophy), (4) hypertrophy, and (5) vascularization and mineralization. Most chondrocytes in the skeletal anlage are not preserved as cartilage tissue by the time of birth, but undergo hypertrophy and facilitate bone formation. There are two exceptions: the epiphysis or growth plate, whose chondrogenic core provides proliferating and hypertrophic chondrocytes for longitudinal bone growth until early adulthood; and the joints, where non-proliferative cartilage on top of the bones meets in the joint space, and these chondrocytes avoid hypertrophy through life [1, 46].

A multitude of growth factors governs these steps, including BMPs and FGFs, as well as *Ihh*, Wnt ligands, parathyroid hormone related protein PTHrP, and TGF $\beta$ s; which regulate key genes such as *Sox9* for cartilage, *Runx2* for bone, as well as a number of homeobox genes [49-51]. The growth factors create a signaling network with many interconnections between them: TGF $\beta$  is connected to PTHrP, which is connected to hedgehog proteins, which are connected to BMPs, which are connected to FGFs, which are connected to Wnts, which are connected to TGF $\beta$ s... [1, 51-54]. A simplified overview of key players in the development of skeletal structures and their interactions can be found in the appendix (Figure A21). In terms of BMP/FGF interaction specifically, both their synergism and their antagonism is part of endochondral ossification.

Knock-out (KO) and conditional knock-out (cKO) studies help to understand this relationship and their individual roles in different cell populations and at different time-points:

BMP signaling via SMAD1/5/8 plays a central role in the generation of bones. Under control of the collagen 2 promotor (targeting chondrocytes), BMP2 cKO mice display defects in chondrocyte proliferation and differentiation, and a more general down-regulation of BMP signaling under the collagen 2 promotor by BMPRIA cKO/BMP1B KO or SMAD1 cKO/SMAD5 cKO results in severe chondrodysplasia [55]. Chondrodysplasias including forms of dwarfism are likewise induced by activating FGFR3 mutations, while FGFR3 or FGF18 null mice show bone overgrowth connected to expanded proliferating and hypertrophic zones. The FGFR3 KO phenotype can be rescued with a BMPRIA cKO (collagen 2 promotor), exemplifying FGF-BMP antagonism at this point of development [51, 56]. TGF $\beta$  ligands have a less central role in chondrocyte and osteoblast differentiation than the BMP ligands do, but they are involved in the early stages of MSC condensation and chondrogenesis [52, 57].

Summarizing, BMPs (mainly BMP2 and BMP4, but also TGF $\beta$ s) promote chondrocyte differentiation and proliferation, while FGFs (mainly FGFR3 mediated signals) inhibit them. This antagonism is mediated at least to some part via negatively influencing each other's expression levels, and via contrary regulation of chondrocyte-inducer and -stabilizer Sox9 [1, 46, 50, 52, 57].

Sox9 antagonist Runx2, a transcription factor, is pivotal in the next step in osteochondral development, namely hypertrophy and osteoblast differentiation [1, 57-59]. BMP ligands such as BMP2 and BMP6 are expressed in hypertrophic zones [56] and can induce *Runx2* expression along with SMAD1/5/8 signaling, while SMAD2/3 signals and TGF $\beta$ s prevent hypertrophy by inhibiting Runx2 [1, 49, 57, 60, 61]. TGF $\beta$ s regain bone-promoting function after birth as mediators of osteoblast-osteoclast communication in bone homeostasis [51, 62]. BMP2 facilitates Runx2 translocation into the nucleus, and FGF2 has been shown to actually be necessary for this induction [1, 51, 63]. Further indicators for the agonism of FGF and BMP signaling in hypertrophy are the consequences of FGF9 KO or FGFR1 cKO under the *Twist2* promoter, which is present in early osteoblastic stages: both phenotypes include smaller hypertrophic zones [56]. Pro-hypertrophic FGF signaling seems to rely on FGF receptors 1 and 2, which are expressed at sites of hypertrophy, while FGFR3 is the FGF receptor predominantly expressed in proliferation zones [1, 59].

So in contrast to the interaction observed for chondrocyte proliferation, BMPs and FGFs synergize to drive chondrocyte hypertrophy and osteoblastic differentiation, both by enhancing Runx2 activity, as well as positively regulating the expression of each other's signal pathway components [1, 51, 52, 63]. While the involved FGF receptors differ, the involved BMP ligands seem to be mostly the same [1].

Some parts of the skull, including the cranial base, likewise go through osteochondral ossification, and are therefore collectively referred to as the chondrocranium. In parallel to growth plates, synchondroses are cartilage sites that persist after birth to provide the basis for bone growth, and the involved mechanisms of bone formation as well as their molecular regulation is highly similar to the ones in growth plates and long bones [1, 56, 64]. Skull parts forming via membranous ossification encompass the facial bones (viscerocranium) and the membranous neurocranium, entailing most of the calvaria [64]. As the calvaria needs to grow and expand after birth as well, membranous bones of the skull are divided sutures, a fibrous connective tissue [1].

Membranous ossification and suture formation and maintenance are quite similar to the later stages of endochondral bone formation. One example is Runx2 as necessary driver of osteoblast differentiation [62], or the regulation of mesenchymal proliferation by TGF $\beta$  ligands, Wnt and FGF signaling [64]. In contrast, Sox9 plays a far less important role in comparison to the appendicular skeleton, as evidenced by the fact that Sox9 haploinsufficiency does not lead to the malformation of the cranial skeleton [62]. As membraneous ossification in the skull does not include the differentiation of chondrocytes, so a transcription factor linked to them would not carry importance. The same is true for other regulators of chondrocytic proliferation and differentiation, namely Ihh and PTHrP. Although they are expressed in the developing calvaria, their absence usually does not cause cranial phenotypes [59, 65, 66]. It seems that membraneous and osteochondral ossification rely on the same key players, although their impact on the developing tissue as well as their role within the signaling network changes depending on the type of bone formation [1].

One of the most common abnormalities in calvarial development is premature suture closure, or

craniosynostosis, which is described to originate from enhanced bone formation rather than altered proliferation, as seems to be the case in growth plate deficiencies [60, 67]. Syndromic forms of craniosynostosis are the result of activating FGFR mutations (mainly FGFR2), as well as *Twist1* insufficiency (a negative regulator of FGFR2 expression [68]), *Msx2* gain-of-function mutations (downstream of BMP signaling), and others [67]. Non-syndromic craniosynostosis are usually not associated with a specific gene, but some can be linked to loss of function mutations in BMP signaling inhibitor SMAD6 or loss of function mutations in MAPK signaling inhibitors Sprouty 1 and 4 [69]. The authors even suggest that SMAD6 haploinsufficiency in combination with BMP2 associated risk alleles may be one of the most common causes of craniosynostosis, second only to FGFR2 mutations. In mouse models, craniosynostosis may also be observed with constitutively active BMPRIA under the neural crest-specific  $P_0$  promoter [54, 66]. It therefore seems that suture maintenance and closure is primarily governed by BMP-FGF interaction. Here, they are connected via Noggin, which is expressed in and vital for patent sutures. Noggin negatively regulates BMP signaling, and is itself regulated in its expression by FGFs in cranial sutures. Premature suture closure caused by activating FGFR2 mutations can be suppressed by the application of Noggin, and the application of recombinant Noggin can also prevent the recurrence of suture closure after they need to be surgically opened [54]. As FGF2 has been described to suppress Noggin only at high concentrations [70] and induce BMP2 expression in cranial suture cells [71], it seems that BMP activity is dependent on FGF signal intensity. Likewise, FGF-driven ossification appears BMP-dependent. It seems that once a certain threshold of ligand concentration is reached, FGF and BMP work together to drive osteoblast differentiation and mineralization, or suture closure, in an additive fashion [1, 54, 71].

Finally, GDF5 occupies a rather unique role for a BMP ligand in osteochondral development. GDF5 is almost exclusively expressed at the sites of future joints, the interzones, and it defines them [72]. However, ectopically applied GDF5 does not induce additional joints [73], suggesting that while it is necessary, it is not sufficient for joint induction. Wnt proteins, specifically Wnt9a (formerly Wnt14), are also described as pre-requisites for joint formation [74].

GDF5 null mice present with brachypodism but unaffected axial skeleton, and patients with homozygous loss of function of GDF5 have shortened limbs and partially disorganized limb joints

causing varying degrees of brachydactylies, such as in Grebe type or Hunter-Thompson type chondrodysplasia [62, 75, 76]. Heterozygous loss of function of GDF5 results in brachydactylies types A2 and C, the shortening of specific fingers [62]. While these phenotypes cement GDF5's role in cartilage maintenance and joint development, they also show that even homozygous GDF5 loss of function does not affect all joints, indicating that GDF5 functions are far more restricted and specific than BMP2 functions.

### 1.3.3. BMPs and FGFs in other tissues

BMP-FGF interaction is not only prevalent in skeletal development, as described above, but in many other tissues as well. For example, teeth development is regulated rather independently from the surrounding tissue by a tight growth factor network including FGFs and BMPs [77, 78], and both instances of synergism and antagonism between BMPs and FGFs can be found. BMP4 and FGF8, for instance, both induce *Msx1*, a key transcription factor that can maintain both their expression; while they antagonize in patterning the border between incisors and molars [78, 79]. On the single tooth level, FGFs (including 4, 9) drive proliferation, which is limited by BMP4-driven apoptosis [79, 80]. The same is true for the development of the optical lens, where both BMPRIA/IB-mediated and FGFR2-mediated signals positively drive lens fiber cell differentiation [81], while BMP/FGF antagonism defines a tissue border in the retina between neural retina (FGF) and pigmented epithelium (BMP) [1, 82, 83].

Neural differentiation is largely driven by the absence of BMP signaling enforced by a number of BMP inhibitors, rather than the presence of an inductive agent [84]. While the necessity of FGFs as inducers of neuralization in antagonism with BMPs is debatable [84-86], it is established that once neural fate is determined, the organization of these central nervous system (CNS) cells along body axes is patterned by various growth factors, including BMPs and their inhibitors as well as FGFs [84, 87]. BMPs and FGFs usually act antagonistically in CNS development, as for instance in the FGF-mediated survival of telencephalic precursors versus SMAD2/3-driven apoptosis [88], or in the tissue border between telencephalic dorsal midline (BMP4) and cerebral cortex (FGF8)[44], among others [1].

In kidney development, BMP4 negatively regulates FGF7,10/FGFR2-driven uterine bud outgrowth, while BMP7, FGF9 and FGF10 synergistically promote the proliferation and maintenance of

nephron progenitors [1, 89]. In heart development, early cardiac subtype patterning is mediated by the combination of Nodal and FGF8 in antagonism to BMPs, while BMP2 and 4 and FGF8 and 4 act synergistically at a later stage of heart development to induce heart-specific markers [1, 90-92]. In lung development on the other hand, BMP/FGF synergism is seen at early stages during fate determination of pulmonary precursors from the foregut epithelium, while BMP4 later antagonizes FGF10/FGFR2IIIb-regulated lung bud outgrowth and hence facilitates branching [1, 93].

#### 1.3.4. Unanswered questions

Despite the seemingly vast knowledge of signal transduction and regulation, both for TGF $\beta$ /BMPs and for FGFs, there are still questions that are unanswered, and phenomena that cannot be explained.

Some questions arise on the mechanistical aspect of signal complex formation: for example, FGF signaling complex stoichiometry is a point of discussion. Crystallographic measurements exist for both 2FGF:2FGFR:1HS and 2FGF:2FGFR:2HS stoichiometries [28] that result in very different geometries [26, 94, 95]. As there is experimental evidence supporting both models, it is potentially possible that signaling complex geometry and stoichiometry are ligand- and/or receptor- and/or HS-specific.

An intriguing question in this context is whether preformed FGFR dimers trans-phosphorylate even in the absence of ligand. This would potentially lead to a leaky and unspecific signal, and therefore seems unlikely. Still, there is experimental evidence suggesting both yes and no, partially dependent on what type of receptor is investigated. A ligand-induced conformational change in receptors would allow ligand-free receptor dimerization without signal induction. While this is conceivable, it is not clear whether such conformational changes actually happen [26, 96, 97].

Similar questions about ligand-free receptor dimerization and subsequent unspecific activation arise concerning TGF $\beta$ /BMP receptors, especially in terms of dimers with one type I and one type II receptor. In observation, type I / type II heterodimers are rare for TGF $\beta$  receptors, which are known not to conformationally change upon ligand binding and hence would generate active heterodimeric complexes. For some BMP receptors on the other hand, conformational

changes after ligand binding are part of the activation process. Here, heterodimers of one type I and one type II receptor can theoretically form without signal activation, and indeed, their formation can be observed [5, 98].

Heterodimer formation in the BMP signaling system is not only an investigatory point on the level of receptors, but on the level of ligands as well. TGF $\beta$ /BMPs are covalently coupled dimers formed during their production within the cell. Some of them are so similar (e.g., BMP2 and BMP4) that a cell expressing two or more of such closely related ligands may theoretically secrete not only homo- but also heterodimers. Such heterodimers would have two different “knuckle” epitopes (binding type II receptors) each one identical to one of the homodimers'. As each “wrist” epitope (binding type I receptors) is build up from both monomers, a heterodimer would also have two “wrist” epitopes that are both distinctly different from either homodimer, and distinctly different from each other. Hence, a heterodimer would potentially elicit distinct biological functions. *In vitro*, this principle has already been put to use in tissue engineering approaches for bone regeneration or for embryonic cell culture [99, 100], but its biological extent and relevance are still unknown.

Apart from signal complex assembly, there are other observations left unexplained. In FGF signaling, these range from missing details (such as, what is the function of the phosphorylation at Y344 in FGFR2 [28]?) to big questions, such as: why is FGFR2IIIb seemingly the only FGF receptor splice variant that is tumor-protective instead of -enhancing [27]? Or, what exactly does the fifth FGF receptor FGFR1 do [25]?

In BMP signaling, we have yet to mechanistically describe how co-receptors (such as repulsive guidance molecules) can enhance a BMP signal if they block the ligand's receptor binding site [101], and we do not understand how some cells distinguish between two TGF $\beta$ /BMP ligands that bind to the same receptors on their surface. Examples of these questions are the basis to this work.

## **1.4. Getting Started: The Findings That Preceded This Work**

### **1.4.1. The co-receptor concept**

Both the BMP and the FGF signaling systems include co-receptors, or cofactors, respectively. In case of FGFs, they are mostly quite vital to signaling: As described above, FGF signaling is highly

dependent on the presence of heparan sulfates as part of the signaling complex (or Klothos, in the case of endocrine FGFs). These co-receptors are usually membrane-anchored, and do not contain a kinase domain [25, 26].

Just as for FGFs, the local retention of BMP ligands is facilitated by heparins or other ECM components, but they do not directly associate with the BMP receptor complex [101, 102]. Genuine TGF $\beta$ /BMP co-receptors such as Betaglycan, Cripto, repulsive guidance molecules (RGMs), or others do not take part in the general signaling mechanism, but they serve specific purposes only for single or a handful of ligands [101]: Betaglycan (or T $\beta$ RIII) for example enables biologically relevant TGF $\beta$ 2 signaling and enhances activin-inhibition by inhibins [101, 103]. Structurally similar Endoglin switches TGF $\beta$  signaling from T $\beta$ RI-mediated to ALK1-mediated, meaning from a SMAD2/3 signal to a SMAD1/5/8 signal [20, 101]. Cripto binds ActRIIB and ActRII, enabling Nodal signaling while partially inhibiting activin signals [104]. Finally, RGMs are specific for BMP2 and BMP4 (and BMP6 in case of RGMc), enhancing their signaling outcome possibly by allowing ActRIIA usage in addition to BMPRII [20]. Some of these co-receptors exist as soluble versions, and as such, they can inhibit signaling by sequestering the ligands, acquiring a dual role [11, 101].

All of these co-receptors are membrane-associated and have no kinase activity, but work by modulating ligand binding to genuine TGF $\beta$ /BMP receptors. Such modulations range from deflecting a ligand from the receptor to altering affinity, to being obligatory for the binding. If multiple ligands are available, the presence or absence of a co-receptor may hence decide which one(s) of them will signal successfully.

### **1.4.2. The ATDC5 / C2C12 discrepancy**

Even with all the processes already known and described for BMP signal regulation, there are still some observations that cannot be explained by any of them. BMP2 and GDF5 are structurally similar ligands that utilize the same receptors: type I receptors BMPRIA and BMPRIB, and type II receptors BMPRII, ActRII, and ActRIIB. The binding affinities of BMP2 and GDF5 are very similar (meaning, equal or less than two-fold different) to all these receptors except for BMPRIA, which binds BMP2 with roughly 20-fold higher affinity as compared to GDF5 [105]. The murine cell lines ATDC5 and C2C12 both express the same subset of these receptors, namely



BMPRII and BMPRIA. Both ligands can induce SMAD1/5/8 phosphorylation in both cell lines, although GDF5 needs to be 10-20 times more concentrated than BMP2 (reflecting the affinity differences at BMPRIA). Still, if downstream target alkaline phosphatase (ALP) is measured three days into treatment, GDF5 only induces it in ATDC5, not C2C12 cells, while BMP2 does it in both. When the BMPRIA affinities are equalized by side-directed mutation of GDF5, the resulting variant GDF5-R57A indeed induces SMAD phosphorylation more efficiently than GDF5wt, but still elicits no ALP expression in C2C12. GDF5wt and GDF5-R57A even antagonize the induction of ALP by BMP2 in C2C12 cells, feasibly by competing for the same receptors without signal. It was confirmed *in vivo* that the ability of GDF5 to induce osteogenic markers is context-dependent: GDF5 was able to induce osteoconduction at an orthotopic site in mice, but no osteoinduction at a heterotopic site, and it antagonized BMP2's osteoinductive properties [106]. Since no known discrepancy could be made responsible for the observed difference, it was concluded that a component must be involved that is hitherto unknown [106]. This component has to be cell-specific, either enhancing GDF5 signal transduction in ATDC5 cells, or interfering with GDF5 signal transduction in C2C12 cells. While it could be assumed that there is a second downstream component next to SMAD1/5/8 needed for ALP induction that is only expressed in ATDC5 cells, this seems improbable: BMP2 and GDF5 recruit the same BMP receptors on both cell lines into an active signaling complex. If two signals were needed for ALP induction, it is hence unlikely that BMP2 would be able to induce them in C2C12 cells, while GDF5 cannot; and given that the expressed receptors are the same, it is unlikely that GDF5 would be able to induce them on one cell, but not the other. Thus, it was postulated that the unknown component is likely membrane-associated like a co-receptor, as this would allow for cell-specific and ligand-specific signal modulation [2, 106] .

## 2. Aim of Work

BMPs have been under investigation ever since their first description as a soluble, bone-inducing agent in 1965. Major break-throughs in early BMP research included the identification of the BMP ligands and their receptors as well as the unraveling of canonical and non-canonical signaling pathways. The concept of a promiscuous receptor set, transducing signals from a large palette of ligands and made specific by a big regulatory machinery, became well-established, and in the last decades, the focus shifted to different questions, namely the role of BMPs in disease as well as their potential benefit in the clinic. The principal assumptions of BMP signal transduction, such as the receptor complex being tetrameric, or SMAD phosphorylation being equivalent to a full BMP signal, are usually not challenged. Still, new ways of fine-tuning BMP signaling outcome are still being discovered, and some observations still remain unexplained.

In this work, I examine the relationship of BMP2 and GDF5 with the FGF receptor 2. In particular, I describe the discovery and the investigation of BMP2/GDF5 - FGFR2 binding, which may open an entirely new chapter of BMP signal regulation: the direct interaction of BMP ligands and receptor tyrosine kinases. In analyzing the intricacies of such a connection to FGFR2, and in revisiting established postulates of BMP signal transduction, I aim to contribute to the understanding of how BMPs generate their specific functions. The better we understand how and when a BMP signal is created, the better we can hope to understand how to manipulate it. In other words: if we achieve knowledge about the developmental and pathological mechanisms governed by BMPs, we learn how to specifically imitate or influence them. BMPs are so pivotal to the integrity of so many tissues that an improvement in the understanding of BMP signaling may touch on a broad range of research fields, including tissue modeling or tissue engineering. The more we understand the processes governing our body, the more we may be able to restore them once they go awry.

## 3. Methods

### 3.1. Addressing Questions of Protein-Protein Interaction and Signal Transduction

In basic research, there are various ways to identify, quantify, and qualify the interaction between two or more proteins. The method of choice depends on the question addressed, but generally speaking, much of the value of the generated data lies in the experimental design rather than in the method itself. The conditions chosen to test or the (protein) alterations chosen to implement will determine whether the experimental outcome is able to provide any new information for a given problem.

Analysis methods that allow for the screening or identification of a hitherto unknown interaction partner (or multiple hitherto unknown interaction partners) include for example 2D gel electrophoresis (how many proteins are in the sample, and how do they differ by mass and isoelectric point?), mass spectroscopy (which proteins are in a sample?), microarrays (how do the transcriptomes differ between two conditions?), or promoter analysis (which transcription factors bind to a given promoter?).

If there is one or more candidates identified that need to be tested for their biological function, an *in vitro* or *in vivo* test system becomes necessary. Any experiment will only evaluate the function of the candidates within this test system. Prominent methods include knock-out, knock-down, or other reduced expression studies (is the candidate necessary for a given function?); and knock-in or over-expression studies (is the candidate sufficient for a given function?), as well as point mutation analysis (what amino acids or epitopes within the candidate are necessary for a given function?). Experiments like these need to be respectful of the properties of the test system: For example, a mutation analysis of a ligand may only yield results in a test system that does not endogenously contain the wildtype ligand.

Antibody-based methods including stainings, western blotting, or ELISA indicate whether a

candidate protein is expressed, whether a candidate protein is phosphorylated (or otherwise functionalized), and may also be suited to quantify protein expression. For the purpose of detection or isolation, many proteins are clonally altered to contain a tag.

If the question is whether two proteins directly interact with each other, appropriate methods include surface plasmon resonance SPR (do they bind each other?), an electrophoretic mobility shift assay EMSA (do they form a complex?), co-immunoprecipitation (do they directly interact in a test system?), or Förster resonance energy transfer FRET (in what conditions do they change their relative distance to each other?). Crystallography of single proteins or protein-protein complexes may shed further light on the mechanisms of the interaction in question.

In trying to understand a phenomenon or interaction, or in testing a working hypothesis, multiple methods are usually combined. The identification of a new interaction candidate for a given protein for example may require a multitude of steps: the protein may be overexpressed as a tagged version in a test system with no endogenous expression. After co-immunoprecipitation that utilizes the tag, the generated sample contains a plethora of the tagged protein's interaction partners. 2D gel electrophoresis and mass spectroscopy will then identify many of them, possibly including candidates not yet described. Interaction must then be verified, e.g. by SPR, and the biological relevance of this interaction may be tested by knock-in and knock-down studies in a suitable test system. If all these data comply, a new interaction partner is successfully identified.

### **3.2. Cell Culture Methods**

All cells were cultured at 37 °C and 5 % CO<sub>2</sub>. Their morphology, growth speed and the absence of contaminations were checked on a daily to semi-daily basis. Maintenance culture medium did not contain antibiotics unless otherwise indicated; however, 100 u/ml penicillin G and 100 µg/ml streptomycin were generally added in starving conditions (2 % FCS). FCS was not heat-inactivated. Medium was changed every 2 to 3 days.

ATDC5 cells were cultured in DMEM/Ham's F12 medium containing 5 % FCS and split at a 1:10 or 1:15 ratio. C2C12 cells and HEK strains were cultured in DMEM medium containing 10% FCS, with additional 100 µg/ml sodium pyruvate added for HEK cells. HEK293T were split at a 1:15 or 1:20 ratio, HEK293AD were split at 1:5 to 1:10. C2C12 cells were split according to their proliferation behavior, ranging from 1:4 after thawing or after puromycin incubation to 1:15 or 1:20 in regular maintenance culture. Cell number and vitality were determined by Neubauer counting chamber, adding 50% trypan blue to a cell suspension aliquot before counting.

#### **3.2.1. Transient transfection**

HEK293AD cells were transiently transfected with FGFR2IIIc-C2 and BMPRIA plasmids to overexpress the corresponding proteins for co-localization stainings in 24 well plates on glass platelets. The 0.8 cm<sup>2</sup> per well were each seeded with 3x10<sup>4</sup> cells in 400 µl a day before transfection. Using the JetPrime transfection reagent and following the manufacturer's protocol, 1 µg of DNA was incubated with 2 µL JetPrime reagent in 100 µl JetPrime buffer for 10 minutes before transfecting each well with 40 µl of this DNA transfection mix. The highest protein expression levels were achieved on day 2, as visually determined by number of fluorescent cells in a control sample transfected with pTurboGFP-C.

#### **3.2.2. Lentiviral transduction**

In a first step, virus particles were produced in HEK293T cells in the absence of antibiotics. After seeding 1 - 2x10<sup>5</sup> cells per well in a 6 well plate, cells were transfected using Xtreme Gene9 as a transfection reagent: Constructs carrying the gene of interest on a eukaryotic expression plasmid were combined with second generation lentivirus production plasmids psPAX2 and

pMD2.G in a molar stoichiometry of 1:2:1, with double molar excess of psPAX2. For each well, 2 µg total DNA were incubated with 6 µl Xtreme Gene9 transfection reagent in 200 µl DMEM basal medium for 30 minutes prior to administration. Growth medium was changed to DMEM containing 30 % FCS on day 1, and virus was harvested on day 3.

In a second step, acceptor cells were cultured in a 6 well plate to a density of ~50 % and transduced with 500 µL virus suspension containing 8 µg/ml polybrene per well. After 3 - 4 hours, 1.5 ml of culture medium were added to avoid drying. Transduction was confirmed by quantitative real-time PCR.

#### **3.2.3. Crystal violet assay**

To plot growth curves, the relative cell number was determined by crystal violet staining over the course of several days. Cells were seeded into 96 well plates and cultured for at least 2 hours, and up to 5 days. For every time point and every condition, 6 – 8 wells were measured. At every time point, the corresponding samples were washed with PBS, incubated with 100 µL/well of 0.5 % (w/v) crystal violet in 20 % (v/v) methanol for 20 min at room temperature, washed thrice with water and dried. After all samples were prepared accordingly at their designated time points, the precipitated crystal violet within the dried wells was measured at the same time by reconstituting it in 200 µl/well methanol on a shaker for 15 minutes, transferring all samples for one growth curve onto one plate, and measuring optical density at 570 nm. The optical density of the crystal violet dye represented a relative measure for cell number, so the values measured in samples cultured for 2 hours were set as the starting population of 100 %.

#### **3.2.4. Alkaline phosphatase assay**

To determine alkaline phosphatase (ALP) expression in response to ligand exposure, cells were firstly seeded into 96 well plates at  $10^4$  cells per well on day -1. On day 0, cells were treated as doublets with BMP ligand alone or in combination with other compounds under starving conditions (2 % FCS). As a standard, cells were treated with a maximum concentration of 250 nM BMP2 and up to ten dilution steps thereof, each diluted by factor 2 (i.e. 250 nM, 125 nM, 62.5 nM, etc). At least two wells per plate were incubated under starving conditions without ligand as a baseline activity control.

On day 3, cells were washed with PBS<sup>-</sup> and incubated in 100 µl per well ALP buffer 1 (see 9.2.4.) on a rocking shaker at room temperature for 1 – 2 hours. To determine ALP activity, 100 µl ALP buffer 2 (see 9.2.4.) per well were added and the optical density at 405 nm was measured every 2 – 5 minutes, until the well on the plate with the highest color intensity reached an optical density of 2. This provided the best resolution of signal differences between wells in the linear range of the measurement.

In the case of highly responsive cells such as ATDC5, the pH of both buffers was lowered to 8.8 and/or the ratio of ALP buffer 1:ALP buffer 2 was changed from 1:1 to 1:3, respectively, to slow down the development time of ALP substrate. Optimally, a measurement would take about 20 minutes.

### **3.3. Immunohistochemistry**

The principle of immunohistochemical stainings is the recognition of an antigen by a specific primary antibody and its detection by mediators binding to the primary antibody's Fc region.

#### **3.3.1. Colocalization staining**

HEK293T cells were transfected as described in 3.2.1., and treated with ligand and stained 48 hours after transfection. Ligand treatment was performed under starving conditions (2% FCS) for 1 hour with 20 nM BMP2, or 100 nM GDF5, respectively. For the staining, all incubation steps were performed at 4°C. Hanks' balanced salt solution with 20mM HEPES and 1% bovine serum albumin was used as a washing buffer as well as diluent for the antibodies, and as blocking solution when additionally supplemented with 5% donkey serum. Firstly, cells were washed with PBS<sup>-</sup>, then fixed for 10 minutes with para-formaldehyde, and blocked for 2h. Primary antibody incubated overnight, followed by three washing steps. Secondary antibody incubation for 1h and washing thrice preceded mounting of the glass platelets on glass slides with Mowiol containing DAPI. This staining protocol was based on previously published protocols [107].

Stainings were analyzed using confocal microscopy (Leica TCS SP8) at a 63x magnification.

### 3.4. Molecular Methods

#### 3.4.1. RNA isolation

RNA isolation and purification was performed using the RNeasy Mini Kit (Qiagen). For each sample,  $5 \times 10^5$  to  $10^6$  cells were pelleted and resuspended in 350  $\mu$ l of RLT buffer. These lysates were either stored at  $-80$  °C or directly processed further.

Manufacturer's instructions were followed: lysates were homogenized with QIAshredder spin columns, supplemented with RNase-free 70% ethanol, and applied to the RNeasy column. The optional DNase digestion step was performed to enhance RNA purity. After the required washing steps, RNA was eluted with 30 – 50  $\mu$ L of RNase-free water. RNA was stored at  $-80$  °C. RNA concentration was determined by nanoDrop microvolume quantification.

#### 3.4.2. cDNA synthesis

cDNA synthesis was performed using the iScript cDNA synthesis kit (BioRad) according to the included instructions, starting with 500 ng to 1  $\mu$ g of RNA per sample, leading to an RNA concentration of 25-50 ng/ $\mu$ l. cDNA was not purified from this reaction, and hence its concentration was not determined. It was stored at  $-20$ °C.

#### 3.4.3. Quantitative real-time PCR

Quantitative real-time PCR (qPCR) was performed using the RT<sup>2</sup> SYBR Green PCR Kit, or the SsoFast™ EvaGreen® Supermix, respectively, depending on availability and according to the manufacturers' protocols. Per sample, 1  $\mu$ L cDNA was amplified (see above for concentration considerations). Each condition was measured as duplet.

The qPCR was run as follows:

10'	95 °C	} repeated 40 times
15"	95 °C	
30"	55 °C	
30"	72 °C	
$\infty$	4 °C	

For analysis, the  $\Delta\Delta C_t$  value was determined, and the fold change  $2^{-\Delta\Delta C_t}$  was calculated by dividing the normalized gene expression ( $2^{-\Delta C_t}$ ) of a test sample by the normalized gene



expression of a control sample. Fold change was then transformed into fold regulation; fold changes greater than one being equal to the fold regulation, while fold changes smaller than one were inverted and presented as negative fold regulation values (e.g. fold change 0.5 equals a -2 fold regulation).

<b>Construct</b>	<b>Primer Sequences</b>
FGFR2	Sense: 5' CAC CGA GAA GAT GGA GAA GC 3' Antisense: 5' GTC TGA CGG GAC CAC ACT TT 3'
HPRT	Sense: 5' GGC AGC GTT TCT GAG CCA TT 3' Antisense: 5' TGG CCT CCC ATC TCC TTC AT 3'
GAPDH	Sense: 5' GGA GAG TGT TTC CTC GTC CC 3' Antisense: 5' ATG AAG GGG TCG TTG ATG GC 3'

*Table 1: PCR-Primers*

### 3.5. Cloning

To introduce a gene of interest into a cell, plasmids containing these genes were generated by standard cloning techniques. Principally, the gene of interest was amplified by PCR either as linear insert or within a transitory plasmid. Both the PCR product and a target plasmid backbone were digested at matching digestion sites, and the insert containing the gene of interest was ligated into the backbone plasmid. Clones were selected based on the antibiotic resistance coded on the plasmid backbone, and verified by sequencing. For any application in eukaryotic cells, especially if the gene was introduced lentivirally, the plasmid pCDH-CMV-MCS-EF1-Puro (henceforth referred to as CD510B) was used as a backbone. As a transitory plasmid, pBlue Script II SK (+) (referred to as pBlue) was utilized.

All (intermediary) products of the cloning process were stored at -20 °C.

#### 3.5.1. Primer Design

Primers were designed to meet the following requirements: The annealing temperature  $T_a$  was calculated to be 60°C with  $T_a = 4^\circ \times (G+C) + 2^\circ \times (A+T)$ . The final annealing 3' base was chosen to be either a C or G. The GC content was preferentially set at > 40%. Thusly created primers were then only used if they yielded no matches over 80 % with non-target sequences when entered

into the basic local alignment search tool (BLAST) of the National Center for Biotechnology Information (NCBI); accessible at <https://blast.ncbi.nlm.nih.gov/>.

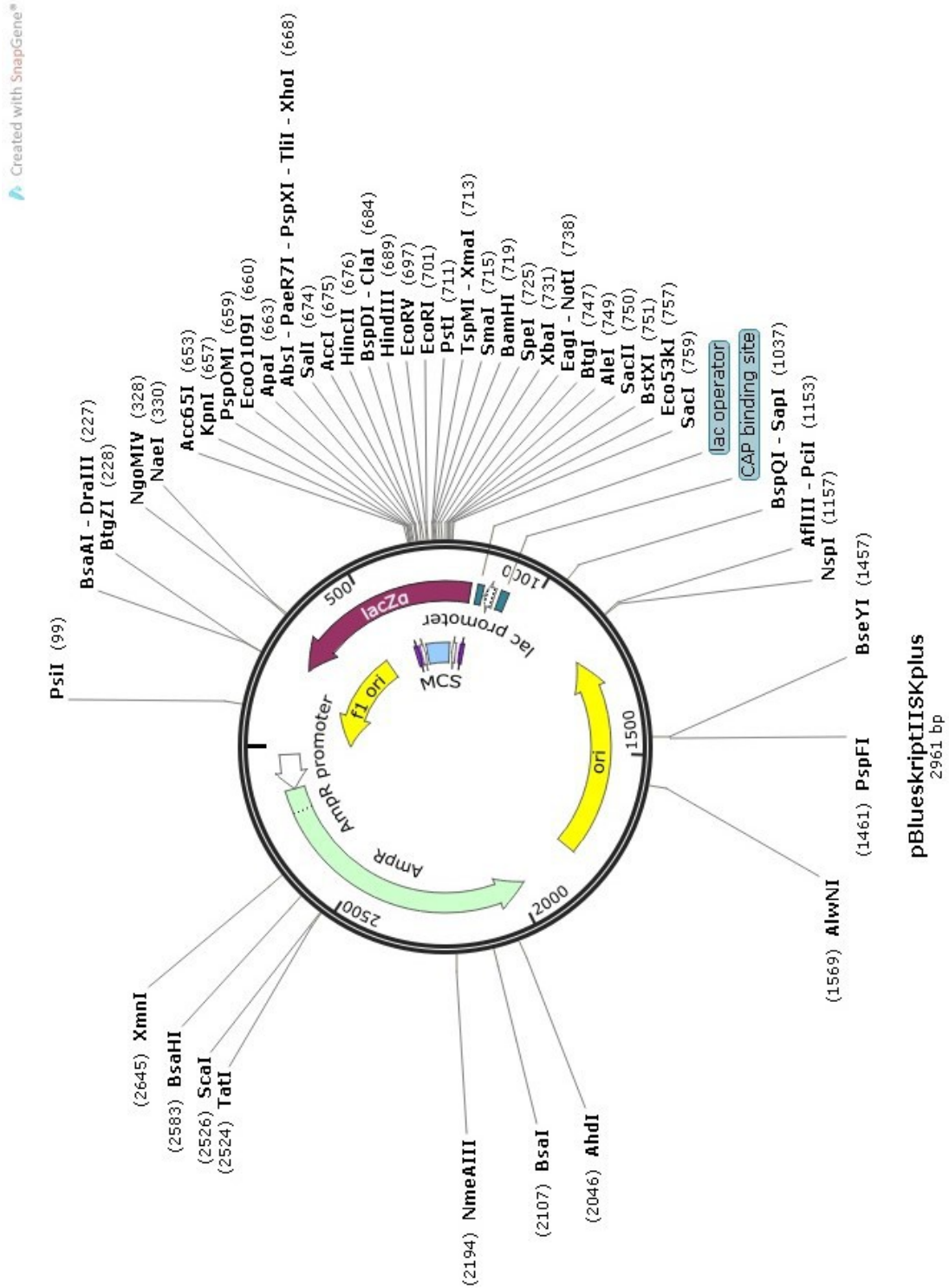


**Figure 4: pBlue Script II SK (+)**

pBlue Script II SK (+) was used as a transitory backbone plasmid. It expresses solely in bacteria and is selectable by its ampicillin resistance.

To introduce restriction sites, primers were elongated by non-annealing bases that contained the respective restriction sequence as well as a few spacer bases. These spacer regions were added to facilitate easier binding of the restriction enzymes to the end of the PCR product.

To introduce point mutations, primers were designed to fully anneal with calculated 60°C on both sides of the wobble bases representing the mutation(s). Point mutations were introduced via both sense and antisense primers, and the construct was amplified in the transitory plasmid pBlue as a circular PCR product.

Construct	Primer Sequences
XbaI_FGFR2_NotI	Sense: 5' CCA GGA T'CT AGA CAG GTA GCC CAT GGT CTC AG 3' Antisense: 5' CCA GGA GC'G GCC GCC AGG AAG ACA CAT TCA CTC ATG 3'
FGFR2 <sup>KD</sup>	Sense: 5' CAG GGA TAT CAA CAA CAT AGA CTT CTT TAA AAA GAC CAC AAA TGG GCG 3' Antisense: 5' CGC CCA TTT GTG GTC TTT TTA AAG AAG TCT ATG TTG ATA TCC CTG 3'

Primer sequences contained **restriction sites** and annealing bases. The sequence „CCA GGA“ served as a spacer region. Inserted mutations are marked yellow.

Table 2: Cloning Primers

### 3.5.2. Generation of the DNA insert by PCR

The insert DNA sequence, containing the gene of interest flanked by specific digestion sites, was generated by PCR with a high fidelity polymerase. For this work, either KAPA high fidelity polymerase (Biosystems) or Q5 hot start high fidelity polymerase (New England Biolab) were used in dependence of availability in the laboratory, and in accordance with the respective manufacturer's protocol. Usually, two PCR reactions of 50 µl containing 50 ng template DNA each were pooled into one sample after amplification. PCR products were then precipitated by adding 10% 3M NaAc (pH 5 ± 0.2), then adding 100 % pure ethanol, and pelleting the precipitating DNA >20,000 xg for 15 minutes in a table-top centrifuge. The pellet was washed once with 70 % ethanol, re-pelleted, air dried, and resuspended in ultrapure H<sub>2</sub>O. The DNA concentration was measured by nanoDrop microvolume quantification.

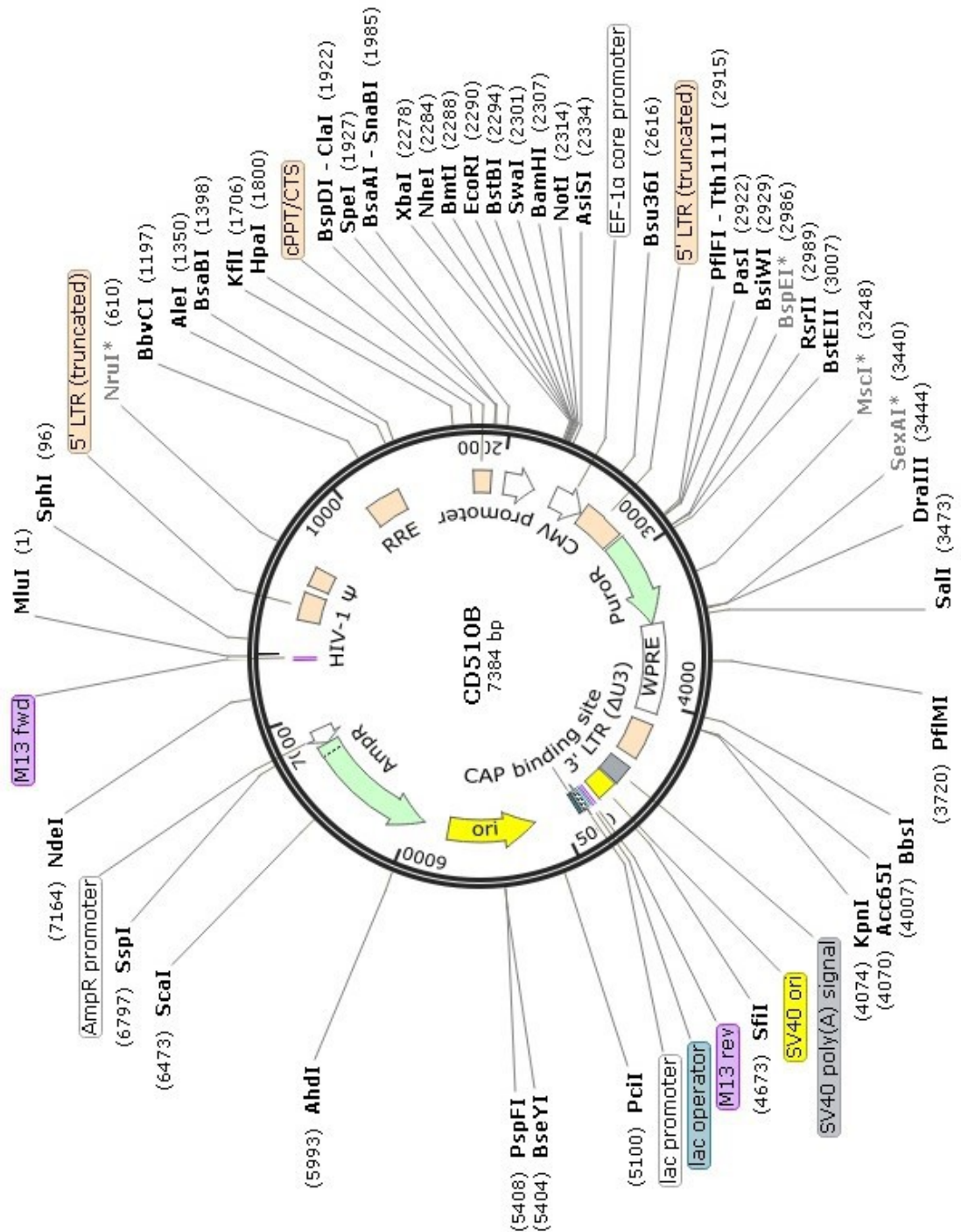


**Figure 5: pCDH-CMV-MCS-EF1-Puro**

pCDH-CMV-MCS-EF1-Puro was used as backbone for transient transfection and lentiviral transduction of eukaryotic cells with a gene of interest. It carries an ampicillin resistance gene for the selection in bacteria and a puromycin resistance gene under a CMV promoter for the selection in eukaryotic cells.

#### 3.5.3. DNA digestion

Plasmids and PCR products were digested using Fast Digest restriction enzymes and buffers (Thermo Fisher). In accordance with the manufacturer's protocols, 1-3 µg of PCR product were digested in a total reaction volume of 40 µl, and 3-5 µg of plasmid were digested in a total reaction volume of 50 µl; both including 10 % (v/v) 10x FD reaction buffer and FD restriction enzyme(s) (units not specified by the manufacturer). The added volumes of the applied FD restriction enzymes did not exceed 10% (v/v) or the total reaction volume. The digestion was incubated at 37°C for at least 1 hour. For the cloning projects in this work, the restriction enzymes XbaI and NotI were used in a 1:1 ratio for PCR products and 1:3 ratio for plasmids.

#### 3.5.4. Gel extraction of DNA plasmids

After digestion, the desired DNA fragments were separated from other digestion products by electrophoresis in a 0.5 % agarose gel, and the respective bands were cut out. Extraction and purification were performed using either the Wizard® SV gel and PCR clean-up system (Promega), or the Zymoclean™ gel recovery kit (Zymo Research), depending on availability in the laboratory, and according to manufacturer's protocols. The DNA was resuspended in ultrapure water and measured by nanoDrop microvolume quantification.

#### 3.5.5. DNA ligation

The digested insert DNA sequence was ligated into the digested plasmid backbone using quick ligase (New England Biolab). 50 ng of backbone DNA were combined with a three-fold molar excess of insert DNA, 10 µl quick ligase buffer, and 1 µl of enzyme in a total volume of 20 µl, according to manufacturer's protocol. The ligation reaction was allowed to proceed for at least 15 min at room temperature. If ligations failed under these conditions, the ligation reaction was repeated for 1 – 2 hours at room temperature or overnight at 4 °C.

To minimize re-ligation, the plasmid backbone DNA was de-phosphorylated by antarctic phosphatase (New England Biolab) according to the manufacturer's protocol and prior to gel extraction. Nonetheless, a re-ligation control without insert DNA was always included at this step.

#### **3.5.6. Bacterial transformation**

For the amplification of plasmids and cloning products, E.coli bacteria were transformed by heat-shock. Simple plasmid amplification was performed in the NovaBlue strain (Novagen), whereas cloning products in eukaryotic plasmid backbones were transformed into the strain C3040 (New England Biolab), which are high efficiency competent bacteria suitable for lentiviral clones and unstable inserts.

After thawing bacteria on ice, 100 ng – 1 µg of DNA was added and the cells were incubated for 30 min on ice. The heat-shock was performed for 30 – 40 seconds at 42 °C. Following 5 minutes resting time on ice, 500 – 1000 µl of antibiotic-free LB medium were added to the bacteria, and they were allowed to grow at 37 °C, shaking at a maximum of 300 rpm, for at least 30 minutes, and up to 3 hours for low-efficiency cloning products. At least 20% of the bacteria suspension (amplification in Novablue) and at most 100 % of it (cloning products in C3040) were plated on antibiotic-containing agar plates, and incubated over night at 37 °C. All clones of cloning products were screened in a control digest before sequencing, confirming the insertion of the gene of interest. Inserts of positive clones were sequenced in their entirety to confirm the desired insert sequence and to exclude the possibility of point mutation insertions during the cloning process.

#### **3.5.7. Plasmid preparation**

Plasmids were amplified and prepared from over-night bacterial culture in LB medium containing the respective antibiotic (here: 100 µg / mL ampicillin). Given that all plasmids used in this work were so-called high copy plasmids, a small-scale plasmid preparation (miniprep) for first analysis was done from 2 mL of bacterial culture, whereas large-scale preparations (maxiprep) for experimental approaches were done from 100 mL of bacterial culture. DNA extraction and purification from the bacteria were performed using plasmid mini and maxi Kits (Qiagen), or the Zyppy™ plasmid miniprep kit (Zymo Research), respectively, and according to the manufacturer's protocols.

## **3.6. Biochemical Methods**

### **3.6.1. Protein isolation**

For protein analysis, cells were lysed in 6 well plates at a cell confluency of 70 – 90 %. Optionally, cells were treated with the indicated agents for the indicated time, before being washed with cold PBS; lysed by adding 200 – 400  $\mu$ l of lysis buffer, and incubating the plate at 4 °C for 30 minutes on a rocking platform. Working on ice, each well was then thoroughly scraped with a cell scraper, the lysate was transferred to a reaction tube and centrifuged at 10,000  $xg$  for 15 minutes to pellet cell remnants. The supernatant constituted the protein lysate and was stored at -80 °C.

### **3.6.2. Determination of total protein concentration**

Total protein concentrations of cell lysates were measured using the DC Protein Assay (Biorad), a Lowry-based quantification method [108]. Standardized samples ranging from 50 to 1000  $\mu$ g /ml bovine serum albumin (BSA), diluted in ultrapure water, were included in every measurement. Lysis buffer served as blank for the samples, and ultrapure water for the BSA standard. The assay was performed according to the manufacturer's protocol, optical density was measured at 750 nm, and protein concentrations were calculated with the values derived from the BSA standard curve samples.

### **3.6.3. Western blotting**

Proteins were separated by electrophoresis under reducing conditions by SDS-PAGE. The separation gel contained 10 % of acrylamide solution (Roth), stacking gel contained 5 %. Lysates were reduced by adding 20 % Laemmli buffer and denatured at 95 °C for 5 – 10 minutes. Usually, 10 – 20  $\mu$ g protein were loaded per sample. Gels were run in running buffer at 25 mA /gel for 50 – 60 minutes. Gels were blotted semi-dry onto a nitrocellulose membrane for 90 minutes at 1 mA /cm<sup>2</sup>.

After blotting, membranes were blocked in TBST (see 9.2.4.), 5 % (w/v) milk for at least one hour and incubated in 5 ml antibody solution over night at 4 °C. Membranes were then washed thrice with TBST for 10 minutes and incubated in 5 mL of secondary antibody solution for 1 hour at room temperature. All antibodies were diluted in TBST, 5 % (w/v) BSA. Membranes were again

washed thrice and developed in 1 ml of a 1:1 mixture of detection reagents 1 and 2 of the Pierce ECL Western Blotting kit (Thermo Fisher) for up to a minute. These contain the substrate Luminol for the secondary antibody-conjugated horse raddish peroxidase (HRP), which is converted into a chemiluminescent product, 3-aminophthalate. Chemiluminescence was visualized using the imaging station FluorChem with an exposure time of maximally 5 minutes.

#### **3.7. Statistical Analysis**

Statistical analysis was performed on the data of a subset of ALP assays as well as on the co-localization staining data and on qPCR results. In general, p-values < 0.05 were considered significant. If more than one group was tested against the same control, p-values were Bonferroni-adjusted to 0.05 divided by the number of these groups. The number of biological repetitions (n) as well as the calculated p-value are specified in the respective figure descriptions.

For the ALP assays, if quantification and significance testing was required, individual experiments had to be normalized to an internal standard in order to become comparable to one another. Mock control cells were included on every plate measured. Their calculated maximal response to each ligand was set as a response of 100 %, and the calculated maxima of the other samples were depicted as percentage of ligand performance on mock control cells. Statistical significance was determined by testing sample values against mock values of each ligand using the Mann-Whitney U (MWU) test.

For the quantification and significance testing of the co-localization stainings, the index of correlation ( $I_{corr}$ ) was determined for at least 8 cells per condition per experiment, at a 63x magnification, using image J. The experiment was repeated three times. Statistical significance was tested with the MWU test.

To test whether expression levels determined by qPCR altered significantly from one another, relative expression levels (normalized on two housekeeping genes HPRT and GAPDH) were tested against each other using the MWU test. Each condition was measured in duplet, and the number of experimental repetitions (n) is specified in the figure legend.



## 4. Results

### 4.1. Testing the Tenability of FGFR2 as Co-Receptor Candidate

The observation that ALP responsiveness differs between ATDC5 and C2C12 cells, despite them having the same BMP receptor expression profiles, led to the microarray-based search for a putative, hitherto unknown signaling component [2](for details, see 1.4.2). Such a component must be differentially expressed in both cell lines to account for the divergency in responsiveness. It was further hypothesized that it must be membrane-bound to mediate divergent signal transduction of the two ligands on C2C12 cells, as a downstream component only recognizing BMPRIA activation would be unlikely able to distinguish GDF5 and BMP2 on the same cell; so most likely a co-receptor. Finally, a component able to allow or subdue signal transduction of BMP2 and/or GDF5 is likely to already be biologically linked to these factors *in vivo*, for example by being co-expressed in the same cellular context and/or causing syndromes/phenotypes in the same tissues. Among the 100 most differentially expressed genes of membrane-associated proteins (see table at 9.1.1.), one candidate that fulfilled all criteria was *Fgfr2*.

In this first part of this thesis, it was investigated whether FGFR2 held the basic properties required for the hypothesized new co-receptor: direct interaction with at least one BMP ligand, and a modulating effect on BMP2/GDF5 signal transduction.

#### 4.1.1. FGFR2IIIc extracellular domain binds BMP ligands GDF5 and BMP2 *in vitro*

Surface plasmon resonance (SPR) measurements can be used to both determine and quantify protein-protein interactions. The laboratory of Prof. Dr. Thomas Müller expressed the extracellular domain of FGFR2 splice variant IIIc isoform  $\alpha$  (FGFR2IIIc<sub>ECD</sub>) in eukaryotic cells and implemented it as analyte in SPR. They then continued to test whether it bound to immobilized BMP2, or GDF5, respectively.

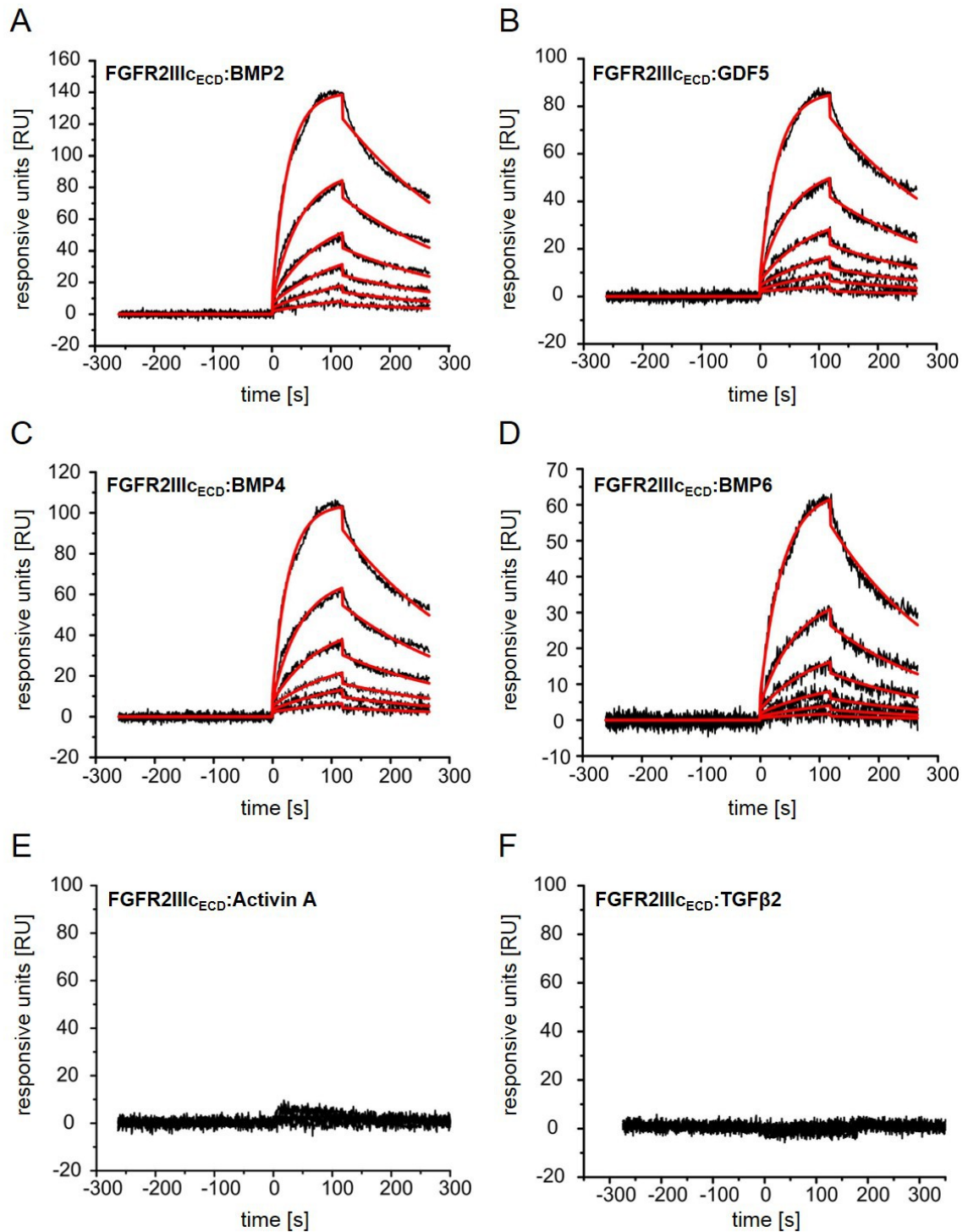


**Figure 6: BMP2 and GDF5 Bind to FGFR2IIIc<sub>ECD</sub>**

In SPR, the extracellular domain of FGFR2 variant IIIc, isoform  $\alpha$  (FGFR2IIIc<sub>ECD</sub>) was tested against immobilized BMP ligand at the concentrations 100 nM, 50 nM, 25 nM, 12.5 nM, 6.25 nM, or 3.125 nM, respectively. FGFR2IIIc<sub>ECD</sub> binds (A) BMP2 ( $K_D = 9.5 \pm 1.8$  nM,  $k_{on} = 3.5 \pm 0.5 \times 10^5$  M<sup>-1</sup>s<sup>-1</sup>,  $k_{off} = 3.3 \pm 0.5 \times 10^{-3}$  s<sup>-1</sup>), (B) GDF5 ( $K_D = 11.0 \pm 2.9$  nM,  $k_{on} = 3.2 \pm 0.8 \times 10^5$  M<sup>-1</sup>s<sup>-1</sup>,  $k_{off} = 3.5 \pm 0.6 \times 10^{-3}$  s<sup>-1</sup>), (C) BMP4 ( $K_D = 10.3 \pm 2.4$  nM,  $k_{on} = 3.5 \pm 0.7 \times 10^5$  M<sup>-1</sup>s<sup>-1</sup>,  $k_{off} = 3.6 \pm 0.6 \times 10^{-3}$  s<sup>-1</sup>), and (D) BMP6 ( $K_D = 17.6 \pm 5.2$  nM,  $k_{on} = 2.3 \pm 0.6 \times 10^5$  M<sup>-1</sup>s<sup>-1</sup>,  $k_{off} = 4.0 \pm 0.8 \times 10^{-3}$  s<sup>-1</sup>), but not (E) Activin A or (F) TGFβ2.

SPR measurements and FGFR2IIIc<sub>ECD</sub> protein were kindly provided by Prof. Dr. Thomas Müller of the Julius-von-Sachs-Institute of Biosciences at the University of Würzburg, Germany.

These graphs are included in [2].

SPR spectroscopy at the Müller laboratory established a direct interaction between BMP ligands and FGFR2IIIc<sub>ECD</sub>: FGFR2IIIc<sub>ECD</sub> bound BMP2 with a  $K_D$  of  $9.5 \pm 1.8$  nM, and GDF5 with a  $K_D$  of  $11.0 \pm 2.9$  nM (Figure 6A,B). This constitutes a very similar and relatively high level of affinity, as the values range lower than the ligands' published affinities to BMP type I receptors in comparable measurements:  $K_D$ [BMPRIA<sub>ECD</sub>:BMP2] =  $48.0 \pm 19.6$  nM,  $K_D$ [BMPRIB<sub>ECD</sub>:BMP2] =  $350.0 \pm 146.0$  nM,  $K_D$ [BMPRIA<sub>ECD</sub>:GDF5] =  $3300.0 \pm 1439.0$  nM, and  $K_D$ [BMPRIB<sub>ECD</sub>:GDF5] =  $300.0 \pm 123.0$  nM [105]. Additionally, they measured BMP4 and BMP6, which turned out to interact in the same nanomolar range of affinity as BMP2 and GDF5 ( $K_D$ [FGFR2IIIc<sub>ECD</sub>:BMP4] =  $10.3 \pm 2.4$  nM,  $K_D$ [FGFR2IIIc<sub>ECD</sub>:BMP6] =  $17.6 \pm 5.2$  nM)(Figure 6C,D); and they tested Activin A and TGF $\beta$ 2, which were not bound by FGFR2IIIc<sub>ECD</sub> (Figure 6E,F).

If an interaction partner that directly binds to BMP ligands is added to a cell culture setup as a soluble agent, it is likely able to inhibit the ligand's biological activity. Conceivably, it does so because its direct binding is (sterically) blocking the ligand's recruitment to cell membrane-bound receptors. This is known for soluble BMP inhibitors such as Noggin [19, 109], and it has also been shown for the extracellular domains of BMP receptors (personal communication, see also 4.3.1), as well as the soluble forms of co-receptors like RGMs [101].

Soluble FGFR2IIIc<sub>ECD</sub> was added to either ATDC5 or C2C12 cells in increasing concentrations, and cells were simultaneously treated with a constant amount of ligand: Both cell lines were treated with BMP2, and ATDC5 cells were also treated with GDF5. C2C12 cells are non-responsive to GDF5; hence, competition experiments with GDF5 on C2C12 were not performed.

After three days, the activity of alkaline phosphatase (ALP), a downstream target of BMP signaling and often-used indicator for the biological activity of BMPs, was measured by quantifying the colored product of its substrate pNPP. Basal levels of ALP activity ("baseline activity") in both cell lines were determined in samples not treated with either BMP2/GDF5 nor FGFR2IIIc<sub>ECD</sub>. Figure 7 shows that FGFR2IIIc<sub>ECD</sub> was able to inhibit BMP2 signaling in both cell lines, as well as GDF5 signaling in ATDC5.  $IC_{50}$  values varied considerably. On average, the  $IC_{50}$  of FGFR2IIIc<sub>ECD</sub> versus BMP2 in ATDC5 was  $51$  nM  $\pm$   $34$  nM;  $26$  nM  $\pm$   $20$  nM versus GDF5 in ATDC5; and  $232$  nM  $\pm$   $124$  nM versus BMP2 in C2C12 ( $n = 6$ ). By  $1$   $\mu$ M of FGFR2IIIc<sub>ECD</sub>, ALP expression was almost at basal levels in all conditions.

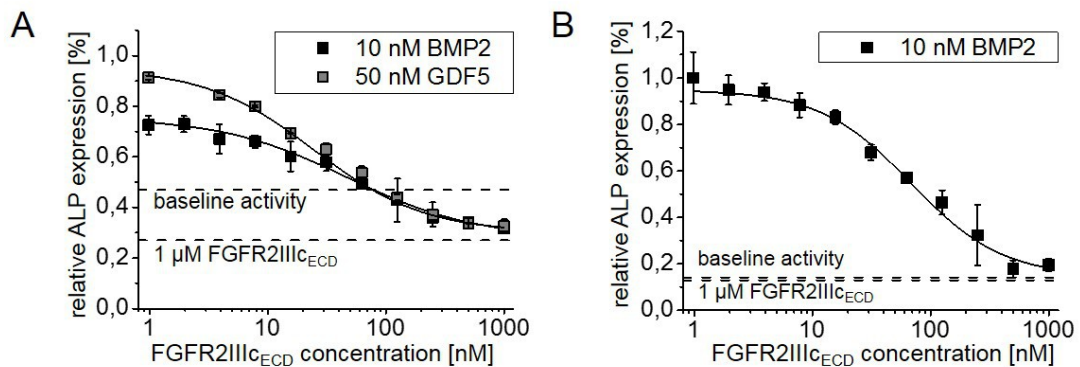


**Figure 7: FGFR2IIIc<sub>ECD</sub> blocks BMP2- and GDF5-induced ALP Expression**

FGFR2IIIc<sub>ECD</sub> was added at increasing concentrations to (A) ATDC5 or (B) C2C12 cells induced with a steady concentration of the BMP ligand indicated, and ALP induction was measured after 3 days. Basal levels of ALP expression were determined in either cell line without ligand or ectodomain stimulation, and depicted as a dotted line („baseline activity“). Administration of 1  $\mu$ M FGFR2IIIc<sub>ECD</sub> without ligand as a control is likewise depicted as a dotted line.

FGFR2IIIc<sub>ECD</sub> protein was kindly provided by Prof. Dr. Thomas Müller of the Julius-von-Sachs-Institute of Biosciences at the University of Würzburg, Germany.

These graphs are included in [2].

#### 4.1.2. FGFR2 shRNA specifically inhibits GDF5-induced ALP expression in ATDC5 cells

After establishing that FGFR2IIIc can bind to both BMP2 and GDF5, it was addressed whether its absence or presence on the cells influenced the signaling outcome for one or both of these ligands. ATDC5 cells express roughly 9 times as much *Fgfr2* RNA as C2C12 (see 9.1.1.), so for ATDC5 cells, *Fgfr2* expression was down-regulated with shRNA. Stable changes to the transcriptome were achieved by lentiviral transduction. Plasmids containing *Fgfr2*-specific shRNA or scrambled shRNA as mock control were packaged into lentiviral vectors in HEK293T cells, and ATDC5 cells were transduced with these viruses. After antibiotic selection, the expression of *Fgfr2* in shRNA containing cells was reduced to about 50 % of the expression in mock control cells (Figure 8B). Cell growth was not influenced by the transduction or by the expression of *Fgfr2* shRNA (Figure 8C).

ATDC5 with reduced *Fgfr2* expression (ATDC5<sub>shRNA</sub>) showed lower ability to express ALP in response to GDF5, but the same ability in response to BMP2, as mock control cells (ATDC5<sub>mock</sub>) (Figure 8A). On average, the relative maximal ALP activity (i.e., the value of the reached plateau

at high concentrations) in ATDC5<sub>shRNA</sub> as compared to ATDC5<sub>mock</sub> was at 101.0% ± 8.0 % in response to BMP2, and at 73.0 % ± 25.0 % in response to GDF5. Only the GDF5 response differed significantly between ATDC5<sub>mock</sub> and ATDC5<sub>shRNA</sub> (Mann-Whitney U: n = 11, p[BMP2] = 0.149, p[GDF5] < 0.001).

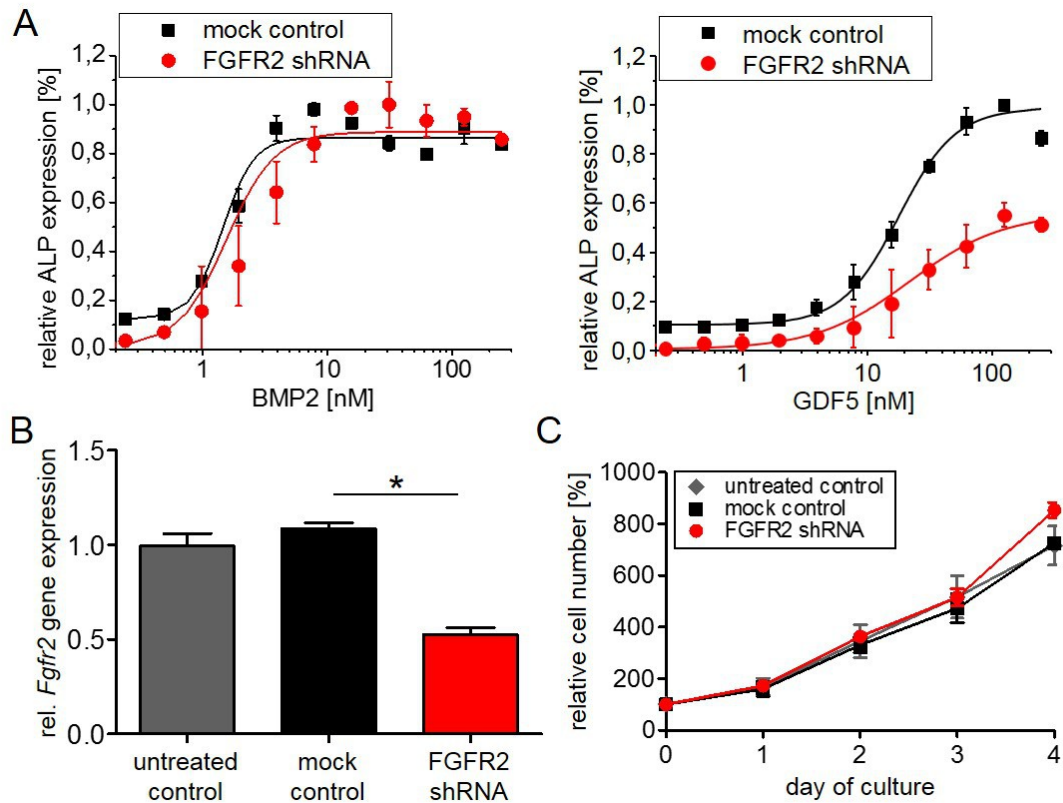


**Figure 8: *Fgfr2* Down-Regulation Specifically Reduces GDF5-induced ALP Expression**

*Fgfr2* gene expression in ATDC5 cells was down-regulated by the lentiviral introduction of *Fgfr2*-specific shRNA. (A) ALP induction by BMP2 or GDF5, respectively, in ATDC5 cells treated with either *Fgfr2* shRNA or scrambled shRNA as mock control. (B) Quantitative real-time PCR confirmed the down-regulation of *Fgfr2* mRNA by about 50 % as compared to mock control cells. *Fgfr2* expression was normalized on HPRT and GAPDH expression levels. Differences in *Fgfr2* expression in *Fgfr2* shRNA-expressing cells versus mock control cells was significant (Mann-Whitney-U: n = 12, p < 0.001). (C) Growth curves obtained by crystal violet staining determined ATDC5 cell growth in dependence of *Fgfr2* gene expression. Changes after four days tested insignificant between mock control cells and *Fgfr2* shRNA-expressing cells (Mann-Whitney-U: n = 3, p = 0.19).

These graphs are included in [2].

This significant alteration in relative maximal ALP expression was accompanied by a significant change in the EC<sub>50</sub> values. The average of EC<sub>50</sub> values increased in response to GDF5 from 29.2 ±

6.9 nM in ATDC5<sub>mock</sub> to  $37.5 \pm 5.7$  nM in ATDC5<sub>shRNA</sub> (Mann-Whitney U:  $n = 8$ ,  $p = 0.018$ ), while they did not change significantly in response to BMP2 (ATDC5<sub>mock</sub>:  $2.4 \text{ nM} \pm 0.8 \text{ nM}$ , ATDC5<sub>shRNA</sub>:  $3.2 \text{ nM} \pm 0.8 \text{ nM}$ ; Mann-Whitney U:  $n = 8$ ,  $p = 0.052$ ).

#### 4.1.3. *Fgfr2IIIc* cDNA boosts BMP ligand-induced ALP expression in C2C12 cells

*Fgfr2*-targeting shRNA in ATDC5 cells indicated a GDF5-specific role for FGFR2 in BMP ligand signal transduction, despite the fact that in SPR, FGFR2IIIc<sub>ECD</sub> bound other BMP ligands as well. If the biological significance of FGFR2/BMP binding was indeed GDF5-specific, it could be suspected that the introduction of *Fgfr2* cDNA into C2C12 cells would likewise only affect GDF5 signaling, and facilitate C2C12-responsiveness to GDF5.

The shRNA introduced into ATDC5 cells binds the kinase domain-coding sequence of *Fgfr2*, so it targets all of ATDC5's splice variants at once [2]. For C2C12, only one splice variant could be lentivirally introduced at a time. In terms of supporting GDF5 signaling, it was feasible to consider only those variant(s) that ATDC5 cells expressed. Barnard et. al. described four splice variants of *Fgfr2* in ATDC5 cells, all variants of the mesenchymal FGFR2IIIc, that differed in length and/or their C-terminal bases [110]. SPR measurements were performed with the ectodomain of FGFR2IIIc isoform  $\alpha$  (FGFR2 $\alpha$ IIIc), the longest extracellular isoform of FGFR2IIIc.

In house, Fabian Prenzlau cloned four variants from the ATDC5 transcriptome, as detailed in his term paper „Die Rolle des FGFR-2 in der chondrogenen Differenzierung“ (*trans. The role of FGFR2 in chondrogenic differentiation*)[111]. These four variants could be identified as FGFR2 $\alpha$ IIIc with either a C1- or a C2-terminus, as well as FGFR2 $\beta$ IIIc with either a C1- or a C2-terminus (for reference, see 1.2.3). These were overlapping but not identical to the variants found by Barnard et al<sup>b</sup>. It was decided to proceed with the splice variants found in house.

Unfortunately, subcloning the *Fgfr2* cDNAs from Fabian Prenzlau's transitory vector constructs to a eukaryotic vector for lentivirus production only successfully yielded clones for FGFR2 $\alpha$ IIIc-C2 and FGFR2 $\beta$ IIIc-C1, although the latter obtained a non-conservative point mutation in the heparin-binding site (E93D). FGFR2 $\beta$ IIIc-C1-E93D was not used in this study because of this mutation, as well as because it would not have been in accordance with the SPR measurements.

b.) The splice variants found by Fabian Prenzlau were Barnard et al.'s FGFR2(i) ( $\Delta$  FGFR2 $\alpha$ IIIc-C1), FGFR2(ii) ( $\Delta$  FGFR2 $\beta$ IIIc-C1), FGFR2(iv) ( $\Delta$  FGFR2 $\alpha$ IIIc-C2), and a variant with the extracellular domain of FGFR2(ii) combined with the intracellular domain of FGFR2(iv) ( $\Delta$  FGFR2 $\beta$ IIIc-C2). He did not find Barnard et al.'s FGFR2(iii), a FGFR2IIIc-C1 isoform missing both Ig1 and the acidic box (as specified in Barnard et al., Figure 2C) [110].

Instead, we proceeded the experiments using FGFR2 $\alpha$ IIIc-C2, hitherto referred to simply as *Fgfr2IIIc* or FGFR2IIIc, respectively.

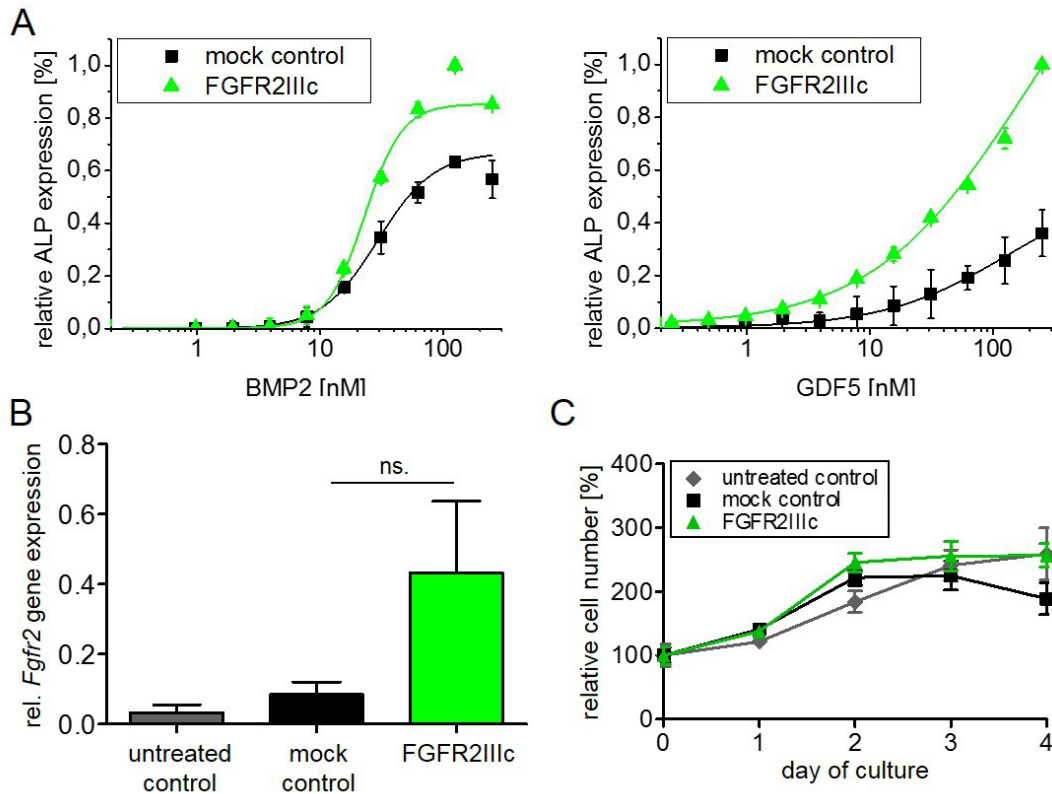


**Figure 9: Elevated FGFR2IIIc Expression Increases C2C12 Responsiveness to BMP2 and GDF5.**

*Fgfr2IIIc* cDNA was lentivirally introduced into C2C12 cells. (A) ALP induction by BMP2 or GDF5, respectively, in C2C12 cells transduced with either *Fgfr2IIIc*-carrying virus, or virus carrying an empty vector as mock control. (B) Quantitative real-time PCR confirmed the up-regulation of *Fgfr2* mRNA as compared to mock control cells by about five-fold. *Fgfr2* expression was normalized on *Hprt* and *Gapdh* expression levels. Differences in *Fgfr2* expression of *Fgfr2IIIc*-expressing cells versus mock cells was not significant (Mann-Whitney-U:  $n = 6$ ,  $p = 0.09$ ). (C) Growth curves obtained by crystal violet staining determined C2C12 cell growth in dependence of *Fgfr2IIIc* gene expression. There was no significant difference between the cell number of mock control cells as compared to *Fgfr2IIIc*-expressing cells on day four (Mann-Whitney-U:  $n = 4$ ,  $p = 0.88$ ).

These graphs are included in [2].

Virus was produced with *Fgfr2IIIc*-containing and empty vector CD510B as mock control. C2C12 cells containing FGFR2IIIc (C2C12<sub>FGFR2IIIc</sub>) exhibited a five-fold increase in *Fgfr2* expression on average, as compared to mock control cells (C2C12<sub>mock</sub>) and when normalized on the expression of housekeeping genes *Hprt* and *Gapdh* (Figure 9B). This tested non-significant in Mann-

Whitney-U (relative expression [mock control] =  $0.085 \pm 0.089$ ; relative expression [*Fgfr2*] =  $0.432 \pm 0.502$ ; Mann-Whitney-U:  $n = 6$ ;  $p = 0.09$ ). If, instead of relative to *Hprt* and *Gapdh*, the expression of *Fgfr2* in C2C12<sub>FGFR2IIIc</sub> is depicted relative to *Fgfr2* expression in non-transduced C2C12 (“untreated control”), relative *Fgfr2* expression levels are at  $210.8 \% \pm 103.2 \%$  in C2C12<sub>mock</sub>, and  $934.4 \% \pm 544.8 \%$  in C2C12<sub>FGFR2IIIc</sub>. The reduced standard deviations due to this normalization step lead to a significant statistical test on these numbers (Mann-Whitney U:  $n = 6$ ,  $p = 0.01$ ). This indicates that the lack of statistical significance of the observed difference in *Fgfr2* expression may have less relevance than the consideration that a five-fold change in mRNA expression usually indicates a robust biological difference.

The virus transduction procedure as well as the increased expression of *Fgfr2IIIc* did not lead to an evident or statistically significant change in cell growth behavior (Figure 9C).

Upon ALP induction with either BMP2 or GDF5, C2C12<sub>FGFR2IIIc</sub> showed improved ALP activity with both ligands (Figure 9A). This effect varied notably between repetitions, so it was performed at least 11 times. On average, BMP2-induced C2C12<sub>FGFR2IIIc</sub> showed a relative maximal ALP activity of  $122.0 \% \pm 32.7 \%$ , as compared to C2C12<sub>mock</sub>, and GDF5-induced C2C12<sub>FGFR2IIIc</sub> showed a relative maximal ALP activity of  $174.0 \% \pm 106.6 \%$  as compared to C2C12<sub>mock</sub>. Average EC<sub>50</sub> values generally decreased in C2C12<sub>FGFR2IIIc</sub>, and shifted from  $26.0 \pm 12.8$  nM in response to BMP2 in C2C12<sub>mock</sub> to  $22.8 \pm 12.2$  nM in C2C12<sub>FGFR2IIIc</sub>, as well as from  $75.4 \pm 21.8$  nM upon GDF5 administration in C2C12<sub>mock</sub> (whenever determinable) to  $66.6 \pm 21.5$  nM in C2C12<sub>FGFR2IIIc</sub>. Quantitatively, none of these changes were significant (Mann-Whitney U [ALP], BMP2:  $n = 13$ ,  $p = 0.079$ ; GDF5:  $n = 11$ ,  $p = 0.262$ . Mann-Whitney U [EC<sub>50</sub>], BMP2:  $n = 15$ ,  $p = 0.709$ ; GDF5:  $n = 4$ ,  $p = 0.470$ ). Qualitatively, however, the switch of C2C12 cells from GDF5 non-responsive to responsive constitutes a biologically relevant event.

The transduction of C2C12 cells with either the mock vector or the *Fgfr2IIIc*-containing vector was performed six independent times. Given that both the qPCR and the ALP data on C2C12<sub>FGFR2IIIc</sub> vs. C2C12<sub>mock</sub> were so heterogeneous that no statistical significance could be reached, it was questioned whether one or more of these six independent transductions were unsuccessful. Hence, it was tested whether low *Fgfr2* expression changes correlated with low changes in ALP induction, constituting a failed transduction and possibly justifying the exclusion of the corresponding data. Surprisingly, the observed correlation was inverse: cells with higher



transduction efficiencies, as measured by elevated *Fgfr2* RNA expression, showed lower changes in GDF5-induced ALP induction, whereas cells with very low *Fgfr2* RNA expression changes showed high changes in GDF5-induced ALP induction (Figure 10). Consequently, no data was excluded from the analysis.

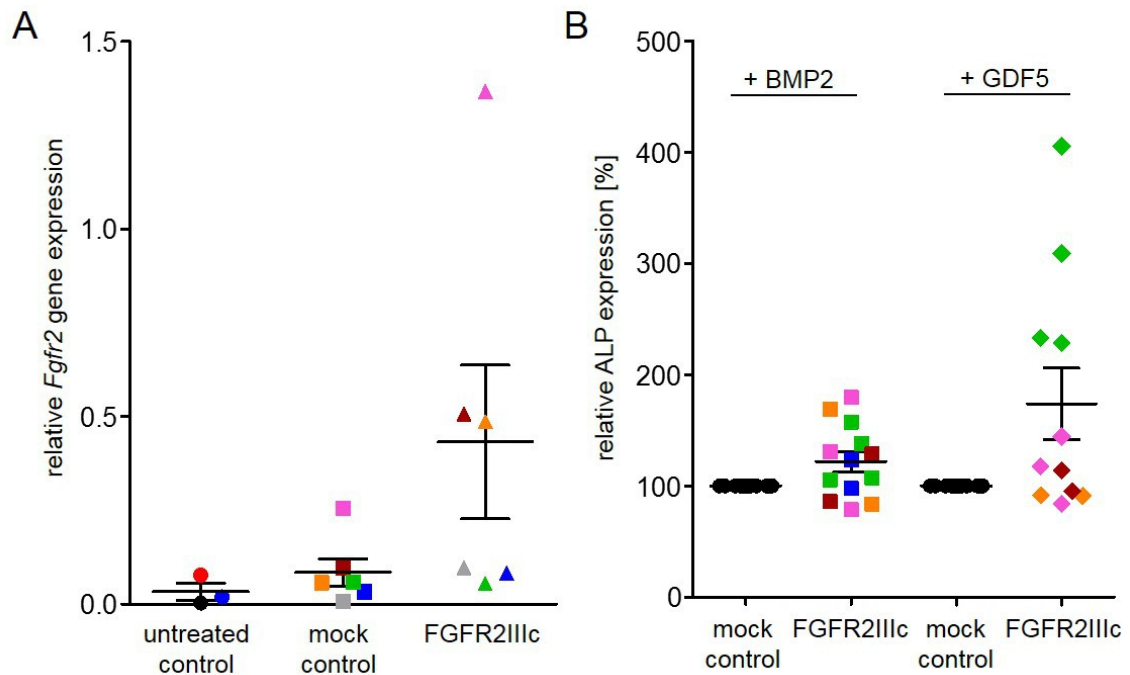


**Figure 10: Correlation between *Fgfr2IIIc* expression levels and ALP performance in C2C12 cells**

The independently performed six transduction experiments in C2C12 were color-coded, and data from the quantitative real-time PCR (A) as well as from the quantification of ALP activity in ligand-induced cells (B) were depicted as scatter blots in order to be able to correlate data from both experimental read-outs for each individual transduction.

In summary, these data show that FGFR2IIIc directly interacts with BMP2 and GDF5, and modulates their biological activity in cell-based assays with a propensity to GDF5.

#### 4.2. Investigating the Mechanism Underlying FGFR2 Mediated GDF5 Responsiveness

Having established that FGFR2IIIc directly binds selected BMP ligands and influences BMP2/GDF5 signaling outcome, the next question must be how. Does the observed elevation in BMP2/GDF5 signaling in the presence of FGFR2IIIc stem from interactions on the cell surface, as

is the case for known TGF $\beta$ /BMP co-receptors such as RGMs [101]? Or is it the net result of downstream events triggered by BMP receptors and the FGFR2IIIc individually, which is usually the case in BMP/FGF cross-talk? In this second part, it was investigated whether BMP and FGF ligands can synergize in ATDC5 or C2C12 cells, and whether the FGFR2 kinase domain is necessary for modulating BMP signaling.

#### **4.2.1. Western blotting does not show synergistic downstream signaling**

Approaching the question whether FGFR2IIIc enhances BMP signaling downstream of the receptors, it was first evaluated whether the activation of FGF receptors and BMP receptors simultaneously would trigger synergistic signals within one of their signaling cascades. BMP2 or GDF5 was added to either C2C12 or ATDC5 cells at one of two concentrations alone or in combination with one of four FGFs (FGF1, 2, 7, 8) for one hour. These ligands were chosen, as FGF1 was reported to bind both FGFR2IIIb and FGFR2IIIc, FGF2 was reported to bind only the IIIc variant of FGFR2, FGF7 to only bind the IIIb variant of FGFR2, and FGF8 was reported to bind neither [25, 112]. After treatment, the phosphorylation of SMAD1/5/8, p42/44 (Erk1/2), Akt, and p38 was evaluated by Western blotting: SMAD1/5/8 are components of canonical BMP2/GDF5 signaling, p42/44 are components of canonical FGF signaling, and Akt and p38 have been implicated in the non-canonical signal transduction of both. In none of the conditions, a BMP/FGF synergism became apparent. Akt phosphorylation was non-observable in any condition, and p38 phosphorylation was only slightly induced in ATDC5 with FGFs, which the BMP ligands seemed to antagonize rather than enhance.

SMAD phosphorylation induced by a BMP ligand remained stable in combination with any FGF, and p42/44 phosphorylation induced by an FGF ligand remained stable in combination with any BMP. If the FGFR2IIIc was indeed activated by BMP ligands to enhance ALP expression, or its basal activity was synergistic with BMP signaling, then it would be unlikely by the means of SMAD1/5/8, p42/44, Akt, or p38 phosphorylation.



**Figure 11: BMP/FGF Cross-Talk on C2C12 Cells**

Four different FGFs 1, 2, 7, and 8, as well as BMP2 (**A**) or GDF5 (**B**), were incubated separately or combined as indicated for 1 hour on C2C12 cells prior to lysate generation. FGFs 1, 2, and 8 were applied at 1nM, FGF7 was applied at 5 nM, BMP2 was applied either at 1 or 10 nM; and GDF5 was applied at either 5 or 50 nM. Lysates were analysed by Western blotting for the expression and phosphorylation status of SMAD1/5, p42/p44 (Erk), Akt, and p38.

These graphs are included in [2].



**Figure 12: BMP/FGF Cross-Talk on ATDC5 Cells**

Four different FGFs 1, 2, 7, and 8, as well as BMP2 (A) or GDF5 (B) were incubated separately or combined as indicated for 1 hour on ATDC5 cells prior to lysate generation. FGFs 1, 2, and 8 were applied at 1nM, FGF7 was applied at 5 nM, BMP2 was applied either at 1 or 10 nM; and GDF5 was applied at either 5 or 50 nM. Lysates were analysed by Western blotting for the expression and phosphorylation status of SMAD1/5, p42/p44 (Erk), Akt, and p38.

These graphs are included in [2].

#### 4.2.2. Erk inhibition does not compromise BMP ligand-mediated ALP expression

To confirm the Western blotting results, it was tested whether the inhibition of FGF signaling components would affect BMP-mediated induction of ALP expression. SU5402 is an RTK inhibitor targeting multiple receptors, including FGFR1, FGFR3, VEGR, EGFR, etc. IC<sub>50</sub> values vary depending on receptor, but are usually between 20 and 500 nM, hence sub-micromolar [113]. U0126 is a selective inhibitor of MEK1/2, kinases upstream of p42/44, with published IC<sub>50</sub> values at 72 nM for MEK1 and 58 nM for MEK2 [114].

SU5402 was not able to inhibit BMP signaling at concentrations up to 1  $\mu$ M in either ATDC5 or C3C12 cells (Figure 13A). Western blotting revealed that it was unable to actually inhibit p42/44 signaling, at least in response to FGF1 (Figure 13B). BMP signaling tended to be reduced at high concentrations of U0126, at least in ATDC5 cells (Figure 13A), although Western blotting showed that it only effectively inhibited p42/44 phosphorylation in C2C12 cells (Figure 13B). Hence, these data remain inconclusive, although they do not support a strong dependency of ALP induction on a FGFR2-mediated MAPK signal.

The Western blotting and inhibitor-based approaches mostly addressed only one signaling component at a time. To target FGF signal transduction in a much broader manner, and to examine whether the receptor's kinase activity is involved in the observed influence on BMP signaling at all, FGFR2IIIc was mutated in its kinase domain to render it kinase-dead (KD). The combination of mutations Y656F and Y657F has been reported to completely ablate all kinase function in the receptor, as it alters the ATP binding site in the kinase domain [115, 116]. Both mutations were introduced into the *Fgfr2aIIIc-C2* clone to create the variant FGFR2IIIc<sup>KD</sup>. To confirm that the construct was indeed kinase-dead, HEK293T and HEK293AD cells were transiently transfected with either mock control vector, or a vector containing either *Fgfr2IIIc*, or *Fgfr2IIIc<sup>KD</sup>*. The high transfection efficiency in these cells, as visually determined by a control construct containing turboGFP, suggested high expression levels of all constructs. Upon FGF ligand administration (1nM FGF1, or FGF2, respectively) for one hour, p42/44 expression and phosphorylation were determined by Western blotting. FGFR2IIIc expression led to elevated responsiveness to both ligands in both HEK cell lines, whereas FGFR2IIIc<sup>KD</sup> expression dominantly suppressed the cells' ability to respond to them, presumably by binding and thereby

sequestering them from the native, kinase-active receptors (Figure 14D).

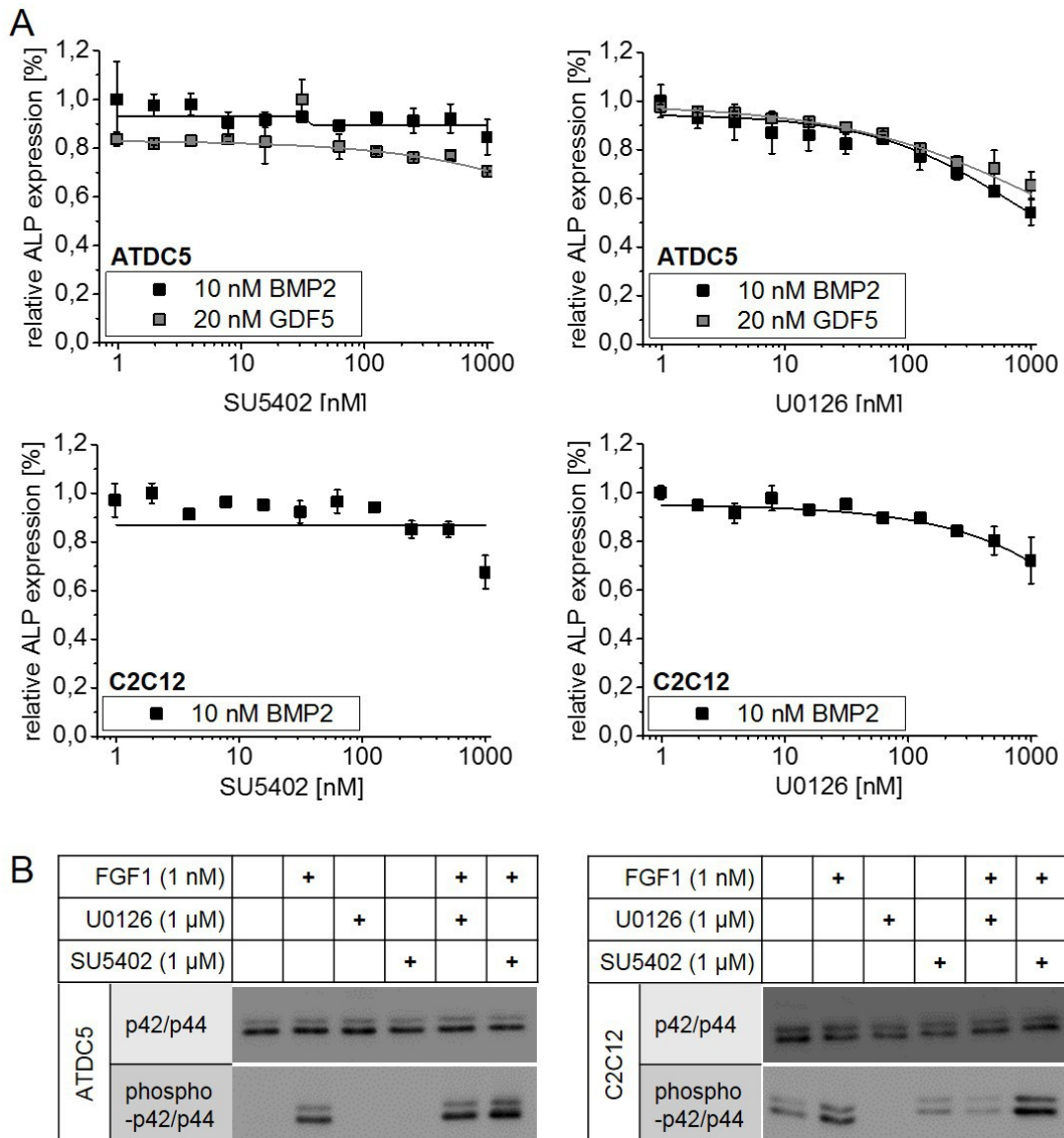


**Figure 13: Influence of p42/p44 Inhibition on BMP-Dependent ALP Induction**

(A) Two inhibitors of FGF signaling, U0126 or SU5402, were added to either ATDC5 or C2C12 cells stimulated with constant amounts of BMP2 or GDF5, and ALP activity was measured after 3 days. U0126 is a MAP kinase kinase inhibitor with a reported  $IC_{50}$  of 0.06 – 0.07 nM; SU5402 is an antagonist to FGFR1, VEGFR, and EGFR, with a reported  $IC_{50}$  of 0.03 nM. (B) The capacity of either inhibitor to inhibit p42/p44 phosphorylation in ATDC5 or C2C12 cells was examined by Western blotting. Cells were pre-treated with inhibitor for 30 minutes, then FGF ligands were added for 5 minutes.

FGFR2IIIc<sup>KD</sup> was expressed in C2C12 cells after lentiviral introduction as well as antibiotic selection. In accordance with other lentiviral transduction experiments, both *Fgfr2* expression levels and growth dynamics were tested prior to the analysis of BMP2/GDF5 responsiveness in the ALP assay. The expression level of *Fgfr2IIIc<sup>KD</sup>* was confirmed to be elevated in transduced cells compared to mock control cells by about five-fold: just as was the case for FGFR2IIIc expressing C2C12, a biologically relevant albeit statistically insignificant change (Figure 14B). The growth behavior over four days did not significantly change between transduced and non-transduced, or between mock control and *Fgfr2IIIc<sup>KD</sup>*-expressing C2C12 cells (Figure 14C).

In the ALP assay, the introduction of FGFR2IIIc<sup>KD</sup> in C2C12 cells not only enhanced ALP activity upon BMP2 or GDF5 application, but it did so more robustly and more extendedly than wildtype FGFR2IIIc (Figure 14A). On average, C2C12 expressing *Fgfr2IIIc<sup>KD</sup>* reached 150.3 % ± 66.1 % relative maximal ALP expression in response to BMP2, as compared to C2C12<sub>mock</sub>. Upon GDF5 application, they exhibited 363.4 % ± 235.2 % relative maximal ALP expression. In contrast to the experiments with wildtype FGFR2IIIc, these changes were both significant, if the significance level of 5 % was considered valid (Mann-Whitney U: n = 12, p[BMP2] = 0.04; p[GDF5] < 0.001). However, taking into account that wildtype and kinase-dead FGFR2IIIc data were tested against the same mock control, it could be considered more appropriate to apply Bonferroni-adjusted significance levels at 0.025 %. In this case, only the increased ALP activity of FGFR2IIIc<sup>KD</sup>-expressing C2C12 cells after GDF5 administration should be considered significantly different from mock control values.

As was the case with C2C12<sub>FGFR2IIIc</sub>, the EC<sub>50</sub> values of both ligands decreased in cells expressing FGFR2IIIc<sup>KD</sup>. For BMP2, the EC<sub>50</sub> values dropped from 26.0 ± 12.8 nM in mock control cells to 19.0 ± 8.7 nM in those expressing FGFR2IIIc<sup>KD</sup>. For GDF5, they decreased from 75.4 ± 21.8 nM (in assays where an EC<sub>50</sub> value could actually be determined) to 35.0 ± 18.2 nM. EC<sub>50</sub> value changes were not significant (Mann-Whitney U: n = 4, p[BMP2] = 0.191, p[GDF5] = 0.061).



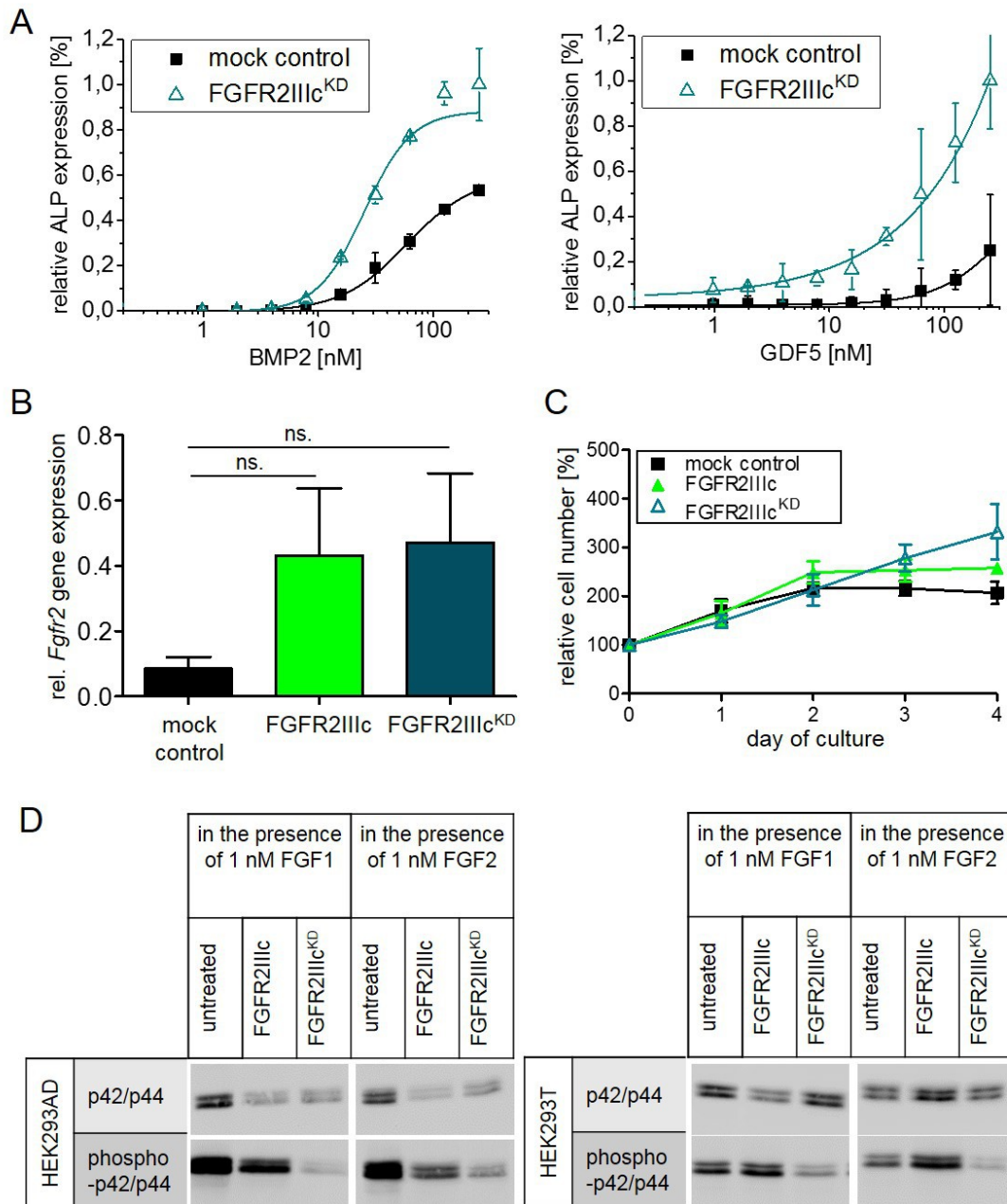


**Figure 14: FGFR2IIIc Kinase Activity Is not Necessary for Its Influence on ALP Activity**

(A) The induction of ALP activity in response to BMP2 or GDF5 in C2C12 cells transduced with either a mock control vector or FGFR2IIIc<sup>KD</sup>. (B) *Fgfr2* mRNA expression was determined by quantitative real-time PCR in C2C12 cells transduced with either mock control vector, *Fgfr2IIIc* or *Fgfr2IIIc*<sup>KD</sup>. Expression levels were normalized on *Hprt* and *Gapdh* expression. Differences in *Fgfr2* expression as compared to C2C12<sub>mock</sub> did not test significantly (Mann-Whitney U: n = 6, p[FGFR2IIIc] = 0.09, p[FGFR2IIIc<sup>KD</sup>] = 0.18). (C) Growth curves obtained by crystal violet staining determined C2C12 cell growth in dependence of *Fgfr2* gene expression. There was no significant difference between the cell number of mock control as compared to *Fgfr2IIIc* or *Fgfr2IIIc*<sup>KD</sup> expressing cells on day four (Mann-Whitney-U: n = 4, p[FGFR2IIIc] = 0.88, p[FGFR2IIIc<sup>KD</sup>] = 0.11). (D) Responsiveness to FGF1 or FGF2 treatment in transiently transduced HEK293AD and HEK293T cells with either FGFR2IIIc or FGFR2IIIc<sup>KD</sup> was determined by Western blotting against the expression and phosphorylation status of p42/p44.

Some of these data were already depicted in Figure 9. A subset of these data are included in [2].



As the variance in qPCR and ALP data between single experiments remained high, *Fgfr2* expression levels and responsiveness to BMP2/GDF5 of C2C12 cells expressing FGFR2IIIc<sup>KD</sup> were correlated in the same fashion as presented for wildtype FGFR2IIIc data (see Figure 10). The inverse correlation between differences in *Fgfr2* RNA expression and differences in induced ALP activity were apparent for FGFR2IIIc<sup>KD</sup> expressing cells, as well. However, ALP activity in response to GDF5 in C2C12 cells expressing *Fgfr2IIIc*<sup>KD</sup> were above mock control values in all experiments, unlike the ALP activity in any other tested condition. This confirmed the observed more robust elevation of ALP responsiveness by FGFR2IIIc<sup>KD</sup> in comparison to wildtype FGFR2IIIc, and gave context to the fact that this condition was the only one testing statistically significant.

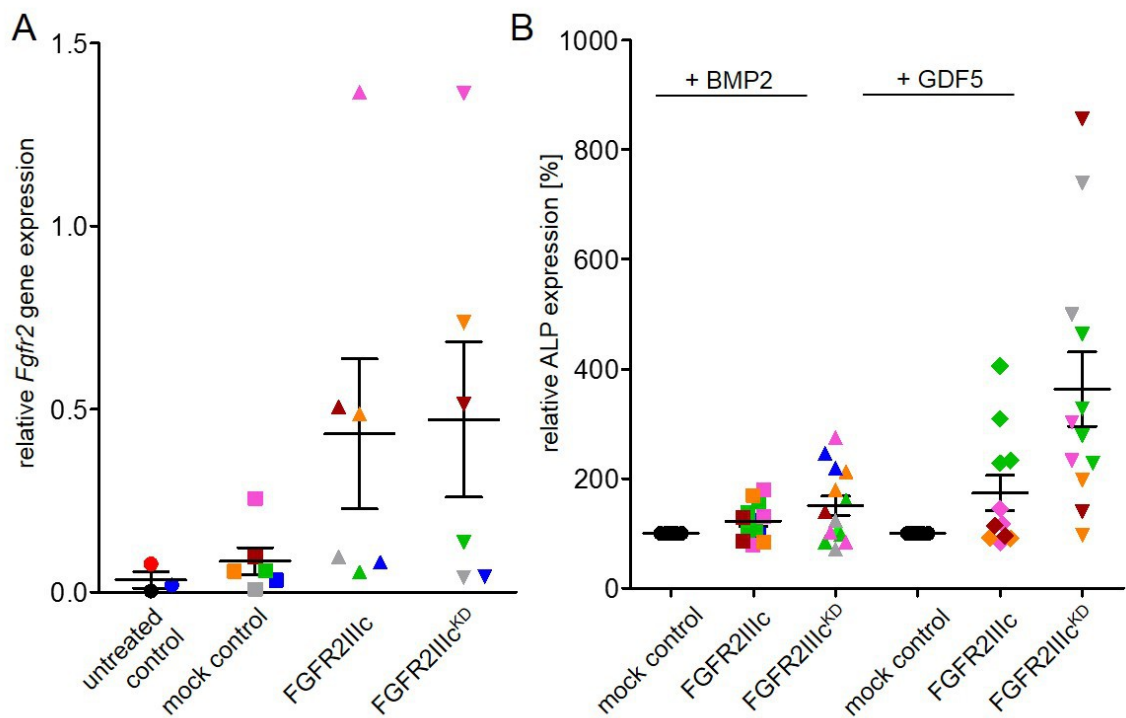


**Figure 15: Correlation between *Fgfr2IIIc* expression levels and ALP performance in C2C12 cells**

The independently performed six transduction experiments in C2C12 were color-coded, and data from the quantitative real-time PCR (A) as well as from the quantification of ALP activity in ligand-induced cells (B) were depicted as scatter blots in order to be able to correlate data from both experimental read-outs for each individual transduction.

A subset of these data was already depicted in Figure 10.

In summary, it can be concluded that the kinase activity of FGFR2IIIc is not relevant to its positive influence on BMP signal transduction. None of the experiments conducted hinted at a mechanism involving crosstalk between BMP and FGF signaling pathways activated within the cell.

### **4.3. Exploring the Possibility of FGFR2IIIc as Part of the BMP Ligand-Receptor-Complex**

The question remains how FGFR2IIIc exerts its influence on BMP mediated signaling, if synergizing downstream events are unlikely. The suggested alternative is a mechanism taking place on the cell surface, namely a direct involvement of FGFR2IIIc in the interaction between BMP ligand and receptor, as is the case for other co-receptors like RGMs [101]. In this third part, it was investigated whether BMPs can bind both BMP receptors and the FGFR2IIIc at the same time, and whether a complex comprising both receptor types is feasible.

#### **4.3.1. Competition behavior of FGFR2IIIc and BMPRIA extracellular domains indicate a common receptor binding site within ligands**

There are two known BMP receptor binding epitopes in BMP ligands like BMP2 and GDF5, the „wrist“ epitope binding BMP type I receptors, and the „knuckle“ epitope binding BMP type II receptors. To test if FGFR2IIIc binds to one of these epitopes, or to another site on the ligand, SPR co-injection measurements were performed by the laboratory of Prof. Thomas Müller that showed whether BMP receptors BMPRIA or ActRIIB could bind BMP2 at the same time as FGFR2IIIc. For this purpose, the first receptor extracellular domain (ECD) was immobilized on the SPR chip, then a BMP ligand was added until the binding interaction was at equilibrium, and then the second receptor ECD was added. For this consecutive approach, it is essential that the ligand added as first analyte and the immobilized receptor ECD have binding dynamics with low off-rates, so that the ligand does not dissociate from the first receptor ECD while adding the second receptor ECD. BMP2-BMPRIA<sub>ECD</sub> interaction shows a sufficiently low off-rate ( $k_{\text{off}} = 0.4 \pm 0.09 \times 10^3 \text{ s}^{-1}$ ), but wildtype BMP2 dissociates from immobilized ActRIIB<sub>ECD</sub> too fast for this co-injection approach ( $k_{\text{off}} = 18.0 \pm 4.68 \times 10^3 \text{ s}^{-1}$ )[105]. Therefore, a BMP2 variant BMP2-L100KN102D (BMP2-KD) with enhanced binding to type II receptors was utilized for co-injection experiments with immobilized ActRIIB<sub>ECD</sub>.

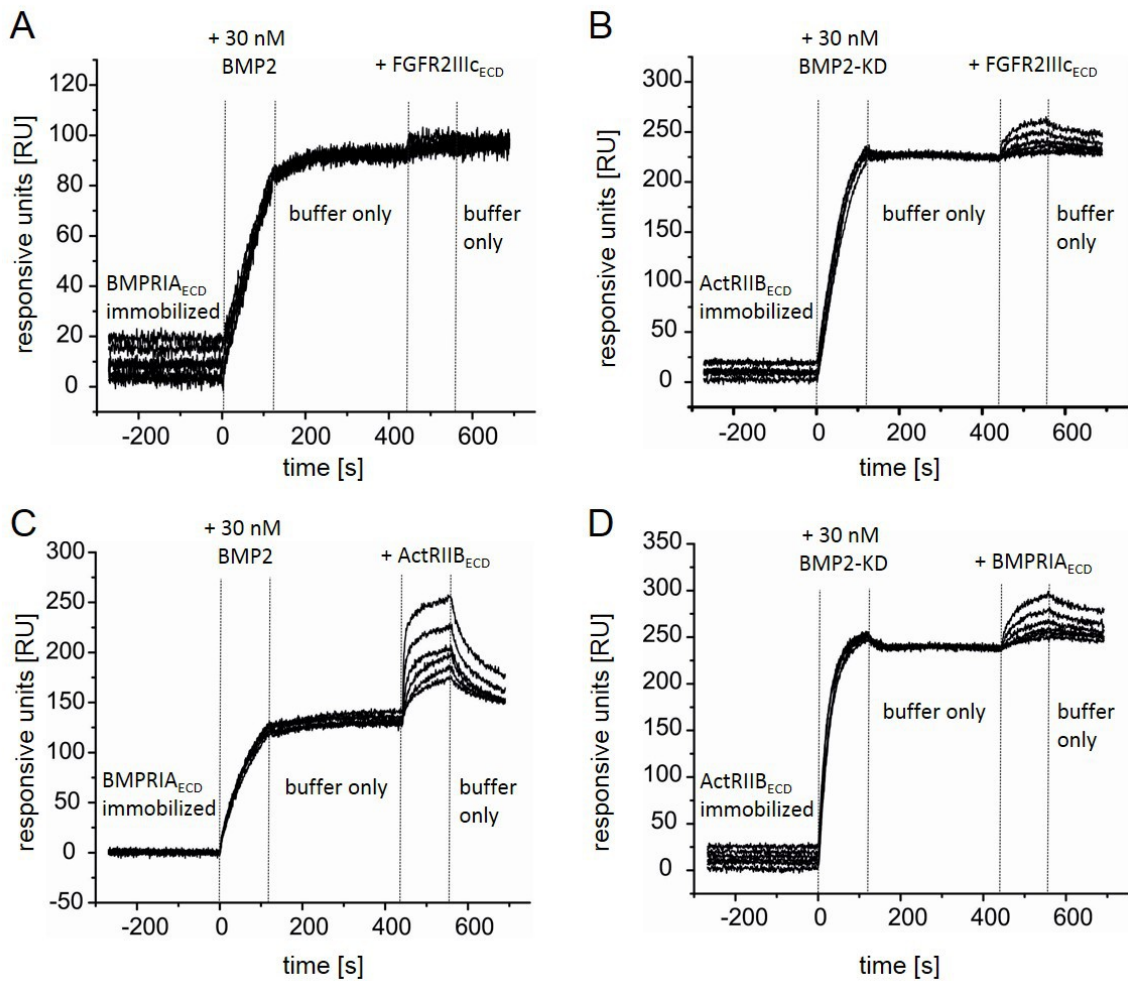


**Figure 16: *FGFR2IIIc<sub>ECD</sub>* Competes with *BMPRIA<sub>ECD</sub>* in SPR Measurements.**

Overlapping binding epitopes between *FGFR2IIIc* and *BMPRIA* or *FGFR2IIIc* and *ActRIIB* for BMP2 were investigated by so-called co-injection SPR measurements. The BMP2 variant BMP2-L100KN102D (BMP2-KD) had to be used when the immobilized receptor extracellular domain was a type II receptor, because wildtype BMP2 would dissociate too fast for a successful co-inject. Second receptor ectodomains were added in two-fold dilutions, in the concentration range specified for each measurement. (A) Co-injection of 200 – 6.25 nM *FGFR2IIIc<sub>ECD</sub>* to *BMPRIA<sub>ECD</sub>* and BMP2. (B) Co-injection of 200 – 6.25 nM *FGFR2IIIc<sub>ECD</sub>* to *ActRIIB<sub>ECD</sub>* and BMP2-KD. (C) Co-injection of 5000 – 156.25 nM *ActRIIB<sub>ECD</sub>* to *BMPRIA<sub>ECD</sub>* and BMP2. (D) Co-injection of 500 – 15.6 nM *BMPRIA<sub>ECD</sub>* to *ActRIIB<sub>ECD</sub>* and BMP2-KD.

SPR co-injection measurement data were kindly provided by Prof. Dr. Thomas Müller of the Julius-von-Sachs-Institute of Biosciences at the University of Würzburg, Germany.

These graphs are included in [2].

Control experiments co-injecting *BMPRIA<sub>ECD</sub>* and *ActRIIB<sub>ECD</sub>* showed that the binding to two different epitopes on BMP2 by the two receptor ECDs can be visualized with this approach: the SPR signal rises upon binding of the ligand to the immobilized ECD, remains in equilibrium

during the washing step, and increases further upon the addition of the second ECD (Figure 16C, D). Hence, in a control setup where both ECDs (BMPRIA<sub>ECD</sub> and ActRIIB<sub>ECD</sub>) are known to bind different epitopes on the utilized ligand, two increases in the SPR signal are observable. SPR co-injections with FGFR2IIIc<sub>ECD</sub> showed that it is likewise able to bind BMP2 immobilized by ActRIIB<sub>ECD</sub>, but is not able to bind to it when immobilized by BMPRIA<sub>ECD</sub> (Figure 16A, B). Hence, it can be assumed that FGFR2IIIc<sub>ECD</sub> binds BMP2 at the “wrist” epitope, or at a site at least overlapping with the “wrist” epitope.

Given the shared binding epitope of FGFR2IIIc and BMPRIA on the ligand, a BMP signaling complex that contains FGFR2IIIc only seems feasible if one or two BMP type I receptors are substituted with FGFR2IIIc, rather than an additional binding of FGFR2IIIc to the “classical” tetrameric BMP receptor complex assembly. To examine whether there is interchangeability of BMPRIA (the only BMP type I receptor expressed on ATDC5 and C2C12 cells) and FGFR2IIIc, competitive ALP assays were performed. ATDC5 or C2C12 cells were treated with constant BMP2 or GDF5 concentrations, and antibodies that reportedly inhibit either BMPRIA or FGFR2 [106, 117, 118] were added at increasing concentrations. Additionally, the efficacy of either extracellular domain (BMPRIA<sub>ECD</sub> or FGFR2IIIc<sub>ECD</sub>) to suppress BMP2- or GDF5-mediated ALP induction was compared.

While the anti-FGFR2 antibody had no effect on ALP induction, the anti-BMPRIA antibody was quite effective in the inhibition of signal transduction, as has been previously described [106, 118]. Here, the IC<sub>50</sub> of the anti-BMPRIA antibody for BMP2 on ATDC5 cells was 8.7 nM<sup>c</sup>, and 12.5 nM ± 6.7 nM for GDF5 (n = 2). Published values of this interaction are 28.3 nM ± 3.8 nM for BMP2, and 4.75 nM ± 1.1 nM for GDF5, respectively [106]. For C2C12, the IC<sub>50</sub> value for BMP2 (measured here) was 24.8 nM<sup>c</sup> (Figure 17).

---

c.) ALP competition assays with anti-BMPRIA antibody were performed twice, but in the case of BMP2 competition, the IC<sub>50</sub> could only successfully be calculated for one of the two experiments.

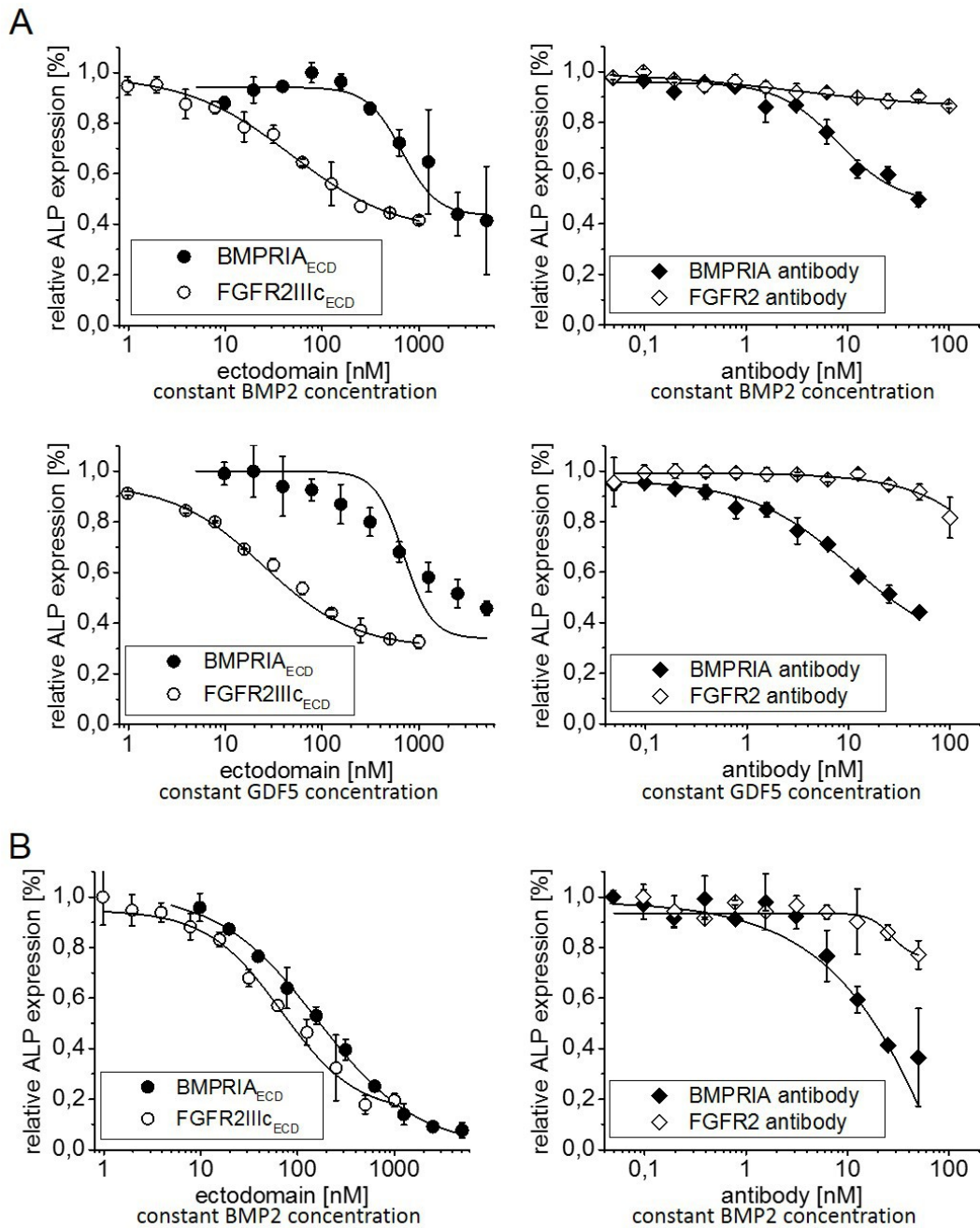


**Figure 17: The Dependence of ALP Induction on BMPRIA and FGFR2IIIc**

To investigate the dependency of ALP induction by BMP2 or GDF5 from the receptors BMPRIA and FGFR2, both ligands were made to compete with either receptor's soluble extracellular domain (ECD), or with an antibody designed to interfere with the respective receptor's function. Competition on ATDC5 (**A**) and C2C12 (**B**) cells was performed with a maximal concentration of 5  $\mu$ M BMPRIA<sub>ECD</sub> and 1  $\mu$ M FGFR2IIIc<sub>ECD</sub> (left side), or a maximal concentration of 50 nM anti-BMPRIA antibody and anti-FGFR2 antibody (right side).

Competition assay data with FGFR2IIIc<sub>ECD</sub> were already depicted in Figure 7.

Comparing the inhibitory capacities of BMPRIA<sub>ECD</sub> and FGFR2IIIc<sub>ECD</sub> (as already shown in Figure 7) revealed that FGFR2IIIc<sub>ECD</sub> was generally more effective in subduing ALP induction than BMPRIA<sub>ECD</sub>, and BMPRIA<sub>ECD</sub> was more effective in C2C12 cells as compared to ATDC5 cells (Figure 17). Measured IC<sub>50</sub> values were 50.5 nM ± 30.8 nM / 26.0 nM ± 19.0 nM for FGFR2IIIc<sub>ECD</sub> competing with BMP2/GDF5 on ATDC5, and 231.8 nM ± 123.7 nM for FGFR2IIIc<sub>ECD</sub> competing with BMP2 on C2C12, as reported above; for BMPRIA<sub>ECD</sub>, IC<sub>50</sub> values were 715.9 nM / 441.8 nM when competing with BMP2/GDF5 on ATDC5, and 218.8 nM when competing with BMP2 on C2C12<sup>d</sup>.

Hence, from published data as well as the shown ALP assays, it can be concluded that anti-BMPRIA antibody as well as soluble BMPRIA<sub>ECD</sub> inhibit BMP signaling. In consequence, this receptor can be considered necessary for ALP induction, and the substitution of both BMPRIA receptor chains in a BMP ligand-receptor complex by FGFR2IIIc should be considered unlikely [105].

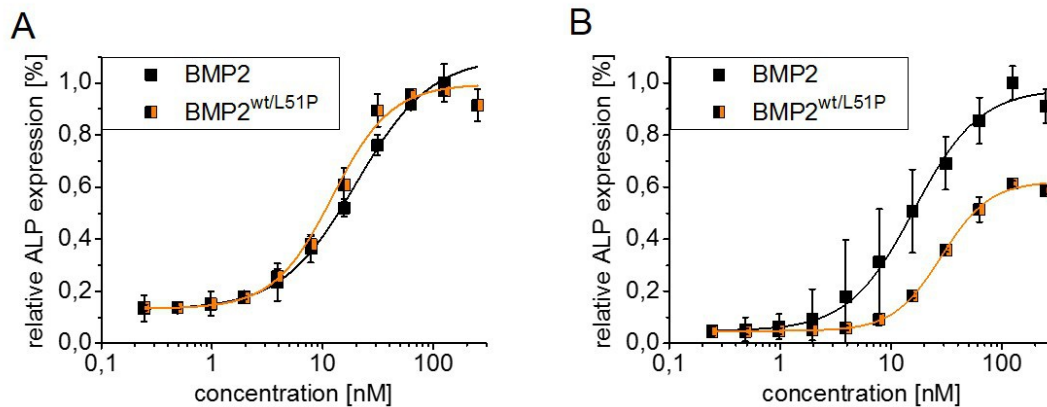


**Figure 18: Heteromeric BMP2<sup>wt/L51P</sup> Is Capable of Inducing ALP Expression.**

ALP activity was induced in (A) ATDC5 or (B) C2C12 cells by either BMP2 (wildtype protein) or heteromeric BMP2<sup>wt/L51P</sup> at increasing concentrations.

The substitution of one out of two of the BMPRIA receptor chains by FGFR2IIIc however remains possible, if one BMPRIA chain per signaling complex would be sufficient for signaling, as has already been suggested for BMP2/BMP6 heteromers [119]. To this end, a BMP2 ligand lacking

d.) ALP competition assays with BMPRIA<sub>ECD</sub> were only performed once, due to the fact that BMPRIA<sub>ECD</sub> protein was limited.

one „wrist“ epitope was used: BMP2-L51P is a mutant with a compromised „wrist“ epitope. Homodimeric BMP2-L51P is not able to induce ALP activity in any capacity [120]. Heteromeric BMP2<sup>wt/L51P</sup> on the other hand retains one binding site to BMP type I receptors. This heteromer was tested for its biological activity. Its capacity to induce ALP activity was identical to that of wildtype BMP2 in ATDC5 cells. In C2C12, it induced a lower, but still considerable, relative maximal ALP activity (Figure 18)[105].

#### 4.3.2. FGFR2IIIc and BMPRIA colocalize when overexpressed in HEK293AD cells

Assuming that FGFR2IIIc can indeed substitute one of the two BMPRIA chains in a ligand-receptor complex, co-localization of FGFR2IIIc and BMPRIA should be measurable in dependence of ligand presence. FGFR2IIIc and HA-tagged BMPRIA were overexpressed and fluorescently stained in HEK293AD cells, a cell line with superior transduction efficiency to either ATDC5 or C2C12 cells, and with stronger adherence to the culture surface than the related HEK293T cells (a pre-requisite for successful staining). Cells positive for FGFR2IIIc were FITC-stained (excitation/emission: 490/525 nm) via the anti-FGFR2 antibody used above as primary antibody and a FITC-conjugated secondary antibody; and cells positive for BMPRIA-HA were stained with a DyLight™ 650 (excitation/emission: 652/672 nm)-conjugated anti-HA antibody. The pictures of single cells positive for both stainings were then analyzed regarding the colocalization of both fluorescent signals, as described by Jaskolski et al. [121]. Here, visualization of colocalization is possible by determining the normalized mean deviation product nMDP values (ranging between exclusion at -1 and colocalization at 1), and color-coding them for each pixel (Figure 19). Quantitative comparison of colocalization is possible by the determination of the index of correlation  $I_{corr}$  (ranging between lack of correlation at 0.5 and total correlation at 1). Average  $I_{corr}$  values were significantly higher in the presence of ligand as compared to the absence of it (MWU,  $n = 3$ ,  $p[\text{BMP2}] = 0.016$ ,  $p[\text{GDF5}] = 0.001$ ). In the absence of ligand, correlation was moderate at  $I_{corr} = 0.738 \pm 0.079$ , increasing upon the addition of 20 nM BMP2 ( $I_{corr} = 0.780 \pm 0.069$ ), and further increasing in the presence of GDF5 ( $I_{corr} = 0.796 \pm 0.061$ ).



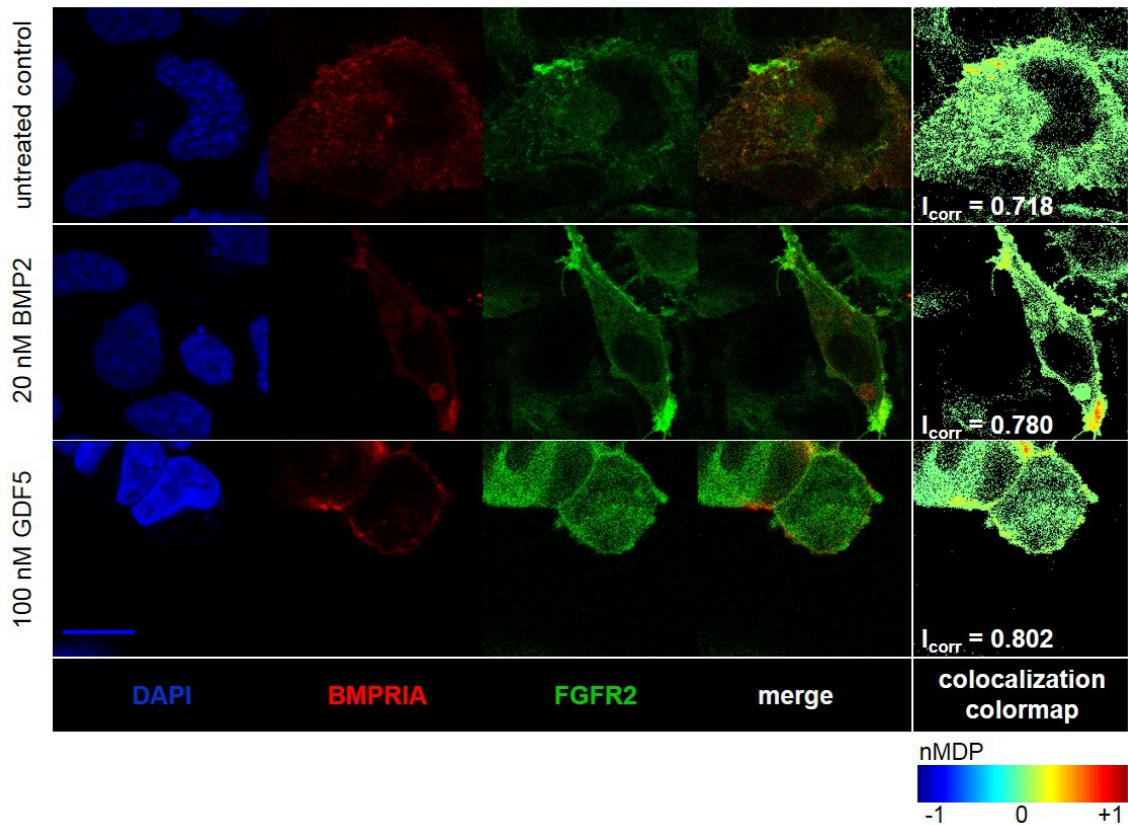


**Figure 19: FGFR2IIIc and BMPRIA Co-Localize In Dependence of Ligand.**

HEK293AD cells were transiently transfected with FGFR2IIIc and HA-tagged BMPRIA. Cells were then treated with 20 nM BMP2, or 100 nM GDF5, respectively, for one hour. FGFR2IIIc was stained indirectly with FITC (excitation/emission: 490/525 nm; color: green); and BMPRIA-HA was directly stained with DyLight™ 650 (excitation/emission: 652/672 nm; color: red). The index of correlation of both stainings was determined in at least 8 double-positive cells per condition, and the staining was repeated three independent times. Representative colocalization colormaps, depicting color-coded normalized mean deviation product nMDP values, indicate areas of high correlation in warm colors. These graphs are included in [2].

#### 4.3.3. Manipulating signaling outcome by changing receptor-ligand interaction parameters

The data presented here indicate that the modulation of BMP signaling by FGFR2IIIc is more likely on the cell surface than downstream. As it is improbable to signal itself in response to BMP ligands, its role then may be to enter the signaling complex and stabilize the interaction between ligand and BMP receptor, which in turn induces and maintains the signal more efficiently. The observation that GDF5 in C2C12 induces SMAD phosphorylation, but not ALP expression, hints to the presence of a threshold in signal transduction to ALP induction that is



higher than for SMAD phosphorylation. As this threshold can be partially overcome by the presence of FGFR2IIIc, altering the properties of the signal-receptor complex such as its stability and integrity may be one way to overcome such a threshold. However, the expression of supportive structures like FGFR2IIIc may not be the only means to influence these properties. Elevating the ligand's affinity to one or more of the BMP receptors should likewise stabilize the signaling complex.

The amino acid exchange R57A in GDF5 alters the „wrist“ epitope. In consequence, GDF5 exhibits an elevated affinity to BMPRIA, with a  $K_D$  to BMPRIA about ten-fold lower than that of wildtype GDF5 and therefore comparable to the one of BMP2. GDF5-R57A has hence been published as a „BMP2 mimic“ [106]. Indeed, in ATDC5 cells, it induces ALP expression with relative maximal ALP activities and  $EC_{50}$  values almost identical to those of BMP2. In C2C12 however, GDF5-R57A does not signal (Figure 20A)[106, 122].

The mutations Y106K and Q108D alter the „knuckle“ epitope. Consequently, GDF5-Y106KQ108D (GDF5-KD) exhibits a higher affinity to BMPRII. It performs markedly better on ATDC5 cells than BMP2, and it is able to signal in C2C12, albeit not as efficiently as BMP2 (Figure 20A). If all three amino acid exchanges are combined (GDF5-R57AY106KQ108D or GDF5-AKD), the resulting ligand signals with 5 – 10-fold lower  $EC_{50}$  values compared to BMP2 in both cell lines (Figure 20A, see Table 3 for details).

<b><i>EC<sub>50</sub> [nM]</i></b>	<b><i>ATDC5</i></b>	<b><i>C2C12</i></b>
BMP2	11.1 ± 6.1	28.8 ± 14.1
GDF5	60.7 ± 22.4	-
GDF5-R57A	8.7 ± 2.4	-
GDF5-KD	5.9 ± 2.4	39.0 ± 24.3
GDF5-AKD	0.6 ± 0.1	2.4 ± 0.1

*Table 3: EC<sub>50</sub> values of ligand variants*

The GDF5 mutant GDF5-R57A, seemingly intermittent between BMP2 and GDF5 [106], was analyzed for its performance on ATDC5<sub>shRNA</sub> and C2C12<sub>FGFR2IIIc</sub>. On ATDC5<sub>shRNA</sub>, GDF5-R57A showed partially reduced relative maximal ALP activities (Figure 20B, C), which were non-significant

upon repetition (Mann-Whitney U:  $n = 7$ ,  $p = 0.18$ ). Notably, the shift in its  $EC_{50}$  values from  $2.8 \pm 0.9$  nM on mock cells to  $4.1 \pm 1.4$  nM in cells expressing *Fgfr2* shRNA was significant (Mann-Whitney U:  $n = 8$ ,  $p = 0.031$ ).

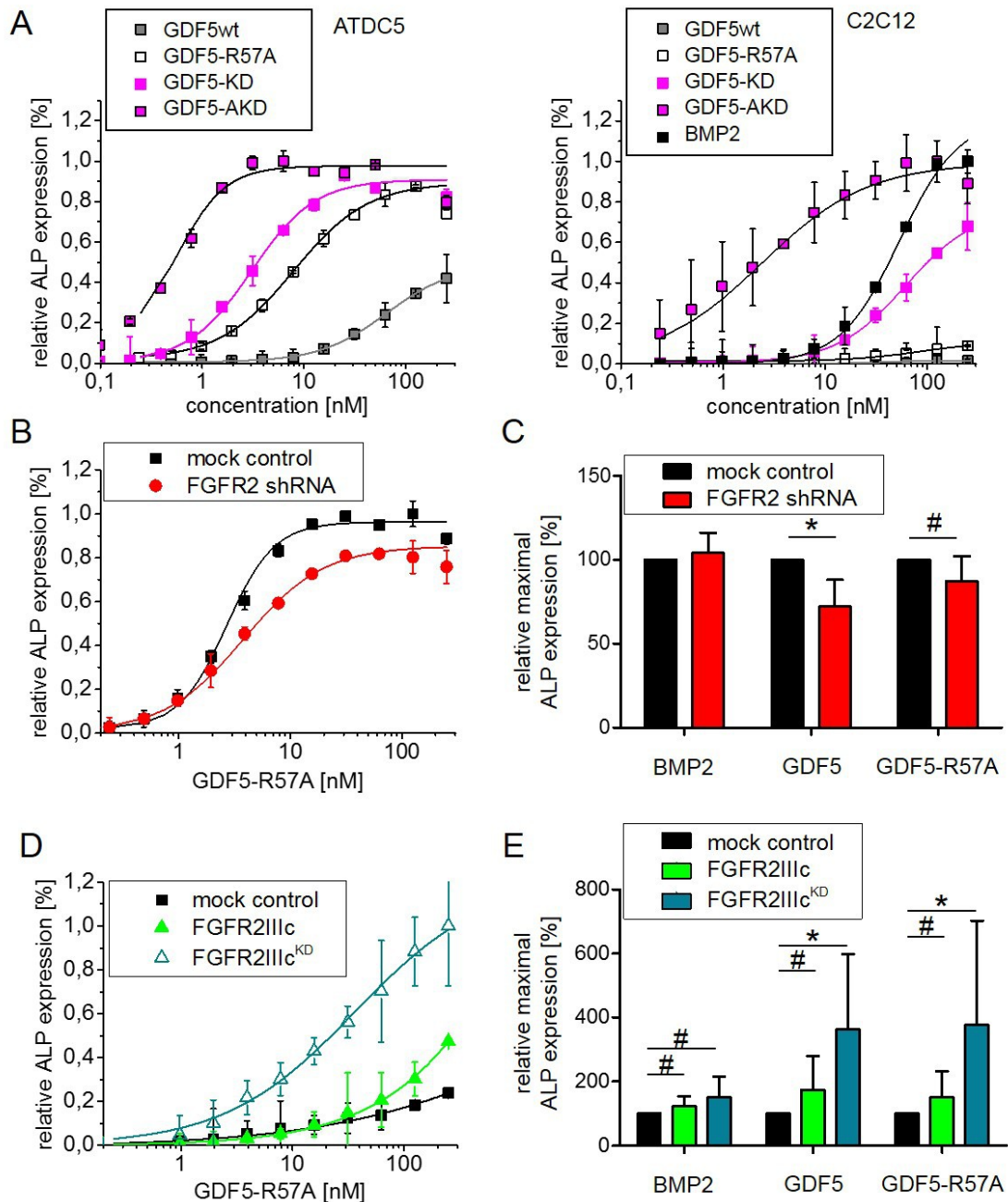


**Figure 20: Performance of GDF5 Mutants in the Presence or Absence of FGFR2**

GDF5 was mutated to enhance receptor binding. While R57A enhances BMPRIA binding, the combination of Y106K and Q108D heightens the affinity to BMPRII. (A) Ability of GDF5-R57A, GDF5-Y106KQ108D (GDF5-KD), and GDF5-R57AY106KQ108D (GDF5-AKD) to induce ALP expression. (B) The induction of ALP activity in response to GDF5-R57A in ATDC5 cells transduced with either mock control or *Fgfr2* shRNA. (D) The induction of ALP activity in response to GDF5-R57A in C2C12 cells transduced with either mock control, FGFR2IIIc, or FGFR2IIIc<sup>KD</sup>. (C, E) Quantification and statistical analysis of maximal ALP expression levels in B, D. (C) Mann-Whitney U:  $p(\text{GDF5}) < 0.001$ ,  $p(\text{GDF5-R57A}) = 0.18$ ,  $n = 7$ . (E) Mann-Whitney U: significance bonferroni-adjusted at 0.025 %,  $p(\text{BMP2/ FGFR2IIIc}) = 0.08$ ,  $p(\text{BMP2/ FGFR2IIIc}^{\text{KD}}) = 0.04$ ,  $p(\text{GDF5/ FGFR2IIIc}) = 0.26$ ,  $p(\text{GDF5/ FGFR2IIIc}^{\text{KD}}) = 0.002$ ,  $p(\text{GDF5-R57A/ FGFR2IIIc}) = 0.15$ ,  $p(\text{GDF5-R57A/ FGFR2IIIc}^{\text{KD}}) < 0.001$ ,  $n \geq 11$ ).

In C2C12<sub>-FGFR2IIIc</sub>, GDF5-R57A induced ALP expression non-significantly, and significantly in C2C12 expressing FGFR2IIIc<sup>KD</sup> (Mann-Whitney U:  $n \geq 12$ ,  $p[\text{FGFR2IIIc}] = 0.15$ ,  $p[\text{FGFR2IIIc}^{\text{KD}}] < 0.001$ ; Figure 20D, E). The shift in EC<sub>50</sub> values however remained insignificant (Mann-Whitney U:  $n = 9$ ,  $p[\text{FGFR2IIIc}] = 0.462$ ,  $p[\text{FGFR2IIIc}^{\text{KD}}] = 0.935$ ).

An overview of the EC<sub>50</sub> values measured in cells with altered *Fgfr2* expression can be found in Table 4.

<i>EC</i> <sub>50</sub> [nM]	<i>ATDC5</i>		<i>C2C12</i>		
	<i>mock control</i>	<i>Fgfr2 shRNA</i>	<i>mock control</i>	<i>Fgfr2IIIc</i>	<i>Fgfr2IIIc</i> <sup>KD</sup>
BMP2	2.4 ± 0.8	3.2 ± 0.8	26.0 ± 12.8	22.8 ± 12.2	19.0 ± 8.7
GDF5	29.2 ± 6.9	37.5 ± 5.7	75.4 ± 21.8	66.6 ± 21.5	35.0 ± 18.2
GDF5-R57A	2.8 ± 0.9	4.1 ± 1.4	4.9 ± 3.7	9.3 ± 9.9	5.9 ± 6.1

Table 4: EC<sub>50</sub> value changes upon *Fgfr2* expression alteration

Taken together, the data support a model of FGFR2IIIc becoming part of the ligand-receptor complex, possibly as substitute for one BMP type I receptor, in order to stabilize the signaling complex.

## 5. Discussion

Growth factor signaling, both in its developmental context and in its molecular details, is very context-dependent and thoroughly interconnected. The investigation of growth factor interaction usually analyzes only small parts of the network at a time. In this thesis, the relationship of FGF receptor 2 with the BMP ligands BMP2 and GDF5 was illuminated in a cell line-based model, new ways of interaction between these proteins were shown, and the underlying mechanisms were examined.

### 5.1. Testing the Tenability of FGFR2 as Co-Receptor Candidate

In this first part of the thesis, it was questioned whether FGFR2, identified as a candidate for a hypothesized new BMP co-receptor in a microarray-based approach [2, 106], possessed the necessary properties: direct binding to BMP ligands, and influencing BMP-mediated signals *in vivo*.

The first step was to test for a direct interaction between FGFR2 and various TGF $\beta$ /BMP ligands by SPR. As such a measurement is performed with two soluble interaction partners, receptors are usually not applied as a whole protein with its hydrophobic transmembranic domain(s), but as smaller soluble domains or peptides. In case of TGF $\beta$ /BMP and FGF receptors, the entire extracellular domain can be expressed as a soluble protein and used as analyte in SPR. While this is quite straight-forward for TGF $\beta$ /BMP receptors, it had to be taken into consideration that FGFR2 is expressed as many different splice variants, and there were a number of possible extracellular domains to potentially employ. One of the major splicing events in the FGFR2 extracellular domain is the switch between the epithelial third Ig-like domain IIIb and the mesenchymal third Ig-like domain IIIc [30]. Here, it was proceeded with FGFR2IIIc, as the microarray that preceded this thesis was performed on mesenchymal cells ATDC5 and C2C12, of which ATDC5 cells are described to only express mesenchymal IIIc variants [110], while C2C12

express only negligible amounts of any splice variant. So as not to exclude any potential binding epitopes, the longest form of FGFR2IIIc containing all three Ig-like domains (dubbed isoform  $\alpha$ ) was utilized. SPR measurements were kindly performed by the laboratory of Prof. Dr. Thomas Müller.

FGFR2IIIc<sub>ECD</sub> bound BMP2, GDF5, BMP4 and BMP6 with affinities in the low nanomolar range, but not Activin A or TGF $\beta$ 2. This indicates a specificity for the BMP subgroup of TGF $\beta$  ligands, rather than specificity for a single ligand. As the biological discrepancy observed between signaling in ATDC5 and C2C12 cells is GDF5-specific, a likewise GDF5-specific binding of FGFR2IIIc<sub>ECD</sub> would have been compelling, but this could not be confirmed in SPR. Instead, the observed propensity for BMP ligands in general may be indicative of a mechanism more broad and general than only GDF5-mediated signals, and the biological relevance of this will be explored to some extent below.

In the next step, it was tested whether FGFR2IIIc<sub>ECD</sub>, as soluble form of FGFR2IIIc, could inhibit BMP-mediated signal transduction in the same way as the soluble forms of other co-receptors such as RGMs [101]. FGFR2IIIc<sub>ECD</sub> was able to inhibit both BMP2- and GDF5-induced ALP activity in a concentration-dependent fashion, confirming the SPR measurements. Analyzing the dynamics of these inhibition data, several differences between ATDC5 and C2C12 cells became apparent: ATDC5 cells showed a higher baseline ALP activity, meaning in the absence of an inducing agent such as a BMP ligand. This baseline activity was reduced upon administration of FGFR2IIIc<sub>ECD</sub> alone, which indicates an endogenously expressed ALP-inducing protein in ATDC5 cells which can be (at least partially) inhibited by FGFR2IIIc<sub>ECD</sub>. It is safe to assume that this is BMP4, as ATDC5 cells are known to express low levels of it [123]. In contrast, ALP activity baseline levels and levels with FGFR2IIIc<sub>ECD</sub> alone in C2C12 cells were low and equivalent, indicating that no intrinsic ALP-inducing factor is produced by these cells. Further, according to the generated IC<sub>50</sub> values, FGFR2IIIc<sub>ECD</sub> inhibited BMP2 two- to four-fold more effectively on ATDC5 cells as compared to C2C12, although the inhibition curve was less sigmoid (implying either a less specific inhibition or multiple interactions). This may indicate that the receptor-ligand complexes formed on either cell line are not identical, and that FGFR2IIIc<sub>ECD</sub> competition with ligand binding to these different complexes causes different inhibition dynamics. As both cell lines express the same BMP receptors, this would likely entail receptor complex components

other than the BMP ligand and type I and II receptors. Alternatively, it is possible that there are different cell surface components expressed on both cell lines that either sequester FGFR2IIIc<sub>ECD</sub> or help recruit it to the membrane surface, influencing the effective FGFR2IIIc<sub>ECD</sub> concentration available on the cell surface, and shifting the IC<sub>50</sub> accordingly. It is also possible that FGFR2IIIc<sub>ECD</sub> interacts with BMP-binding extracellular components such as heparins, which are differentially expressed on both cell lines. This interaction could theoretically release ECM-bound BMP ligands, which are then available to bind the receptor and increase the signal. While a definite mechanism cannot be concluded from these data, it is worth noting that apparently, other components besides the expressed BMP receptors influence BMP signal transduction in a cell type-specific manner.

After establishing that FGFR2IIIc directly binds to GDF5 and BMP2, it was investigated whether its expression in the model cell lines also has an influence on the ligands' signal transduction properties. As *Fgfr2* RNA is expressed 9-fold higher in ATDC5 cells as compared to C2C12 cells, its expression was inhibited in ATDC5 cells and elevated in C2C12 cells, and its influence on GDF5- and BMP2-induced ALP activity was evaluated.

All *Fgfr2* splice variants expressed in ATDC5 cells were down-regulated by lentivirally introducing a *Fgfr2*-specific shRNA binding the kinase domain-coding sequence of *Fgfr2* mRNA. A number of control experiments were performed to ensure the integrity of the ALP induction analysis. For example, it could be confirmed by qPCR that mock cells (transduced with scrambled shRNA) did not show a difference in *Fgfr2* expression when compared to wildtype cells (untreated control), whereas shRNA-containing ATDC5 cells showed a significant reduction to about 50% of *Fgfr2* expression in mock control cells (an expectable decrease for shRNA approaches). It was further investigated whether transduced and selected ATDC5 cells showed altered growth dynamics. Measured ALP activity levels are relative not only to the ability of the measured cells to respond to an ALP-inducing stimulus, but also to their absolute number. Hence, the comparison of ALP induction in two different conditions relies on an equal amount of cells in each measured well. Over the course of four days, which is the length of one ALP induction experiment, wildtype and transduced ATDC5 cells showed comparable cell growth. Based on these control experiments, the produced cells were considered suitable for analyzing ALP induction.

Inducing ALP activity in ATDC5<sub>mock</sub> and ATDC5<sub>shRNA</sub> cells with either BMP2 or GDF5 revealed that the reduction in *Fgfr2* expression only caused a reduction in GDF5 responsiveness. BMP2-induced ALP activity was not altered. This finding stood in contrast to SPR analysis and to competition experiments, where no distinction between BMP2 and GDF5 interaction with FGFR2IIIc<sub>ECD</sub> could be determined.

In theory, the efficiency of signal transduction with a given ligand concentration should be directly dependent on the receptor chain with the lower affinity to the ligand, which, in the case of BMP2 and GDF5, is the type II receptor. ATDC5 and C2C12 cells only express BMPRII as type II receptor. However, while EC<sub>50</sub> values of BMP2 in C2C12 are around 20 nM (22.8 ± 12.8 in these experiments), the measured EC<sub>50</sub> values for BMP2 in ATDC5 cells are lower, at between 1 and 10 nM (2.4 ± 0.8 nM in these experiments). This leads to the assumption that the ligand-receptor interaction and/or the ligand-receptor complex in ATDC5 cells is stabilized by additional components that may not be expressed on C2C12 cells, or that BMP2 gets trapped on the surface by cell-specific membrane proteins, elevating its local concentration on the cell surface. In the first case of different signaling complexes, the BMP2 signal transduction complex might be stable enough to compensate for the partial loss of *Fgfr2*, or not employ FGFR2IIIc for signal transduction at all. GDF5 in turn may be more dependent on it, either because not all structures stabilizing BMP2 signal transduction can stabilize GDF5 signaling as well, or because the GDF5 receptor-ligand complex is less stable to begin with, possibly as a consequence of a less favorable geometry or less favorable binding kinetics. On the other hand, ATDC5 cells do express more matrix proteins than C2C12 do due to their chondrogenic nature, so it is likewise a feasible assumption that membrane-associated proteins influence the local ligand concentration both in a cell type-specific and a ligand-specific manner.

In C2C12 cells, FGFR2 was lentivirally introduced as the splice variant FGFR2αIIIc-C2. Prior to this work, Fabian Prenzlau had cloned *Fgfr2* splice variants from the ATDC5 cell transcriptome, as it was considered feasible that an ATDC5-expressed splice variant was involved in BMP2/GDF5 signaling, and hence should be tested in C2C12 (for reference, see his term paper [111]). He found four splice variants, FGFR2αIIIc with either a C1- or a C2-terminus, as well as FGFR2βIIIc with either a C1- or a C2-terminus.

Only one of these variants, FGFR2 $\alpha$ IIIc-C2, could be successfully transferred into the lentiviral vector. This was considered unfortunate, as the C2-terminus is not part of the consensus sequence, but the C1-terminus is. Hence, obtaining the sequence of FGFR2 $\alpha$ IIIc-C1 in a lentiviral construct would have been favorable. It had to be questioned whether FGFR2 $\alpha$ IIIc-C2 was actually appropriate to use: In terms of consistency with prior experiments, FGFR2 $\alpha$ IIIc with either C-terminus would have been appropriate. SPR measurements and competition assays only used the extracellular domain of FGFR2 $\alpha$ IIIc, and the shRNA introduced into ATDC5 cells indiscriminately down-regulated all variants expressed by these cells. Still, the biological differences between the consensus C1 and the utilized C2 needed to be taken into account.

Unfortunately, C2 (as well as the third c-terminal isoform C3) have only really been investigated as variants of FGFR2IIIb, and reports on carboxyl-terminal variants of FGFR2IIIc are practically non-existent. C1 and C2 carboxyl-termini of FGFR2IIIb can be found in normal epithelial cells [124], while FGFR2IIIb-C3 is only expressed and associated with cancer cells [125]. This is not surprising, as FGFR2IIIb-C3 exhibits higher levels of activation, less dependency on ligand, and an indicated lower likelihood of being internalized, as compared to FGFR2IIIb-C1, thus promoting cell transformation [125, 126]. FGFR2IIIb-C2 has likewise been linked to cancer and epithelial to mesenchymal transformation, although supporting data is much more scarce. Lonic et al. even make a case for a lower activation status of FGFR2IIIb-C2 and -C3 in comparison to -C1. They state that amino acid S783<sup>e</sup>, only present in FGFR2IIIb-C1, is necessary for full FGFR2 activation [127]. Another serine, S781, is retained in the C1- and C2-termini, and its homologous serine 777 in FGFR1 has been linked to the inhibition of FGFR activation by a negative feedback mechanism [128]. FGFR2IIIb-C2 retains ligand-sensitivity, shows no elevated basal activity, and still has all amino acid residues necessary for receptor internalization and degradation after ligand-binding. Notably, like non-canonical carboxy-termini, the switch from FGFR2IIIb to FGFR2IIIc in epithelial cells is likewise connected to cancer progression, and is arguably a stronger transformation indicator than the switch from FGFR2IIIb-C1 to -C2 [35, 126]. In terms of the C2 variant of FGFR2IIIc, Fabian Prenzlau's work as well as Barnard et al. showed that it too is expressed in non-cancerous cells, at least in ATDC5, osteoblastic cell lines and in primary

---

e.) Lonic et al. refer to this residue as S779. However, they specify the residue in question as the second serine in the c-terminal QYSPSY motif, which is at position 779 in FGFR1, not FGFR2. Actually, 783 is the correct position in FGFR2IIIb [127].



chondrocytes and osteoblasts (although Barnard et al. failed to identify the isoform they found as FGFR2IIIc-C2)[110].

In summary, it can only be assumed that the high homology of the C2 to the C1 variant, as well as its expression in normal tissues and the collective scientific disinterest in either FGFR2IIIb or FGFR2IIIc with C2-terminus, translate into neglectable biological differences between C1 and C2. On this basis, work was proceeded with FGFR2αIIIc-C2, henceforth referred to simply as FGFR2IIIc.

In accordance with the ATDC5 transduction experiments, *Fgfr2IIIc*-transduced C2C12 cells were confirmed to not significantly change their growth dynamics within four days, and further confirmed to exhibit altered *Fgfr2* expression by qPCR analysis after transduction and selection. C2C12<sub>FGFR2IIIc</sub> showed an average five-fold elevation in *Fgfr2* mRNA levels as compared to C2C12<sub>mock</sub> (transduced with an empty backbone vector). This presented a biologically relevant, but not statistically significant change, due to the heterogeneity between single experiments. ALP induction produced likewise heterogeneous results. On average, the introduction of *Fgfr2IIIc* mediated higher levels of ALP activity in C2C12 both in response to BMP2 and GDF5, although the difference was greater for GDF5 both qualitatively and quantitatively. One of the reasons for the heterogeneity in the quantification may be that the ALP induction did not reach plateau phase with the highest used concentration of GDF5 on C2C12. This could not be remedied, as GDF5 is not soluble above the used concentrations at a physiological pH, so the relative maximal ALP expression was always mathematically determined as projection from the obtained data, and quantification data may therefore be imprecise. However, the qualitative data also varied, so there are likely other underlying reasons for the observed heterogeneity as well (see below).

In any case, it can be stated that FGFR2IIIc had an influence on both the BMP2 and the GDF5 signal in C2C12 cells, whereas its influence seemed entirely GDF5-specific in ATDC5 cells, suggesting that BMP2 signal transduction (and possibly its receptor-ligand complex) in C2C12 cells may be less stable when compared to ATDC5 cells, as has been discussed above.

The high variance between single experiments became a focus point, because even raising the

number of repetitions to over 10 (an unusually high number of repetitions for a cell line-based standard assay) did not grant statistical significance. Examining this heterogeneity in both the qPCR and ALP assay data more closely revealed that there was an inverse correlation between elevated *Fgfr2* mRNA levels and elevated GDF5-induced ALP activity. The smaller the difference in *Fgfr2* expression, the higher was the impact on ALP induction. Hence, not only could no data set be excluded from the analysis, which kept the variance high and prevented statistical significance; this finding also implied a dose-dependent effect: while low levels of FGFR2IIIc on C2C12 cells could enhance ALP activity induction, higher levels seemingly failed to do so.

Dose-dependent switches from BMP-FGF agonism to antagonism so far have been described for ligand concentration changes [129, 130], not receptor concentration changes. However, just like the ligands, the receptors may cause a concentration-dependent elevation of FGF signaling: It has been suggested that FGFR-mediated, ligand-independent signaling increases with the number of receptors on the cell, both by overexpression experiments [97] and by the association of FGFR overexpression with cancer [27]. Elevated FGF signaling in turn has been associated with BMP antagonism in C2C12 cells [41]. Hence, the observed dose-dependent effect may constitute either a gradual shift in balance between synergistic effects of the presence of FGFR2IIIc on the cell surface, and antagonistic effects of FGF signaling; or it could be indicative of a switch between a BMP-synergistic low FGF signal and a BMP-antagonistic high FGF signal. Additionally, it cannot be excluded that other intrinsic and unidentified growth factors or signaling molecules are connected to BMP and FGF signal transduction in C2C12 in a broader network, as is usually the case in developmental environments (see 1.3. ), so conceivably, *Fgfr2IIIc* expression levels may also have an indirect influence on the transduction of BMP signals via proteins of other signaling cascades.

In summary, FGFR2 splice variant IIIc directly binds to TGF $\beta$  family members of the BMP subgroup, including BMP2 and GDF5, and can modulate their signal transduction with a propensity for GDF5. However, the underlying mechanism is neither entirely GDF5-specific nor “on/off”, as the presence of FGFR2IIIc does not automatically translate into a strong GDF5 responsiveness. Further, from the data shown, it is feasible to assume that apart from the BMP receptors, FGFR2IIIc is not the only protein influencing BMP2/GDF5 receptor-ligand interaction and signal transduction efficiency in this model system, especially regarding ATDC5 cells. It is

however one component with noticeable influence, and the molecular basis for this became the next focus of investigation.

## **5.2. Investigating the Mechanism Underlying FGFR2 Mediated GDF5 Responsiveness**

FGFR2IIIc has a measurable influence on GDF5- (and BMP2-) mediated signal transduction. Based on the data presented so far, the molecular mechanism behind this influence can only be hypothesized: maybe there is a downstream signal generated either by the mere expression of FGFR2IIIc, or by its binding to BMP2/GDF5, that can synergize with BMP receptor-mediated signals to induce ALP expression. Alternatively, FGFR2IIIc may have an influence on BMP signaling on the cell surface, without the involvement of downstream signals. Previous experiments provide some support for either theory: considering that BMP2 and GDF5 variant R57A can induce SMAD1/5/8 phosphorylation in C2C12 to a similar extent, but only BMP2 can induce ALP activity [106], it seems apparent that SMAD1/5/8 phosphorylation is not sufficient for the elevation of *Alp* expression levels. Inhibition studies with SMAD and MAPK inhibitors imply that sustained SMAD phosphorylation is nonetheless necessary, and that a MAP kinase may be the additional signal needed for ALP induction [105]. These findings suggest that the presence of FGFR2IIIc may enable GDF5 to induce a MAPK signal necessary for ALP induction; a signal which, in consequence, BMP2 would then have to be able to elicit in C2C12 (and ATDC5) even in the absence of FGFR2IIIc. On the other hand, FGFR2 was identified as candidate for a new co-receptor. Other TGF $\beta$ /BMP co-receptors generate ligand specificity exclusively on the cell surface. A co-receptor-mediated downstream signal is seemingly not involved, as they usually do not have a kinase domain, and sometimes not even an intracellular domain [101]. Even in the case of muscle-specific kinase MuSK, a recently identified BMP co-receptor and fellow receptor tyrosine kinase, MuSK's kinase domain is not part of its influence on BMP signaling [131]. These observations would give reason to assume that the co-receptor function of FGFR2IIIc to GDF5 (and BMP2) has likewise nothing to do with its kinase.

To evaluate which hypothetical mechanism is more likely, it was examined which pathways are activated in ATDC5 and C2C12 cells by BMP2, GDF5, FGF ligands 1, 2, 7, or 8, as well as by dual combinations of one BMP and one FGF. The expression and phosphorylation of representative signaling molecules for both canonical and non-canonical signaling of the applied growth factors

were determined. BMP2 and GDF5 induced SMAD phosphorylation in any condition, and FGF ligands induced p42/44 in any condition (except for FGF8 on C2C12 cells). p38 was phosphorylated in none of the conditions, and Akt phosphorylation was likewise absent, or low but inconsistent in response to FGF ligands. In these data, there was no hint that BMP2 or GDF5 induce different signaling cascades in C2C12, despite the fact that one can induce ALP and one cannot; there was no hint that GDF5 could induce more or different signals in ATDC5 as compared to C2C12, although it induces ALP only in the former; and there was no hint for synergistic signaling between a tested BMP ligand and a tested FGF ligand. Hence, this approach did not support the hypothesis of an FGFR2-mediated downstream signal.

Still, looking at the data more closely, there are a few things to be noted. The FGF ligands 1, 2, 7, and 8 were chosen for their reported receptor splice variant specificities in human: FGF1 binds to both FGFR2IIIb and FGFR2IIIc, FGF2 only binds to FGFR2IIIc, FGF7 only binds to FGFR2IIIb, and FGF8 binds to neither [25, 112]. Hence, looking at the cell lines' FGFR2 expression, it should be expected that FGF1 and FGF2 only signal in ATDC5 cells, and FGF7 and FGF8 should not be able to signal in either cell line. This was not the case. The reason why robust FGF1 and FGF2 responses in both cell lines can be observed is likely due to the fact that both ATDC5 and C2C12 cells also express FGFR1 [2], which binds to both FGF1 and FGF2 with either of its IgIII splice variants. FGF8 can signal via FGFR3, which is present only on ATDC5 cells, so the observed ATDC5-specific FGF8 response here can also be explained [2, 25, 112]. Only p42/p44 phosphorylation in response to FGF7 in both cell lines is surprising, because FGF7 is described to only signal via FGFR2IIIb, a splice variant expressed in neither cell line [2, 110]. Possibly, the chosen FGF7 concentration was so high that it bound non-specifically to other receptor variants, or the described specificity for FGF7 to FGFR2IIIb is not as exclusive as suggested; or there are underlying species differences between mice and men.

Further, it seems dissatisfactory that no distinction can be made between BMP2 and GDF5 signaling on C2C12 cells in these data. Clearly, they do not induce all the same signaling events, as one leads to ALP activity, and the other does not. While the details of this discrepancy are not known, the lack of any observable difference makes it apparent that the selected signaling components do not represent the entirety of the ALP-inducing signaling cascade(s). In light of

these considerations, as well as the assumption that FGFR1 is likely the activated receptor in this experiment rather than FGFR2 (at least in C2C12 cells), the conclusions that can be drawn from these Western blots in terms of the underlying question are actually quite limited. As stated above, there are no indications in these data that FGFR-mediated signaling events include a downstream signal that synergizes with BMP signal transduction with regards to ALP induction. However, the design of this experiment does not allow excluding the existence of such a signal either, as other downstream mediators that were not considered here might play a role.

Hence, to target (classical) FGF signaling in a more relevant context, namely in BMP-mediated ALP induction, two inhibitors were introduced to the ALP assay. SU5402 is a receptor tyrosine kinase inhibitor used for the inhibition of FGF signaling [44, 113], while U0126 inhibits p42/p44 phosphorylation by MEK1/2 and is hence used as a p42/p44 inhibitor [114]. Neither was able to efficiently inhibit BMP2- or GDF5-induced ALP expression in ATDC5 cells. SU5402 not only failed to inhibit ALP induction, but was also unable to inhibit FGF1-induced p42/p44 phosphorylation in either cell line, as determined by Western blotting. It must be said that the ability of SU5402 to inhibit FGFR2-mediated signaling is debatable in general, as  $IC_{50}$  values are usually only specified for FGFR1 or non-FGF receptors such as VEGF [113]. However, the observed phosphorylation of p42/p44 in response to FGF1 on C2C12 cells must be mediated by FGFR1, the only FGF receptor they express [2]. Still, even if the inhibitor was applied with a concentration 30-fold of its reported  $IC_{50}$  ( $IC_{50} = \sim 30$  nM for FGFR1, according to manufacturer), no inhibition of p42/p44 phosphorylation could be observed in Western blotting. As this inhibition should be considered a prerequisite to the ALP assays, the generated data should be disregarded. U0126 was able to inhibit FGF1-induced p42/p44 phosphorylation only in C2C12 cells, as determined by Western blotting, while it could slightly to moderately inhibit ALP induction only in ATDC5 cells. This inhomogeneity between experiments renders the generated data rather inconclusive. Assuming that the observed reduction in ALP activity is genuine, the linear form of the inhibition curve would indicate an unspecific, rather than a specific, underlying interaction, and the level of inhibition at the highest concentration, exceeding the described  $IC_{50}$  values more than 10-fold ( $IC_{50} = 60 - 70$  nM, according to manufacturer), would then show that p42/p44 phosphorylation is not an essential signal for ALP induction. In this

context however, it cannot be excluded that inhibiting the FGF signaling cascade may have reduced cell proliferation, and that the reduced ALP activity may simply be caused by a reduced cell number per well at high inhibitor concentrations.

While the Western blotting and inhibitor-based approaches did not hint at a dependency of BMP signaling or BMP-mediated ALP induction on FGFR2-mediated signaling events, they could not effectively disprove it either. The redundancy in signaling pathways or the involvement of not tested non-canonical signaling events could not be excluded, and the experimental design was not optimal to investigate the question at hand. To both address FGFR2 specifically (without affecting FGFR1 or FGFR3), and to inhibit FGFR2's signaling as broadly as possible, two mutations were introduced clonally to generate FGFR2IIIc-Y656FY657E, a kinase-dead FGFR2 variant (FGFR2IIIc<sup>KD</sup>)[115, 116]. Overexpression in HEK293AD or HEK293T cells showed FGFR2IIIc<sup>KD</sup>'s dominant-negative effect on FGF1- and FGF2-mediated p42/p44 phosphorylation, likely by sequestering the FGF ligands without inducing a signal. This confirmed the kinase-dead nature of the cloned FGFR2 variant. The lentiviral transduction and selection of FGFR2IIIc<sup>KD</sup> in C2C12 was performed in parallel to wildtype FGFR2IIIc, and a required biologically relevant average increase in *Fgfr2* expression as well as a non-significant influence on cell growth within four days could likewise be shown, as was done for the other lentivirally altered cells. Notably, the *Fgfr2* expression change between C2C12 with mock vector and with *Fgfr2IIIc<sup>KD</sup>* containing vector as determined by qPCR was, again, not statistically significant. In contrast, the responsiveness to GDF5 in terms of ALP induction was robustly and significantly increased between these two cell types. C2C12 cells expressing FGFR2IIIc<sup>KD</sup> not only showed higher ALP activity in response to both BMP2 and GDF5 in comparison to C2C12<sub>mock</sub>, but in comparison to C2C12<sub>FGFR2IIIc</sub> as well. Consequently, it became very unlikely that an FGFR2-triggered signal synergizes with BMP signaling to induce ALP. On the contrary, the fact that the change in GDF5 responsiveness is only statistically significant in C2C12 cells expressing FGFR2IIIc<sup>KD</sup>, not wildtype FGFR2IIIc, suggests that downstream events triggered by the presence of FGFR2IIIc are actually able to partially reduce the BMP2/GDF5-synergistic capacities of the receptor itself. As discussed above, this could be due to more phosphorylated p42/p44 antagonizing SMAD signaling [11, 38, 41], or it could be more indirectly via an influence of FGF signaling on the expression of genes coding for

components connected to the BMP signal cascade, as is the case in most cross-talking contexts (for reference, see 1.3.1.), or via interaction in an even more complex network of growth factors, as is the case in some developmental contexts (for reference, see 1.3.2. and 1.3.3.).

If the inverse correlation between *Fgfr2* mRNA expression levels and BMP2-mediated ALP induction in C2C12 transduced with wildtype FGFR2IIIc is indeed due to kinase domain-mediated, BMP-antagonizing signals, there should be no such correlation between qPCR and ALP assay data in the kinase-dead variant experiments. Indeed, comparing *Fgfr2IIIc<sup>KD</sup>* expression and BMP2-induced ALP activity indicated no correlation (or rather, showed a tendency for direct correlation). On the other hand, qPCR data still inversely correlated with GDF5-induced ALP activity in FGFR2IIIc<sup>KD</sup> expressing cells. The fact that FGFR2IIIc<sup>KD</sup> introduction facilitates higher and more robust GDF5 responsiveness in C2C12 than wildtype FGFR2IIIc indicated the involvement of some downstream component of FGFR2 that negatively influences the induction of ALP activity. However, if this inverse correlation between qPCR and GDF5-mediated ALP data is valid, the presence of high amounts of FGFR2IIIc<sup>KD</sup> likewise negatively influences the induction of ALP activity independently of downstream signals, which would lead to the assumption that there is more than one way for FGFR2IIIc to negatively influence BMP-mediated ALP induction. Interestingly, this only seems true for C2C12 cells, as ATDC5 cells express much more FGFR2IIIc as even the most efficiently transduced C2C12 (as compared to *Hprt* and *Gapdh* in qPCR).

The question how FGFR2IIIc<sup>KD</sup> expression may negatively influence the induction of ALP expression in C2C12 independently from its kinase domain cannot be answered here, but may become clear once it is known how the interaction between FGFR2IIIc and BMP ligands BMP2 and GDF5 on the cell surface leads to higher ALP level induction in the first place.

### **5.3. Exploring the Possibility of FGFR2 as Part of the BMP Ligand-Receptor-Complex**

After establishing that a cross-talk downstream of BMP and FGF receptors is not likely to be responsible for the influence of FGFR2IIIc on BMP-induced ALP activity, the alternative hypothesis of an interaction on the cell surface was pursued.

The first question was whether BMP receptors and FGFR2IIIc could bind BMP ligands simultaneously. For this purpose, so-called co-injection experiments in SPR were performed

which showed that ActRIIB could bind to BMP2 in the presence of FGFR2IIIc, whereas the presence of BMPRIA apparently blocked the FGFR2IIIc binding site on BMP2. Hence, it can be assumed that FGFR2IIIc binds to the “wrist” epitope in BMP2, or to a site overlapping with the “wrist” epitope. This finding likely excludes the possibility that FGFR2IIIc is recruited by the BMP ligand as an additional component to the tetrameric BMP/GDF receptor complex. Does then the FGFR2IIIc bind BMP ligands independently of the BMP receptor complex, enhancing its signaling without becoming activated itself, or does FGFR2IIIc actually substitute BMPRIA in the complex? Considering the first option, there are indeed components of BMP signaling that bind the ligands independently of the receptor complex, and in doing so enhance or even facilitate BMP signaling: matrix components like heparin sulfates locally trap BMP ligands, binding and releasing them, effectively reducing the ligand's diffusion and hence elevating local concentrations [102, 132]. It is however safe to assume that this is not the case for FGFR2IIIc for two reasons: first, heparin binding of BMP ligands only has a positive influence on BMP signaling in an *in vivo* context, where diffusion actually reduces BMP levels below biologically active concentrations. In a cell culture system, the ligands have nowhere to diffuse to, and hence heparin-binding of BMPs reduces signaling capacity, as becomes apparent when comparing ALP induction by BMPs with and without heparin binding sites in cell culture (in house data). Second, local retention of the BMP ligand by heparin sulfates actually needs a constant bind-and-release, otherwise heparins would sequester BMP ligands, competing with their binding to the receptor complex. This would require low binding affinities, but the measured affinities for BMP ligands to FGFR2IIIc even exceed the ones to BMP receptors at the 1:1 ratio. Taken together, it seems unlikely that FGFR2IIIc would function in the same way as heparin sulfates in the context of BMP signaling.

In consequence, it was considered whether FGFR2IIIc could replace BMPRIA in the signaling complex. Hence, the necessity and interchangeability of these two receptors in BMP2/GDF5-mediated signaling was tested by competitive ALP induction assays. Comparing the inhibitory capacities of the soluble BMPRIA<sub>ECD</sub> and soluble FGFR2IIIc<sub>ECD</sub>, they showed similar inhibitory curves and IC<sub>50</sub> values for BMP2 signaling in C2C12. This outcome is to be expected, as they compete for the same binding site on the ligand with similar affinity against the same receptor-ligand interaction. However, BMPRIA<sub>ECD</sub> performed less well on ATDC5, while FGFR2IIIc<sub>ECD</sub>



performed better. As the ligand and the ECD's affinities to it remain the same, it seems possible that the extracellular domains are competing with different binding interactions in both cell lines, meaning that the signaling complex is composed differently.

The necessity of each receptor chain for ALP induction was determined by the addition of signal-inhibiting antibodies to the ALP assay. The anti-BMPRIA antibody employed had been tested for its signal-neutralizing ability [106, 118], and was confirmed to inhibit both BMP2- and GDF5-mediated signaling in the ALP assay. Hence, it can be assumed (and has already been stated [120]), that BMPRIA is necessary for BMP signal transduction. The anti-FGFR2 antibody is commercialized as neutralizing antibody, and could be confirmed to bind to the extracellular domain of FGFR2IIIc in western blotting (in house) as well as published to inhibit FGF signaling [117]. However, it had no effect on ALP induction by BMP2 or GDF5 in either cell line, although it should have been expected to negatively influence GDF5-signaling in ATDC5 cells in particular, similar to the shRNA. From Western blotting and immunofluorescence experiments utilizing the very same antibody to recognize FGFR2IIIc<sub>ECD</sub> or FGFR2IIIc, respectively, it can be excluded that the antibody does not bind the receptor at all. Its failure in the ALP assays to influence GDF5-signaling may simply be because it does not mask the BMP binding site on FGFR2, but this needs to be confirmed once this site is actually known.

Following the observation that BMPRIA is necessary for ALP induction in response to BMP2 or GDF5, and it can be concluded that FGFR2IIIc is unlikely to substitute both BMPRIA chains in the BMP signaling complex. However, it may substitute one. To investigate whether this is feasible, a BMP2 heterodimer consisting of one wildtype BMP2 homodimer and one BMP2-L51P was employed. BMP2-L51P is a BMP2 variant with compromised type I receptor epitope, and the efficacy of this mutation has been shown by the lack of biological activity of BMP2-L51P homodimers [120]. The BMP2<sup>wt/L51P</sup> heterodimer can consequently only activate one type I receptor in a signaling complex. Its biological activity, as shown by its ability to induce ALP in both ATDC5 and C2C12, provides evidence that a BMP receptor-ligand complex with only one (activated) type I BMP receptor chain can successfully transduce BMP2-mediated signals (at least in case of BMPRIA). A lower overall ALP signal compared to wildtype BMP2 may be expected, as BMP2<sup>wt/L51P</sup> may activate less BMPRIA receptors than the wildtype ligand, which can be observed in C2C12 (and has already been published, [105]). In ATDC5 cells however, wildtype

BMP2 and BMP2<sup>wt/L51P</sup> induce the same amount of ALP. This is unlikely due to identical abilities to activate the receptor complex and BMP signaling, as evidenced by the discrepancy observed in C2C12. Rather, these results again lead to the assumption that ATDC5 cells contain signaling complex-stabilizing components (which, in this case, may very well be the FGFR2IIIc expressed on ATDC5). The finding that BMP2<sup>wt/L51P</sup> is biologically active makes a theoretical receptor complex containing one BMPRIA, one FGFR2IIIc, and two BMP type II receptor chains a possibility.

In trying to find evidence for a complex containing both FGFR2IIIc and BMPRIA, both receptors were overexpressed in HEK293AD cells and fluorescently stained in the absence and presence of BMP2 or GDF5. The ligand-dependent colocalization of both receptors was then accessed by correlating the two fluorescent signals obtained from confocal microscopy. While the colocalization of the two stainings was moderate in all conditions, it increased significantly upon the addition of either 20 nM BMP2 or 100 nM GDF5, as compared to cells without ligand. Studying the generated colocalization colormaps revealed that colocalization did not take place over the entirety of the cell membrane, but in small, focused areas. This explained why the index of correlation (generated for the entire image) did not reach values indicating very high, overall colocalization. While this approach cannot be interpreted as proof of the hypothesized complex, it gives a strong hint to a close association of BMPRIA and FGFR2IIIc in the presence of ligand.

As has been laid out repeatedly in this discussion, the stability of the receptor-ligand complex seems to influence both the presence and the robustness of the induced ALP levels in response to ligand; and it has been argued that FGFR2IIIc possibly fills the role of a complex stabilizer, as seemingly do other, unknown components – especially in ATDC5. Another means of increasing complex stability is directly increasing ligand-receptor binding. Hence, the influence of enhanced BMP receptor type I and/or BMP receptor type II binding affinities in GDF5 on ALP induction was tested: three GDF5 mutants were compared to wildtype GDF5 or BMP2 in the ALP assay: GDF5-R57A, a mutant with enhanced affinity to type I receptors, GDF5-Y106KQ108D (GDF5-KD), a mutant with enhanced affinity to type II receptors, and GDF5-R57AY106KQ108D (GDF5-AKD), a combination mutant of the former two. In ATDC5 cells, all mutants showed higher maximal ALP

induction and lower  $EC_{50}$  values when compared to GDF5 wildtype (as has been already reported for GDF5-R57A, [106]), with GDF5-AKD performing best, and GDF5-KD second best. In C2C12 cells, both wildtype GDF5 and GDF5-R57A were not able to induce ALP (as has been reported, [106]), while GDF5-KD and GDF5-AKD could: GDF5-KD showed lower maximal ALP activity and higher  $EC_{50}$  values than BMP2, and GDF5-AKD performed better than BMP2 on both accounts. Apparently, if the receptor-ligand interaction is altered “right”, C2C12 become GDF5 responsive.

Given that the affinity of wildtype GDF5 and BMP2 is higher to type I receptors than to type II receptors, it seems straightforward that the type II receptor interaction would be more limiting than the type I receptor interaction to the overall efficacy of signal transduction by these ligands, and that therefore the elevation of type II receptor affinity in GDF5-KD would have a higher impact on the ability to induce ALP, as compared to the elevation of type I receptor affinity in GDF5-R57A. The observation that the combination of both mutations leads to an even better performance in the ALP assay shows that their influence is additive, rather than being limited by the type II receptor interaction only. It can be assumed that other factors that positively influence the assembly or stability of the signaling complex would likewise be additive to some extent, and it has been hypothesized repeatedly above that ATDC5 cells express more such factors than C2C12 do, including the FGFR2IIIc. However, the fact that GDF5-R57A on C2C12 cells does not perform better than wildtype GDF5 at all also indicates that there may be a minimum threshold that needs to be met; and while this threshold can be overcome by alterations to the receptor-ligand complex, it manifests somewhere downstream between SMAD phosphorylation and the induction of *Alp* expression.

GDF5-R57A, the mutant “intermediate” between BMP2 and GDF5 and altered in the BMP type I receptor binding site, was tested on the ATDC5 and C2C12 cells with lentivirally changed FGFR2IIIc expression. On ATDC5<sub>shRNA</sub> cells, GDF5-R57A performed as BMP2, with a non-significant decrease in ALP induction; whereas on C2C12 cells expressing either FGFR2IIIc or FGFR2IIIc<sup>KD</sup>, it performed as GDF5 with higher induced ALP levels that were only significantly increased in the presence of FGFR2IIIc<sup>KD</sup>, not FGFR2IIIc. Therefore, ALP induction by GDF5-R57A is influencable by the presence of FGFR2IIIc, but to a lesser extent than wildtype GDF5, confirming that GDF5-R57A is not a simple “BMP2-mimic”, but is comparable either to BMP2 or GDF5, depending on

context (see [106]).

#### **5.4. Drawing Conclusions**

The central question of this thesis is, how does the FGFR2 exert its influence on BMP signal transduction?

The findings presented indicate that it is interactions on the cell surface that are crucial. This assumption is in line with the original hypothesis of an unknown co-receptor being responsible for the observed ligand-specific differences, as other known co-receptors such as betaglycan, endoglin, cripto, or RGMs, all operate by altering ligand-receptor interaction on the cell surface, and have no direct influence on signal transduction within the cell. However, the mechanisms behind this differ. As FGFR2IIIc (at least partially) binds to the same epitope in BMP2 as type I receptors, its mode of action may be a “release or replace mechanism”, as it has been suggested for RGMs and other co-receptors [101]: raising the likelihood of a BMP ligand-receptor assembly without becoming part of the signaling complex. On the other hand, it may have to replace one BMPRIA chain and enter the complex, as has been already suggested above. Similar mechanisms have been described for endoglin with TGFβs, or Cripto with Nodal [101].

It is beyond the experiments put forth in this thesis to definitely determine whether the FGFR2IIIc replaces one BMPRIA chain and becomes part of the complex, or whether it elicits its influence by another mechanism more akin to the ones suggested for other co-receptors. What can be stated based on the described findings is that FGFR2IIIc functions as a co-receptor, meaning it directly influences the BMP signal transduction on the cell surface by interacting with the core ligand-receptor complex.

How then does stabilizing the signaling complex elevate signal transduction? To answer this question, particularly in regards to TGFβ/BMP signaling, it is worth remembering that signal transduction via SMADs is no cascade of repeated phosphorylation leading to signal amplification, as is the case e.g. for MAP kinase signaling. On the contrary, receptor activation and SMAD phosphorylation are quite linear events; the same SMAD molecule that gets activated by the receptor translocates into the nucleus and acts as transcription factor. Thus, ligand-induced receptor activation does not “switch on” a cell response that is amplified and

hence stabilized inside the cell by a phosphorylation cascade, but rather elicits an easily modifiable and readily reversible activated cell state [8, 11]. If then the same concentration of ligand can activate more receptors or keep the same amount of receptors activated longer in the presence of a co-receptor, more SMAD proteins become phosphorylated and the downstream signal is more pronounced.

While this is quite straightforward, it does not explain all observable discrepancies, such as: how can a ligand like GDF5 activate SMAD phosphorylation in C2C12 cells, but not elevate *Alp* expression? And how is the threshold in the induction of ALP that was observed with the GDF5 mutants on C2C12 cells achieved? In other words: how does an alteration in signal complex stability translate into different signals downstream of phospho-SMAD?

One possibility is that the quantitative amount of phospho-SMAD plays a major role. SMAD-responsive elements in the genome are weak-binding, but may occur multiple times in close proximity as cooperative binding sites [8, 11]. This phenomenon may be responsible for translating different quantities of phosphorylated SMAD into different degrees of translational responses, and begs to address both intensity and duration of SMAD phosphorylation, overall SMAD expression levels, and localization of phosphorylated SMAD complexes, when assessing the biological activity of a BMP ligand.

Another possibility is the necessity of a second downstream component for some targets of BMP signaling. Several additional signaling molecules have been implicated to play a non-redundant role in BMP signaling in ATDC5 and/or C2C12 and/or for ALP induction. For example, it has been shown that the biological activity of BMP4 in C2C12 cells is widely dependent on Notch signaling (although not all target genes were affected by the presence of Notch). Apparently, BMP4 can directly induce downstream components of Notch such as *Hes1* and *Hey1* in dependency of an active Notch signal, and it has been suggested that it does so by transcription complexes containing both SMAD1 and Notch intracellular domain [133]. While the up-regulation of Notch effector genes by an active BMP signal can be found in some other cellular contexts [13, 134], the opposite is likewise described [135].

Several MAP kinases have also been linked to BMP-dependent signal transduction, although the findings here are likewise not entirely consistent. For example, the comparison of early studies shows that one of them claims BMP2 induces p38, but not p42/p44 phosphorylation in C2C12

[136], while the next claims the induction of both p38 and p42/p44 phosphorylation by the same ligand in the same cells, but not JNK [14], yet another study reports p38 and JNK phosphorylation induction by BMP2 in other osteoblastic cells, but only neglectible activation of p42/p44 [137], and another one claims early p38 activation, late JNK activation, and constant p42/p44 activation by BMP2 in osteoblastic HOB cells [138]. All four studies examine the influence of phospho-p38 on ALP and osteocalcin (OC) induction by BMP2 using the same p38 inhibitor SB203580, which actually fails to inhibit all forms of p38 [139]. One study concludes that p38 inhibition has a negative effect on both ALP and OC levels [14], two conclude that it has a positive effect on both [136, 138], and one finds a negative effect on ALP and a positive effect on OC induction [137]. What all four studies agree upon is the transient nature of p38 phosphorylation by BMP2, peaking at between 1 and 2 hours and vanishing by hour 6-8 (while the earliest induction of *Alp* mRNA is shown after 8 hours [14], and ALP protein levels rise even later [105]). In ATDC5 cells, it was shown that GDF5-induced p38 did not influence the induction of ALP by GDF5 [140].

More recent studies often show the (strong) induction of p38 phosphorylation by BMP2 only in the presence of a secondary activating components [141-143] or in hypoxia as opposed to normoxia [144].

Today, the notion that BMPs activate p38 is more accepted than the contrary, and quite frequently referenced in respective articles and reviews [21, 36, 145, 146]. It should be mentioned that some do not distinguish between BMP and TGF $\beta$  ligands, and hence quote references that only investigated the latter (e.g., [21]), while others do not distinguish between BMP2/BMPRIA and BMP7/ALK2 signaling (e.g. [145, 147]). One study equated ATF-2<sup>f</sup> phosphorylation with p38 activation, although they did not show p38 phosphorylation in response to BMP2 despite the fact that they employed a respective antibody in another setup [148].

Still, BMP ligand induction of p38 has been shown (e.g. Lee et. al. [150], who do not lean on SB203580 for their experiments, as well as the examples above), sometimes along with one of its upstream regulators, TAK1. TAK1 has also been reported to directly associate with SMADs 1 through 7, and to influence the cellular localization of SMADs 1, 2, and 3 [151], as well as the

---

f). Activating transcription factor-2 (ATF-2) is a downstream component either of p38 or of JNK [149].

phosphorylation status of SMADs 1, 5, and 8 [9]. TAK1/p38 activation by BMPs is mostly functionally linked either to chondrogenesis rather than osteogenesis, as evidenced by cellular assays [140, 148] and conditional knock-out models [51, 52, 147]; or it has been associated with BMP-induced apoptosis [152-154].

In our hands, we could not find an active p38 signal in response to BMP2 or GDF5. While we are aware that others have found one in comparable setups [98, 140, 150], the literature reviewed above suggests that BMP-mediated p38 phosphorylation is not a robust outcome. It has even been suggested that most observations could likewise be explained by p38 acting as a co-activator of SMADs and/or Runx2, rather than being a downstream effector of BMPs [155]. In any case, p38 most likely is a fine-tuner of BMP2 activity in osteochondral tissues [51, 52], rather than a central part of it.

Considerations of a second signal may plausibly account for cell-specific differences, but they fail to sufficiently explain why two ligands BMP2 and GDF5, utilizing the same receptors BMPRIA and BMPRII, on the same cell C2C12, should induce different downstream targets. How would a second signal be induced by one, and not the other? GDF5 would have to recruit a signaling complex that is different from that recruited by BMP2, and as it would unlikely differ in its core components (other than the ligand itself), it would have to incorporate additional, unknown complex components, or exhibit a different complex geometry, stoichiometry, or assembly sequence.

Unfortunately, the exact dynamics of assembling a ternary signaling complex is a difficult field of study. While many aspects of both BMP and FGF signaling are considered proven and enjoy universal consensus in the community (for example the existence of certain receptor-ligand pairs, or the necessity of key signal transduction components including SMADs or MAPKs, respectively), the details of signaling complex assembly are very much under debate, carried out on a proverbial „battle scene“ [26]. In terms of the above mentioned geometry, stoichiometry, or assembly sequence of even the core ligand-receptor complexes, there is no consensus in either family – is there one mechanism, or several? And as right now there are more likely to be several, what are the components that they have in common, how exactly do they differ, and what does it depend on to follow one rather than the others? Is the activity of a co-receptor or

other involved component determined by these properties, or do they determine them? Answering these questions is complicated, because we have no means of directly observing the formation of a complex. We rely on indirect measurements in smartly designed experiments to then deduce what is most likely, and more often than not we can then only make statements for very defined circumstances.

This thesis aimed to identify a co-receptor that enables GDF5 signaling, expecting a qualitative biological effect: if the factor is present, GDF5 signaling is there, if it is absent, then so is the signal. What we observed with FGFR2 was a much more heterogeneous, gradual biological effect, that could even be called unpredictable in regards to the wildtype protein. While this did not meet the original expectations, it can be consolidated in the context of developmental mechanisms: It is in the nature of morphogens that they do not elicit a qualitative on/off effect, but a quantitative one. In development, different morphogen gradients usually meet, and the concentration of each growth factor as well as their quantitative relation to each other is what determines cell fate in any particular point of the embryo. Looking at skeletal development in particular, the key factors regulating endochondral ossification in both long bones and the chondrocranium, as well as regulating membranous ossification in the calvaria, are the same: TGF $\beta$ s and hedgehog proteins drive precursor proliferation, FGFR3-mediated signaling hinders it in antagonism with BMPs, while FGFR1/2-mediated signaling drives osteochondral differentiation in concert with them and with Runx2, and so forth. It has been repeatedly suggested that differences between different parts of the skeleton arise from fine-tuning the plethora of signals present, rather than from different players at each site [56, 66]. While severe phenotypes identify key factors such as BMP2, Sox9, or Runx2 [22, 23, 156, 157], the origin of mild or moderate phenotypes is often not understood: different GDF5 mutations affect a small and very distinct number of bones or joints; some mutations of FGFR3 mostly affect the craniofacial bones, leaving other bones of the skeleton intact, while others cause severe dwarfism with normal calvarial development [158], and as of now, it cannot be explained how these different mutations in the same protein have such distinct and different effects on development. However, it provides context to the observation that the effect of FGFR2's presence on GDF5-mediated signaling is moderate, and dependent on cell type and expression



levels. It is likely that we do not only measure direct FGFR2-GDF5 interaction, but the sum of a larger number of involved proteins, shifted by the manipulation of FGFR2 expression levels.

FGFR2 could be identified as one component to influence BMP/GDF signal transduction in ATDC5 and C2C12 cells, and the biological significance of this interaction may lie in the fine-tuning of BMP-FGF interaction. In the shift from BMP-FGF antagonism during chondrocyte proliferation to BMP-FGF synergism during hypertrophy, the involved BMP ligands are mostly the same, but the involved FGF receptors change from FGFR3 to FGFRs 1 and 2. The data presented here may help to understand this shift in growth factor communication. It also suggests that a BMP signaling complex may have far more interaction partners and modulators than are currently known. The identification of more such components may consolidate the observed BMP ligand promiscuity to their receptors with the plethora of BMP-mediated biological functions.

## 6. Outlook

In this thesis, it was shown that FGFR2 functions as a co-receptor to BMP ligands such as GDF5 and BMP2. Further investigations of this new FGF receptor/BMP ligand interaction promise to touch many fields of research in the future. Its implications for growth factor family networks, as well as the potential influence of RTKs in general on BMP signal diversity and specificity must be intriguing to the basic researcher, while its relevance in programming osteochondral cell types must be important to the applied scientist, and its potential benefits for understanding and counteracting diseases of osteochondral tissues especially must seem rewarding to a clinician.

The steps taken next depend on the questions we ask: Does FGFR2IIIc really become part of the BMP signaling complex? Experiments involving co-immunoprecipitation or FRET of BMP receptor chains and FGFR2IIIc in the absence and presence of BMP ligands may shed further light on this.

Do other ligands apart from GDF5 (and BMP2) need FGFR2IIIc for a subset of their biological functions, and can other RTKs likewise act as co-receptor to BMPs? Initial SPR measurements would open the door to investigations similar to the ones detailed in this thesis, only with different ligands or a different receptor tyrosine kinase: FGFR1 and FGFR3 would be interesting candidates if considering the osteochondral environment further, while a theoretical interaction of VEGF with BMPs could have ramifications in vessel development and maintenance.

Apart from the interaction with RTKs, other questions remain open. What other components are involved in BMP signaling on ATDC5 cells that are absent in C2C12? Going back to the microarray data that were produced prior to this thesis may give some hints as to what it is that makes a BMP2 signal in ATDC5 seemingly more effective and robust than in C2C12. Generating membrane fractions of ATDC5 in the presence of BMP2 or GDF5, and identifying new membrane-bound binding partners of these ligands, may give indications as to how signaling complexes in ATDC5 and C2C12 cells are composed in dependence of the cell type. If candidates

can be identified, experimental set-ups like the ones detailed in this thesis may be employed again. Depending on the candidate, it might also be feasible to utilize a BMP non-responsive cell line in which to overexpress single components including the BMP receptors, and investigating their influence on signal transduction dynamics independently of the multi-factored networks found in our model cell lines.

Finally, the central question of this thesis remains: how exactly do the signals induced by GDF5 and BMP2 differ in C2C12? Why does GDF5 signal differently in ATDC5 and C2C12 cells? This question has not been answered here, as the data presented in this thesis showed that, while FGFR2IIIc played a role, it is not the central, mediating (“on/off”) component underlying this observation. One way to address these questions would be additional Western blotting experiments, aiming to identify signaling components that are differentially activated. For example, Notch signaling has been implied in BMP-mediated ALP induction, as described above, and has not been tested here. Broader approaches may include Western blotting based on arrays for the activation of many signaling components at the same time, or microarray analysis comparing the transcriptomes of the cells in the absence and presence of the ligands. The additional identification of more modulators of BMP/GDF signal transduction will help to understand the discrepancy between the biological activities of GDF5 and BMP2.

# 7. Index

## 7.1. Table of Abbreviations

<b><i>Abbreviation</i></b>	<b><i>Meaning</i></b>
A	Adenosine
AB	Antibody
ALK	Activin Receptor-Like Kinase
ALP	Alkaline Phosphatase
BMP	Bone Morphogenetic Protein
BMPR	BMP Receptor
BRIA	BMP Receptor IA
BSA	Bovine Serum Albumin
C	Cytosine
CBP	CREB-Binding Protein
CD510B	pCDH-CMV-MCS-EF1-Puro
CDC42	Cell Division Control protein 42 homolog
CDK	Cyclin-Dependent Kinase
CI	Co-Localization Index
Co-SMAD	Common Mediator/Partner SMAD
Crk	Other name for p38
CRKL	Crk-Like Protein
DAG	Diacylglycerol
Daxx	Death associated protein 6
DMEM	Dulbecco's Modified Eagle Medium
DMSO	DiMethyl SulfOxide
DNA	DesoxyriboNucleic Acid
Dusp	Dual Specificity Phosphatase
ECM	ExtraCellular Matrix
FCS	Fetal Calf Serum
FGF	Fibroblastic Growth Factor

<b><i>Abbreviation</i></b>	<b><i>Meaning</i></b>
FGFR2	FGF Receptor 2
FGFR2-ECD	ExtraCellular Domain of FGFR2
FGFR2-trunc	FGFR2 truncated
FGFR2 <sup>KD</sup>	Kinase-Dead FGFR2
FGFRL1	FGFR Like 1
FOP	Fibrodysplasia Ossificans Progressiva
FR2	FGFR2
FRS2 $\alpha$	FGFR Substrate 2 $\alpha$
G	Guanine
Gab1	Grb2-Associated Binding Protein
GDF	Growth/Differentiation Factor
Grb2	Growth Factor Receptor-Bound 2
GS	Glycine-/Serine-Rich Domain
GSK3	Glycogen Synthase Kinase 3
HEPES	IUPAC: 4-(2-hydroxyethyl)-1-piperazineethanesulfonic acid
HS	Heparan Sulfate
HSPG	HS Proteoglycan
I-SMAD	Inhibitory SMAD
Ig	Immunoglobulin-like Domain
IP <sub>3</sub>	Inositol Triphosphate
JNK	C-Jun N-terminal Kinase
KLPH	Klotho/Lactase-Phlorizin Hydrolase-Related Protein ( $\gamma$ Klotho)
LIMK	LIM domain Kinase
MAN1	Inner nuclear Membrane protein 1
MAPK	Mitogen-Activated Protein Kinase
maxiprep	Large-Scale DNA Plasmid Preparation
MEK	MAPK kinase
miniprep	Small-Scale DNA Plasmid Preparation
MWU	Mann-Whitney U
NP40	Nonidet P-40 (IUPAC: 4-Nonylphenyl-polyethylene glycol)
p300	histone acetyltransferase p300
pBlue	pBlue Skript II SK (+)
PBS	Phosphate Buffered Saline
PCR	Polymerase Chain Reaction

<b>Abbreviation</b>	<b>Meaning</b>
PDP	Pyruvate Dehydrogenase Phosphatase
PI3K	Phosphadidylinositol-4,5-Biphosphate 3-Kinase
PLC $\gamma$	Phospholipase C $\gamma$
pNPP	Paranitrophenyl-Phosphate Disodium Hexahydrate
PPM1A	Mg <sup>2+</sup> /Mn <sup>2+</sup> dependent protein phosphatase 1A
qPCR	Quantitative Real-Time PCR
R-SMAD	Receptor-Regulated SMAD
RGM	Repulsive Guidance Molecule
RNA	Ribonucleic Acid
RTK	Receptor Tyrosine Kinase
SBE	SMAD-Binding Element
Shb	Sh2 Domain-Containing Adapter Protein B
Shc1	Src Homology 2 domain Containing transforming protein 1
SHP2	The Tyrsine-Protein Phosphatase Non-Receptor Type 11
Smurf	SMAD specific E3 Ubiquitination Regulatory Factor
SnoN	SKI like protein
SOS	Sons of Senseless
Spry	Sprouty
STAT	Signal Transducer and Activator of Transcription
T	Thymine
TAK1	TGF $\beta$ -Activated Kinase 1
TBS	Tris Buffered Saline
TGF $\beta$	Transforming Growth Factor $\beta$
TRAF6	Tumor Necrosis Factor (TNF) Receptor-Associated Factor 6
T $\beta$ R	TGF $\beta$ Receptor
WB	Western Blotting
wt	Wildtype

*Table 5: Abbreviations*

## 7.2. List of Figures

Figure 1: BMP Signal Transduction .....	14
Figure 2: FGF Signal Transduction .....	20
Figure 3: FGFR2 Splice Variants.....	22
Figure 4: pBlue Script II SK (+).....	42
Figure 5: pCDH-CMV-MCS-EF1-Puro.....	44
Figure 6: BMP2 and GDF5 Bind to FGFR2IIIcECD.....	50
Figure 7: FGFR2IIIcECD blocks BMP2- and GDF5-induced ALP Expression.....	52
Figure 8: Fgfr2 Down-Regulation Specifically Reduces GDF5-induced ALP Expression.....	53
Figure 9: Elevated FGFR2IIIc Expression Increases C2C12 Responsiveness to BMP2 and GDF5.....	55
Figure 10: Correlation between Fgfr2IIIc expression levels and ALP performance in C2C12 cells.....	57
Figure 11: BMP/FGF Cross-Talk on C2C12 Cells .....	59
Figure 12: BMP/FGF Cross-Talk on ATDC5 Cells .....	60
Figure 13: Influence of p42/p44 Inhibition on BMP-Dependent ALP Induction .....	62
Figure 14: FGFR2IIIc Kinase Activity Is not Necessary for Its Influence on ALP Activity.....	64
Figure 15: Correlation between Fgfr2IIIc expression levels and ALP performance in C2C12 cells.....	65
Figure 16: FGFR2IIIcECD Competes with BMPRIAECED in SPR Measurements.....	67
Figure 17: The Dependence of ALP Induction on BMPRIA and FGFR2IIIc .....	69
Figure 18: Heteromeric BMP2wt/L51P Is Capable of Inducing ALP Expression.....	70
Figure 19: FGFR2IIIc and BMPRIA Co-Localize In Dependence of Ligand.....	72
Figure 20: Performance of GDF5 Mutants in the Presence or Absence of FGFR2 .....	74
Figure A21: Regulatory Components in the Development of the Cranial and Appendicular Skeleton .....	122
Figure A22: Examples of BMP-FGF Interactions in Development .....	124

### 7.3. List of Tables

Table 1: PCR-Primers.....	41
Table 2: Cloning Primers.....	43
Table 3: EC50 values of ligand variants.....	73
Table 4: EC50 value changes upon Fgfr2 expression alteration.....	75
Table 5: Abbreviations.....	102
Table A1: The 100 most differentially expressed membrane-associated genes between ATDC5 and C2C12 cells.....	119
Table A2: Pairings of TGF $\beta$ ligands and their receptors.....	120
Table A3: Pairings of FGF ligands and their receptors.....	121
Table A4: Equipment.....	126
Table A5: Laboratory Material and Consumables.....	127
Table A6: Chemicals.....	129
Table A7: Solutions.....	132
Table A8: Cell Lines.....	132
Table A9: Proteins.....	133
Table A10: Antibodies.....	133
Table A11: Plasmids.....	134
Table A12: Kits.....	135
Table A13: Software.....	136
Table A14: Figure References to the Laboratory Notebook.....	138



## 8. Literature

1. Schliermann A, Nickel J: **Unraveling the Connection between Fibroblast Growth Factor and Bone Morphogenetic Protein Signaling.** *International journal of molecular sciences* 2018, **19**(10).
2. Schliermann A; Seher, A; Prenzlau, F; Siverino, C; Sasse, F; Kneitz, S; Mueller, TD; Nickel, J: **A Receptor with Identity Crisis: Fibroblast Growth Factor Receptor 2 Directly Binds BMPs to modulate their signaling outcome.** In: *PNAS* (submitted).
3. Vogel C, Chothia C: **Protein family expansions and biological complexity.** *PLoS computational biology* 2006, **2**(5):e48.
4. Mueller TD, Nickel J: **Promiscuity and specificity in BMP receptor activation.** *FEBS letters* 2012, **586**(14):1846-1859.
5. Nickel J, Sebald W, Groppe JC, Mueller TD: **Intricacies of BMP receptor assembly.** *Cytokine & growth factor reviews* 2009, **20**(5-6):367-377.
6. Kotzsch A, Nickel J, Seher A, Heinecke K, van Geersdaele L, Herrmann T, Sebald W, Mueller TD: **Structure analysis of bone morphogenetic protein-2 type I receptor complexes reveals a mechanism of receptor inactivation in juvenile polyposis syndrome.** *The Journal of biological chemistry* 2008, **283**(9):5876-5887.
7. Macias MJ, Martin-Malpartida P, Massague J: **Structural determinants of Smad function in TGF-beta signaling.** *Trends in biochemical sciences* 2015, **40**(6):296-308.
8. Schmierer B, Hill CS: **TGFbeta-SMAD signal transduction: molecular specificity and functional flexibility.** *Nature reviews Molecular cell biology* 2007, **8**(12):970-982.
9. Greenblatt MB, Shim JH, Glimcher LH: **TAK1 mediates BMP signaling in cartilage.** *Annals of the New York Academy of Sciences* 2010, **1192**:385-390.
10. Moustakas A, Heldin CH: **Non-Smad TGF-beta signals.** *Journal of cell science* 2005, **118**(Pt 16):3573-3584.
11. Weiss A, Attisano L: **The TGFbeta superfamily signaling pathway.** *Wiley interdisciplinary reviews Developmental biology* 2013, **2**(1):47-63.
12. Lee MY, Lim HW, Lee SH, Han HJ: **Smad, PI3K/Akt, and Wnt-dependent signaling pathways are involved in BMP-4-induced ESC self-renewal.** *Stem cells* 2009, **27**(8):1858-1868.
13. Zhang T, Wen F, Wu Y, Goh GS, Ge Z, Tan LP, Hui JH, Yang Z: **Cross-talk between TGF-beta/SMAD and integrin signaling pathways in regulating hypertrophy of mesenchymal stem cell chondrogenesis under deferral dynamic compression.** *Biomaterials* 2015, **38**:72-85.
14. Gallea S, Lallemand F, Atfi A, Rawadi G, Ramez V, Spinella-Jaegle S, Kawai S, Faucheu C, Huet L, Baron R *et al*: **Activation of mitogen-activated protein kinase cascades is involved in regulation of bone morphogenetic protein-2-induced osteoblast differentiation in pluripotent C2C12 cells.** *Bone* 2001, **28**(5):491-498.

15. Kretschmar M, Doody J, Massague J: **Opposing BMP and EGF signalling pathways converge on the TGF-beta family mediator Smad1**. *Nature* 1997, **389**(6651):618-622.
16. Hatsell SJ, Idone V, Wolken DM, Huang L, Kim HJ, Wang L, Wen X, Nannuru KC, Jimenez J, Xie L *et al*: **ACVR1R206H receptor mutation causes fibrodysplasia ossificans progressiva by imparting responsiveness to activin A**. *Science translational medicine* 2015, **7**(303):303ra137.
17. Olsen OE, Wader KF, Hella H, Mylin AK, Turesson I, Nesthus I, Waage A, Sundan A, Holien T: **Activin A inhibits BMP-signaling by binding ACVR2A and ACVR2B**. *Cell communication and signaling : CCS* 2015, **13**:27.
18. Ruppert R, Hoffmann E, Sebald W: **Human bone morphogenetic protein 2 contains a heparin-binding site which modifies its biological activity**. *European journal of biochemistry* 1996, **237**(1):295-302.
19. Song K, Krause C, Shi S, Patterson M, Suto R, Grgurevic L, Vukicevic S, van Dinther M, Falb D, Ten Dijke P *et al*: **Identification of a key residue mediating bone morphogenetic protein (BMP)-6 resistance to noggin inhibition allows for engineered BMPs with superior agonist activity**. *The Journal of biological chemistry* 2010, **285**(16):12169-12180.
20. Corradini E, Babitt JL, Lin HY: **The RGM/DRAGON family of BMP co-receptors**. *Cytokine & growth factor reviews* 2009, **20**(5-6):389-398.
21. Derynck R, Zhang YE: **Smad-dependent and Smad-independent pathways in TGF-beta family signalling**. *Nature* 2003, **425**(6958):577-584.
22. Goldman DC, Donley N, Christian JL: **Genetic interaction between Bmp2 and Bmp4 reveals shared functions during multiple aspects of mouse organogenesis**. *Mechanisms of development* 2009, **126**(3-4):117-127.
23. Wang RN, Green J, Wang Z, Deng Y, Qiao M, Peabody M, Zhang Q, Ye J, Yan Z, Denduluri S *et al*: **Bone Morphogenetic Protein (BMP) signaling in development and human diseases**. *Genes & diseases* 2014, **1**(1):87-105.
24. Dudley AT, Robertson EJ: **Overlapping expression domains of bone morphogenetic protein family members potentially account for limited tissue defects in BMP7 deficient embryos**. *Developmental dynamics : an official publication of the American Association of Anatomists* 1997, **208**(3):349-362.
25. Ornitz DM, Itoh N: **The Fibroblast Growth Factor signaling pathway**. *Wiley interdisciplinary reviews Developmental biology* 2015, **4**(3):215-266.
26. Pomin VH: **Paradigms in the structural biology of the mitogenic ternary complex FGF:FGFR:heparin**. *Biochimie* 2016, **127**:214-226.
27. Turner N, Grose R: **Fibroblast growth factor signalling: from development to cancer**. *Nature reviews Cancer* 2010, **10**(2):116-129.
28. Luo Y, Yang C, Jin C, Xie R, Wang F, McKeehan WL: **Novel phosphotyrosine targets of FGFR2IIIb signaling**. *Cellular signalling* 2009, **21**(9):1370-1378.
29. Belov AA, Mohammadi M: **Grb2, a double-edged sword of receptor tyrosine kinase signaling**. *Science signaling* 2012, **5**(249):pe49.
30. Eswarakumar VP, Lax I, Schlessinger J: **Cellular signaling by fibroblast growth factor receptors**. *Cytokine & growth factor reviews* 2005, **16**(2):139-149.
31. Hatch NE, Hudson M, Seto ML, Cunningham ML, Bothwell M: **Intracellular retention, degradation, and signaling of glycosylation-deficient FGFR2 and craniosynostosis**

- syndrome-associated FGFR2C278F.** *The Journal of biological chemistry* 2006, **281**(37):27292-27305.
32. Xia X, Kumru OS, Blaber SI, Middaugh CR, Li L, Ornitz DM, Sutherland MA, Tenorio CA, Blaber M: **Engineering a Cysteine-Free Form of Human Fibroblast Growth Factor-1 for "Second Generation" Therapeutic Application.** *Journal of pharmaceutical sciences* 2016, **105**(4):1444-1453.
33. Matsuda Y, Ueda J, Ishiwata T: **Fibroblast growth factor receptor 2: expression, roles, and potential as a novel molecular target for colorectal cancer.** *Pathology research international* 2012, **2012**:574768.
34. Amann T, Bataille F, Spruss T, Dettmer K, Wild P, Liedtke C, Muhlbauer M, Kiefer P, Oefner PJ, Trautwein C *et al*: **Reduced expression of fibroblast growth factor receptor 2IIIb in hepatocellular carcinoma induces a more aggressive growth.** *The American journal of pathology* 2010, **176**(3):1433-1442.
35. Cha JY, Lambert QT, Reuther GW, Der CJ: **Involvement of fibroblast growth factor receptor 2 isoform switching in mammary oncogenesis.** *Molecular cancer research : MCR* 2008, **6**(3):435-445.
36. Itoh H, Hattori Y, Sakamoto H, Ishii H, Kishi T, Sasaki H, Yoshida T, Koono M, Sugimura T, Terada M: **Preferential alternative splicing in cancer generates a K-sam messenger RNA with higher transforming activity.** *Cancer research* 1994, **54**(12):3237-3241.
37. Roghani M, Moscatelli D: **Prostate cells express two isoforms of fibroblast growth factor receptor 1 with different affinities for fibroblast growth factor-2.** *The Prostate* 2007, **67**(2):115-124.
38. Guo X, Wang XF: **Signaling cross-talk between TGF-beta/BMP and other pathways.** *Cell research* 2009, **19**(1):71-88.
39. Bierie B, Moses HL: **Tumour microenvironment: TGFbeta: the molecular Jekyll and Hyde of cancer.** *Nature reviews Cancer* 2006, **6**(7):506-520.
40. Shi Q, Chen YG: **Interplay between TGF-beta signaling and receptor tyrosine kinases in tumor development.** *Science China Life sciences* 2017, **60**(10):1133-1141.
41. Sapkota G, Alarcon C, Spagnoli FM, Brivanlou AH, Massague J: **Balancing BMP signaling through integrated inputs into the Smad1 linker.** *Molecular cell* 2007, **25**(3):441-454.
42. Dorey K, Amaya E: **FGF signalling: diverse roles during early vertebrate embryogenesis.** *Development* 2010, **137**(22):3731-3742.
43. Tuazon FB, Mullins MC: **Temporally coordinated signals progressively pattern the anteroposterior and dorsoventral body axes.** *Seminars in cell & developmental biology* 2015, **42**:118-133.
44. Srinivasan S, Hu JS, Currle DS, Fung ES, Hayes WB, Lander AD, Monuki ES: **A BMP-FGF morphogen toggle switch drives the ultrasensitive expression of multiple genes in the developing forebrain.** *PLoS computational biology* 2014, **10**(2):e1003463.
45. Basson MA: **Signaling in cell differentiation and morphogenesis.** *Cold Spring Harbor perspectives in biology* 2012, **4**(6).
46. Berendsen AD, Olsen BR: **Bone development.** *Bone* 2015, **80**:14-18.
47. Norrie JL, Lewandowski JP, Bouldin CM, Amarnath S, Li Q, Vokes MS, Ehrlich LIR, Harfe BD, Vokes SA: **Dynamics of BMP signaling in limb bud mesenchyme and polydactyly.** *Developmental biology* 2014, **393**(2):270-281.
48. Verheyden JM, Sun X: **An Fgf/Gremlin inhibitory feedback loop triggers termination of**

- limb bud outgrowth.** *Nature* 2008, **454**(7204):638-641.
49. Nishimura R, Hata K, Matsubara T, Wakabayashi M, Yoneda T: **Regulation of bone and cartilage development by network between BMP signalling and transcription factors.** *Journal of biochemistry* 2012, **151**(3):247-254.
50. Olsen BR, Reginato AM, Wang W: **Bone development.** *Annual review of cell and developmental biology* 2000, **16**:191-220.
51. Wu M, Chen G, Li YP: **TGF-beta and BMP signaling in osteoblast, skeletal development, and bone formation, homeostasis and disease.** *Bone research* 2016, **4**:16009.
52. Chen CG, Thuillier D, Chin EN, Alliston T: **Chondrocyte-intrinsic Smad3 represses Runx2-inducible matrix metalloproteinase 13 expression to maintain articular cartilage and prevent osteoarthritis.** *Arthritis and rheumatism* 2012, **64**(10):3278-3289.
53. Ferguson CM, Schwarz EM, Reynolds PR, Puzas JE, Rosier RN, O'Keefe RJ: **Smad2 and 3 mediate transforming growth factor-beta1-induced inhibition of chondrocyte maturation.** *Endocrinology* 2000, **141**(12):4728-4735.
54. Mishina Y, Snider TN: **Neural crest cell signaling pathways critical to cranial bone development and pathology.** *Experimental cell research* 2014, **325**(2):138-147.
55. Jing J, Ren Y, Zong Z, Liu C, Kamiya N, Mishina Y, Liu Y, Zhou X, Feng JQ: **BMP receptor 1A determines the cell fate of the postnatal growth plate.** *International journal of biological sciences* 2013, **9**(9):895-906.
56. Wei X, Hu M, Mishina Y, Liu F: **Developmental Regulation of the Growth Plate and Cranial Synchronosis.** *Journal of dental research* 2016, **95**(11):1221-1229.
57. Studer D, Millan C, Ozturk E, Maniura-Weber K, Zenobi-Wong M: **Molecular and biophysical mechanisms regulating hypertrophic differentiation in chondrocytes and mesenchymal stem cells.** *European cells & materials* 2012, **24**:118-135; discussion 135.
58. Dy P, Wang W, Bhattaram P, Wang Q, Wang L, Ballock RT, Lefebvre V: **Sox9 directs hypertrophic maturation and blocks osteoblast differentiation of growth plate chondrocytes.** *Developmental cell* 2012, **22**(3):597-609.
59. Kozhemyakina E, Lassar AB, Zelzer E: **A pathway to bone: signaling molecules and transcription factors involved in chondrocyte development and maturation.** *Development* 2015, **142**(5):817-831.
60. Marie PJ, Debiais F, Hay E: **Regulation of human cranial osteoblast phenotype by FGF-2, FGFR-2 and BMP-2 signaling.** *Histology and histopathology* 2002, **17**(3):877-885.
61. van der Kraan PM, van den Berg WB: **Chondrocyte hypertrophy and osteoarthritis: role in initiation and progression of cartilage degeneration?** *Osteoarthritis and cartilage* 2012, **20**(3):223-232.
62. Kornak U, Mundlos S: **Genetic disorders of the skeleton: a developmental approach.** *American journal of human genetics* 2003, **73**(3):447-474.
63. Agas D, Sabbieti MG, Marchetti L, Xiao L, Hurley MM: **FGF-2 enhances Runx-2/Smads nuclear localization in BMP-2 canonical signaling in osteoblasts.** *Journal of cellular physiology* 2013, **228**(11):2149-2158.
64. Tubbs RS, Bosmia AN, Cohen-Gadol AA: **The human calvaria: a review of embryology, anatomy, pathology, and molecular development.** *Child's nervous system : ChNS : official journal of the International Society for Pediatric Neurosurgery* 2012, **28**(1):23-31.
65. Abzhanov A, Rodda SJ, McMahon AP, Tabin CJ: **Regulation of skeletogenic differentiation in cranial dermal bone.** *Development* 2007, **134**(17):3133-3144.

66. Levi B, Wan DC, Wong VW, Nelson E, Hyun J, Longaker MT: **Cranial suture biology: from pathways to patient care.** *The Journal of craniofacial surgery* 2012, **23**(1):13-19.
67. Johnson D, Wilkie AO: **Craniosynostosis.** *European journal of human genetics : EJHG* 2011, **19**(4):369-376.
68. Franco HL, Casasnovas J, Rodriguez-Medina JR, Cadilla CL: **Redundant or separate entities?--roles of Twist1 and Twist2 as molecular switches during gene transcription.** *Nucleic acids research* 2011, **39**(4):1177-1186.
69. Timberlake AT, Choi J, Zaidi S, Lu Q, Nelson-Williams C, Brooks ED, Bilguvar K, Tikhonova I, Mane S, Yang JF *et al*: **Two locus inheritance of non-syndromic midline craniosynostosis via rare SMAD6 and common BMP2 alleles.** *eLife* 2016, **5**.
70. Warren SM, Greenwald JA, Spector JA, Bouletreau P, Mehrara BJ, Longaker MT: **New developments in cranial suture research.** *Plastic and reconstructive surgery* 2001, **107**(2):523-540.
71. Jiang T, Ge S, Shim YH, Zhang C, Cao D: **Bone morphogenetic protein is required for fibroblast growth factor 2-dependent later-stage osteoblastic differentiation in cranial suture cells.** *International journal of clinical and experimental pathology* 2015, **8**(3):2946-2954.
72. Decker RS, Koyama E, Pacifici M: **Genesis and morphogenesis of limb synovial joints and articular cartilage.** *Matrix biology : journal of the International Society for Matrix Biology* 2014, **39**:5-10.
73. Pacifici M, Koyama E, Iwamoto M: **Mechanisms of synovial joint and articular cartilage formation: recent advances, but many lingering mysteries.** *Birth defects research Part C, Embryo today : reviews* 2005, **75**(3):237-248.
74. Kan A, Ikeda T, Fukai A, Nakagawa T, Nakamura K, Chung UI, Kawaguchi H, Tabin CJ: **SOX11 contributes to the regulation of GDF5 in joint maintenance.** *BMC developmental biology* 2013, **13**:4.
75. Mundlos S: **The brachydactylies: a molecular disease family.** *Clinical genetics* 2009, **76**(2):123-136.
76. Zelzer E, Olsen BR: **The genetic basis for skeletal diseases.** *Nature* 2003, **423**(6937):343-348.
77. Lan Y, Jia S, Jiang R: **Molecular patterning of the mammalian dentition.** *Seminars in cell & developmental biology* 2014, **25-26**:61-70.
78. Cudney SM, Vieira AR: **Molecular factors resulting in tooth agenesis and contemporary approaches for regeneration: a review.** *European archives of paediatric dentistry : official journal of the European Academy of Paediatric Dentistry* 2012, **13**(6):297-304.
79. Li CY, Prochazka J, Goodwin AF, Klein OD: **Fibroblast growth factor signaling in mammalian tooth development.** *Odontology* 2014, **102**(1):1-13.
80. Caton J, Tucker AS: **Current knowledge of tooth development: patterning and mineralization of the murine dentition.** *Journal of anatomy* 2009, **214**(4):502-515.
81. Cvekl A, Duncan MK: **Genetic and epigenetic mechanisms of gene regulation during lens development.** *Progress in retinal and eye research* 2007, **26**(6):555-597.
82. Yang XJ: **Roles of cell-extrinsic growth factors in vertebrate eye pattern formation and retinogenesis.** *Seminars in cell & developmental biology* 2004, **15**(1):91-103.
83. Dias da Silva MR, Tiffin N, Mima T, Mikawa T, Hyer J: **FGF-mediated induction of ciliary body tissue in the chick eye.** *Developmental biology* 2007, **304**(1):272-285.

84. Ozair MZ, Kintner C, Brivanlou AH: **Neural induction and early patterning in vertebrates**. *Wiley interdisciplinary reviews Developmental biology* 2013, **2**(4):479-498.
85. Liu S, Zhang H, Duan E: **Epidermal development in mammals: key regulators, signals from beneath, and stem cells**. *International journal of molecular sciences* 2013, **14**(6):10869-10895.
86. Tang K, Peng G, Qiao Y, Song L, Jing N: **Intrinsic regulations in neural fate commitment**. *Development, growth & differentiation* 2015, **57**(2):109-120.
87. Germain N, Banda E, Grabel L: **Embryonic stem cell neurogenesis and neural specification**. *Journal of cellular biochemistry* 2010, **111**(3):535-542.
88. Paek H, Hwang JY, Zukin RS, Hebert JM: **beta-Catenin-dependent FGF signaling sustains cell survival in the anterior embryonic head by countering Smad4**. *Developmental cell* 2011, **20**(5):689-699.
89. McMahon AP: **Development of the Mammalian Kidney**. *Current topics in developmental biology* 2016, **117**:31-64.
90. Bhattacharya S, Macdonald ST, Farthing CR: **Molecular mechanisms controlling the coupled development of myocardium and coronary vasculature**. *Clinical science* 2006, **111**(1):35-46.
91. Meganathan K, Sotiriadou I, Natarajan K, Hescheler J, Sachinidis A: **Signaling molecules, transcription growth factors and other regulators revealed from in-vivo and in-vitro models for the regulation of cardiac development**. *International journal of cardiology* 2015, **183**:117-128.
92. Nakajima Y, Sakabe M, Matsui H, Sakata H, Yanagawa N, Yamagishi T: **Heart development before beating**. *Anatomical science international* 2009, **84**(3):67-76.
93. Hines EA, Sun X: **Tissue crosstalk in lung development**. *Journal of cellular biochemistry* 2014, **115**(9):1469-1477.
94. Pellegrini L, Burke DF, von Delft F, Mulloy B, Blundell TL: **Crystal structure of fibroblast growth factor receptor ectodomain bound to ligand and heparin**. *Nature* 2000, **407**(6807):1029-1034.
95. Schlessinger J, Plotnikov AN, Ibrahimi OA, Eliseenkova AV, Yeh BK, Yayon A, Linhardt RJ, Mohammadi M: **Crystal structure of a ternary FGF-FGFR-heparin complex reveals a dual role for heparin in FGFR binding and dimerization**. *Molecular cell* 2000, **6**(3):743-750.
96. Comps-Agrar L, Dunshee DR, Eaton DL, Sonoda J: **Unliganded fibroblast growth factor receptor 1 forms density-independent dimers**. *The Journal of biological chemistry* 2015, **290**(40):24166-24177.
97. Sarabipour S, Hristova K: **Mechanism of FGF receptor dimerization and activation**. *Nature communications* 2016, **7**:10262.
98. Nohe A, Hassel S, Ehrlich M, Neubauer F, Sebald W, Henis YI, Knaus P: **The mode of bone morphogenetic protein (BMP) receptor oligomerization determines different BMP-2 signaling pathways**. *The Journal of biological chemistry* 2002, **277**(7):5330-5338.
99. Morimoto T, Kaito T, Matsuo Y, Sugiura T, Kashii M, Makino T, Iwasaki M, Yoshikawa H: **The bone morphogenetic protein-2/7 heterodimer is a stronger inducer of bone regeneration than the individual homodimers in a rat spinal fusion model**. *The spine journal : official journal of the North American Spine Society* 2015, **15**(6):1379-1390.
100. Valera E, Isaacs MJ, Kawakami Y, Izpisua Belmonte JC, Choe S: **BMP-2/6 heterodimer is**

- more effective than BMP-2 or BMP-6 homodimers as inductor of differentiation of human embryonic stem cells. *PLoS one* 2010, **5**(6):e111167.
101. Nickel J, Ten Dijke P, Mueller TD: **TGF-beta family co-receptor function and signaling.** *Acta biochimica et biophysica Sinica* 2018, **50**(1):12-36.
102. Bier E, De Robertis EM: **EMBRYO DEVELOPMENT. BMP gradients: A paradigm for morphogen-mediated developmental patterning.** *Science* 2015, **348**(6242):aaa5838.
103. Villarreal MM, Kim SK, Barron L, Kodali R, Baardsnes J, Hinck CS, Krzysiak TC, Henen MA, Pakhomova O, Mendoza V *et al*: **Binding Properties of the Transforming Growth Factor-beta Coreceptor Betaglycan: Proposed Mechanism for Potentiation of Receptor Complex Assembly and Signaling.** *Biochemistry* 2016, **55**(49):6880-6896.
104. Gray PC, Vale W: **Cripto/GRP78 modulation of the TGF-beta pathway in development and oncogenesis.** *FEBS letters* 2012, **586**(14):1836-1845.
105. Heinecke K, Seher A, Schmitz W, Mueller TD, Sebald W, Nickel J: **Receptor oligomerization and beyond: a case study in bone morphogenetic proteins.** *BMC biology* 2009, **7**:59.
106. Klammert U, Mueller TD, Hellmann TV, Wuerzler KK, Kotzsch A, Schliermann A, Schmitz W, Kuebler AC, Sebald W, Nickel J: **GDF-5 can act as a context-dependent BMP-2 antagonist.** *BMC biology* 2015, **13**:77.
107. Gilboa L, Nohe A, Geissendorfer T, Sebald W, Henis YI, Knaus P: **Bone morphogenetic protein receptor complexes on the surface of live cells: a new oligomerization mode for serine/threonine kinase receptors.** *Molecular biology of the cell* 2000, **11**(3):1023-1035.
108. Lowry OH, Rosebrough NJ, Farr AL, Randall RJ: **Protein measurement with the Folin phenol reagent.** *The Journal of biological chemistry* 1951, **193**(1):265-275.
109. Seemann P, Schwappacher R, Kjaer KW, Krakow D, Lehmann K, Dawson K, Stricker S, Pohl J, Ploger F, Staub E *et al*: **Activating and deactivating mutations in the receptor interaction site of GDF5 cause symphalangism or brachydactyly type A2.** *The Journal of clinical investigation* 2005, **115**(9):2373-2381.
110. Barnard JC, Williams AJ, Rabier B, Chassande O, Samarut J, Cheng SY, Bassett JH, Williams GR: **Thyroid hormones regulate fibroblast growth factor receptor signaling during chondrogenesis.** *Endocrinology* 2005, **146**(12):5568-5580.
111. Prenzlau F: **Die Rolle des FGFR-2 in der chondrogenen Differenzierung.** *term paper.* Wuerzburg: Julius-Maximilians-University; 2014.
112. Tiong KH, Mah LY, Leong CO: **Functional roles of fibroblast growth factor receptors (FGFRs) signaling in human cancers.** *Apoptosis : an international journal on programmed cell death* 2013, **18**(12):1447-1468.
113. Sun L, Tran N, Liang C, Tang F, Rice A, Schreck R, Waltz K, Shawver LK, McMahon G, Tang C: **Design, synthesis, and evaluations of substituted 3-[(3- or 4-carboxyethylpyrrol-2-yl)methylidene]indolin-2-ones as inhibitors of VEGF, FGF, and PDGF receptor tyrosine kinases.** *Journal of medicinal chemistry* 1999, **42**(25):5120-5130.
114. Duncia JV, Santella JB, 3rd, Higley CA, Pitts WJ, Wityak J, Frieze WE, Rankin FW, Sun JH, Earl RA, Tabaka AC *et al*: **MEK inhibitors: the chemistry and biological activity of U0126, its analogs, and cyclization products.** *Bioorganic & medicinal chemistry letters* 1998, **8**(20):2839-2844.
115. Belleudi F, Leone L, Aimati L, Stirparo MG, Cardinali G, Marchese C, Frati L, Picardo M,

- Torrise MR: **Endocytic pathways and biological effects induced by UVB-dependent or ligand-dependent activation of the keratinocyte growth factor receptor.** *FASEB journal : official publication of the Federation of American Societies for Experimental Biology* 2006, **20**(2):395-397.
116. Bernard-Pierrot I, Ricol D, Cassidy A, Graham A, Elvin P, Caillaud A, Lair S, Broet P, Thiery JP, Radvanyi F: **Inhibition of human bladder tumour cell growth by fibroblast growth factor receptor 2b is independent of its kinase activity. Involvement of the carboxy-terminal region of the receptor.** *Oncogene* 2004, **23**(57):9201-9211.
117. Di Maggio N, Mehrkens A, Papadimitropoulos A, Schaeren S, Heberer M, Banfi A, Martin I: **Fibroblast growth factor-2 maintains a niche-dependent population of self-renewing highly potent non-adherent mesenchymal progenitors through FGFR2c.** *Stem cells* 2012, **30**(7):1455-1464.
118. Harth S, Kotsch A, Hu J, Sebald W, Mueller TD: **A selection fit mechanism in BMP receptor IA as a possible source for BMP ligand-receptor promiscuity.** *PLoS one* 2010, **5**(9).
119. Isaacs MJ, Kawakami Y, Allendorph GP, Yoon BH, Izpisua Belmonte JC, Choe S: **Bone morphogenetic protein-2 and -6 heterodimer illustrates the nature of ligand-receptor assembly.** *Molecular endocrinology* 2010, **24**(7):1469-1477.
120. Keller S, Nickel J, Zhang JL, Sebald W, Mueller TD: **Molecular recognition of BMP-2 and BMP receptor IA.** *Nature structural & molecular biology* 2004, **11**(5):481-488.
121. Jaskolski F, Mülle C, Manzoni OJ: **An automated method to quantify and visualize colocalized fluorescent signals.** *Journal of neuroscience methods* 2005, **146**(1):42-49.
122. Nickel J, Kotsch A, Sebald W, Mueller TD: **Purification, crystallization and preliminary data analysis of the ligand-receptor complex of the growth and differentiation factor 5 variant R57A (GDF5R57A) and BMP receptor IA (BRIA).** *Acta crystallographica Section F, Structural biology and crystallization communications* 2011, **67**(Pt 5):551-555.
123. Shukunami C, Akiyama H, Nakamura T, Hiraki Y: **Requirement of autocrine signaling by bone morphogenetic protein-4 for chondrogenic differentiation of ATDC5 cells.** *FEBS letters* 2000, **469**(1):83-87.
124. Tannheimer SL, Rehemtulla A, Ethier SP: **Characterization of fibroblast growth factor receptor 2 overexpression in the human breast cancer cell line SUM-52PE.** *Breast cancer research : BCR* 2000, **2**(4):311-320.
125. Moffa AB, Ethier SP: **Differential signal transduction of alternatively spliced FGFR2 variants expressed in human mammary epithelial cells.** *Journal of cellular physiology* 2007, **210**(3):720-731.
126. Cha JY, Maddileti S, Mitin N, Harden TK, Der CJ: **Aberrant receptor internalization and enhanced FRS2-dependent signaling contribute to the transforming activity of the fibroblast growth factor receptor 2 IIIb C3 isoform.** *The Journal of biological chemistry* 2009, **284**(10):6227-6240.
127. Lonic A, Barry EF, Quach C, Kobe B, Saunders N, Guthridge MA: **Fibroblast growth factor receptor 2 phosphorylation on serine 779 couples to 14-3-3 and regulates cell survival and proliferation.** *Molecular and cellular biology* 2008, **28**(10):3372-3385.
128. Zakrzewska M, Haugsten EM, Nadratowska-Wesolowska B, Oppelt A, Hausott B, Jin Y, Otlewski J, Wesche J, Wiedlocha A: **ERK-mediated phosphorylation of fibroblast growth factor receptor 1 on Ser777 inhibits signaling.** *Science signaling* 2013, **6**(262):ra11.



129. Liu W, Selever J, Murali D, Sun X, Brugger SM, Ma L, Schwartz RJ, Maxson R, Furuta Y, Martin JF: **Threshold-specific requirements for Bmp4 in mandibular development.** *Developmental biology* 2005, **283**(2):282-293.
130. Nakamura Y, Tensho K, Nakaya H, Nawata M, Okabe T, Wakitani S: **Low dose fibroblast growth factor-2 (FGF-2) enhances bone morphogenetic protein-2 (BMP-2)-induced ectopic bone formation in mice.** *Bone* 2005, **36**(3):399-407.
131. Yilmaz A, Kattamuri C, Ozdeslik RN, Schmiedel C, Mentzer S, Schorl C, Oancea E, Thompson TB, Fallon JR: **MuSK is a BMP co-receptor that shapes BMP responses and calcium signaling in muscle cells.** *Science signaling* 2016, **9**(444):ra87.
132. Yan D, Lin X: **Shaping morphogen gradients by proteoglycans.** *Cold Spring Harbor perspectives in biology* 2009, **1**(3):a002493.
133. Dahlqvist C, Blokzijl A, Chapman G, Falk A, Dannaeus K, Ibanez CF, Lendahl U: **Functional Notch signaling is required for BMP4-induced inhibition of myogenic differentiation.** *Development* 2003, **130**(24):6089-6099.
134. Kuribayashi H, Baba Y, Watanabe S: **BMP signaling participates in late phase differentiation of the retina, partly via upregulation of Hey2.** *Developmental neurobiology* 2014, **74**(12):1172-1183.
135. Cook BD, Evans T: **BMP signaling balances murine myeloid potential through SMAD-independent p38MAPK and NOTCH pathways.** *Blood* 2014, **124**(3):393-402.
136. Vinals F, Lopez-Rovira T, Rosa JL, Ventura F: **Inhibition of PI3K/p70 S6K and p38 MAPK cascades increases osteoblastic differentiation induced by BMP-2.** *FEBS letters* 2002, **510**(1-2):99-104.
137. Guicheux J, Lemonnier J, Ghayor C, Suzuki A, Palmer G, Caverzasio J: **Activation of p38 mitogen-activated protein kinase and c-Jun-NH2-terminal kinase by BMP-2 and their implication in the stimulation of osteoblastic cell differentiation.** *Journal of bone and mineral research : the official journal of the American Society for Bone and Mineral Research* 2003, **18**(11):2060-2068.
138. Lai CF, Cheng SL: **Signal transductions induced by bone morphogenetic protein-2 and transforming growth factor-beta in normal human osteoblastic cells.** *The Journal of biological chemistry* 2002, **277**(18):15514-15522.
139. Cuenda A, Rousseau S: **p38 MAP-kinases pathway regulation, function and role in human diseases.** *Biochimica et biophysica acta* 2007, **1773**(8):1358-1375.
140. Nakamura K, Shirai T, Morishita S, Uchida S, Saeki-Miura K, Makishima F: **p38 mitogen-activated protein kinase functionally contributes to chondrogenesis induced by growth/differentiation factor-5 in ATDC5 cells.** *Experimental cell research* 1999, **250**(2):351-363.
141. Baek SH, Choi SW, Park SJ, Lee SH, Chun HS, Kim SH: **Quinoline compound KM11073 enhances BMP-2-dependent osteogenic differentiation of C2C12 cells via activation of p38 signaling and exhibits in vivo bone forming activity.** *PloS one* 2015, **10**(3):e0120150.
142. Moon SH, Kim I, Kim SH: **Mollugin enhances the osteogenic action of BMP-2 via the p38-Smad signaling pathway.** *Archives of pharmacal research* 2017, **40**(11):1328-1335.
143. Yang B, Lin X, Yang C, Tan J, Li W, Kuang H: **Sambucus Williamsii Hance Promotes MC3T3-E1 Cells Proliferation and Differentiation via BMP-2/Smad/p38/JNK/Runx2 Signaling Pathway.** *Phytotherapy research : PTR* 2015, **29**(11):1692-1699.

144. Lafont JE, Poujade FA, Padeloup M, Neyret P, Mallein-Gerin F: **Hypoxia potentiates the BMP-2 driven COL2A1 stimulation in human articular chondrocytes via p38 MAPK.** *Osteoarthritis and cartilage* 2016, **24**(5):856-867.
145. Greenblatt MB, Shim JH, Zou W, Sitara D, Schweitzer M, Hu D, Lotinun S, Sano Y, Baron R, Park JM *et al*: **The p38 MAPK pathway is essential for skeletogenesis and bone homeostasis in mice.** *The Journal of clinical investigation* 2010, **120**(7):2457-2473.
146. Yoon BS, Lyons KM: **Multiple functions of BMPs in chondrogenesis.** *Journal of cellular biochemistry* 2004, **93**(1):93-103.
147. Shim JH, Greenblatt MB, Xie M, Schneider MD, Zou W, Zhai B, Gygi S, Glimcher LH: **TAK1 is an essential regulator of BMP signalling in cartilage.** *The EMBO journal* 2009, **28**(14):2028-2041.
148. Jin EJ, Lee SY, Choi YA, Jung JC, Bang OS, Kang SS: **BMP-2-enhanced chondrogenesis involves p38 MAPK-mediated down-regulation of Wnt-7a pathway.** *Molecules and cells* 2006, **22**(3):353-359.
149. Rudraraju B, Droog M, Abdel-Fatah TM, Zwart W, Giannoudis A, Malki MI, Moore D, Patel H, Shaw J, Ellis IO *et al*: **Phosphorylation of activating transcription factor-2 (ATF-2) within the activation domain is a key determinant of sensitivity to tamoxifen in breast cancer.** *Breast cancer research and treatment* 2014, **147**(2):295-309.
150. Lee KS, Hong SH, Bae SC: **Both the Smad and p38 MAPK pathways play a crucial role in Runx2 expression following induction by transforming growth factor-beta and bone morphogenetic protein.** *Oncogene* 2002, **21**(47):7156-7163.
151. Hoffmann A, Preobrazhenska O, Wodarczyk C, Medler Y, Winkel A, Shahab S, Huylebroeck D, Gross G, Verschuere K: **Transforming growth factor-beta-activated kinase-1 (TAK1), a MAP3K, interacts with Smad proteins and interferes with osteogenesis in murine mesenchymal progenitors.** *The Journal of biological chemistry* 2005, **280**(29):27271-27283.
152. Kimura N, Matsuo R, Shibuya H, Nakashima K, Taga T: **BMP2-induced apoptosis is mediated by activation of the TAK1-p38 kinase pathway that is negatively regulated by Smad6.** *The Journal of biological chemistry* 2000, **275**(23):17647-17652.
153. Shibuya H, Iwata H, Masuyama N, Gotoh Y, Yamaguchi K, Irie K, Matsumoto K, Nishida E, Ueno N: **Role of TAK1 and TAB1 in BMP signaling in early Xenopus development.** *The EMBO journal* 1998, **17**(4):1019-1028.
154. Yamaguchi K, Nagai S, Ninomiya-Tsuji J, Nishita M, Tamai K, Irie K, Ueno N, Nishida E, Shibuya H, Matsumoto K: **XIAP, a cellular member of the inhibitor of apoptosis protein family, links the receptors to TAB1-TAK1 in the BMP signaling pathway.** *The EMBO journal* 1999, **18**(1):179-187.
155. Reilly GC, Golden EB, Grasso-Knight G, Leboy PS: **Differential effects of ERK and p38 signaling in BMP-2 stimulated hypertrophy of cultured chick sternal chondrocytes.** *Cell communication and signaling : CCS* 2005, **3**(1):3.
156. Akiyama H, Chaboissier MC, Martin JF, Schedl A, de Crombrughe B: **The transcription factor Sox9 has essential roles in successive steps of the chondrocyte differentiation pathway and is required for expression of Sox5 and Sox6.** *Genes & development* 2002, **16**(21):2813-2828.
157. Takarada T, Hinoi E, Nakazato R, Ochi H, Xu C, Tsuchikane A, Takeda S, Karsenty G, Abe T, Kiyonari H *et al*: **An analysis of skeletal development in osteoblast-specific and**

- chondrocyte-specific runt-related transcription factor-2 (Runx2) knockout mice.** *Journal of bone and mineral research : the official journal of the American Society for Bone and Mineral Research* 2013, **28**(10):2064-2069.
158. Helsten T, Schwaederle M, Kurzrock R: **Fibroblast growth factor receptor signaling in hereditary and neoplastic disease: biologic and clinical implications.** *Cancer metastasis reviews* 2015, **34**(3):479-496.

## 9. Appendix

This appendix to the thesis titled “The role of FGF receptor 2 in GDF5 mediated signal transduction” contains the following items:

- Additional figures/overviews
- Lists of materials used in this study
- References of the depicted figures to the laboratory notebook kept during this study
- Supplemental References

### 9.1. Additional Figures and Overviews

#### 9.1.1. The 100 most differentially expressed membrane-associated genes in ATDC5 vs C2C12 cells

<i><b>MGI Symbol</b></i>	<i><b>Description</b></i>	<i><b>Fold Change: ATDC5 - C2C12</b></i>
Selp	selectin, platelet	71,064
Nrn1	neuritin 1	64,918
Pzca	prostate stem cell antigen	58,564
Eltf1	EGF, latrophilin seven transmembrane domain containing 1	55,215
Galnt13	UDP-N-acetyl-alpha-D-galactosamine:polypeptide N-acetylgalactosaminyltransferase 13	45,719
Hs6st2	heparan sulfate 6-O-sulfotransferase 2	40,553
Gabbr3	gamma-aminobutyric acid (GABA) A receptor, subunit beta 3	39,351
Scn3a*	sodium channel, voltage-gated, type III, alpha	38,276
Gpc4	glypican 4	37,379
Arrdc4	arrestin domain containing 4	34,759
St3gal6	ST3 beta-galactoside alpha-2,3-sialyltransferase 6	20,004
Plce1	phospholipase C, epsilon 1	17,398

## 9. Appendix

<b>MGI Symbol</b>	<b>Description</b>	<b>Fold Change: ATDC5 - C2C12</b>
Galnt9	UDP-N-acetyl-alpha-D-galactosamine:polypeptide N-acetylgalactosaminyltransferase 9	16,676
Gramd2	GRAM domain containing 2	15,514
Mgat4a	mannoside acetylglucosaminyltransferase 4, isoenzyme A	15,167
Nhedc1	Na <sup>+</sup> /H <sup>+</sup> exchanger domain containing 1	11,886
Scn2a1*	sodium channel, voltage-gated, type II, alpha 1	10,741
Scn9a*	sodium channel, voltage-gated, type IX, alpha	10,741
Tmem22	transmembrane protein 22	10,678
Slc2a3	solute carrier family 2 (facilitated glucose transporter), member 3	10,538
Gcnt1	glucosaminyl (N-acetyl) transferase 1, core 2	10,202
Lctf	lactase-like	9,871
Vldlr	very low density lipoprotein receptor	9,847
Slc25a13	solute carrier family 25 (mitochondrial carrier, adenine nucleotide translocator), member 13	9,752
Tmem56	transmembrane protein 56	9,352
<b>Fgfr2</b>	<b>fibroblast growth factor receptor 2</b>	<b>9,255</b>
Cacng7	calcium channel, voltage-dependent, gamma subunit 7	8,765
Glpr1	GLI pathogenesis-related 1 (glioma)	8,561
Tmem20	transmembrane protein 20	8,435
Il15ra	interleukin 15 receptor, alpha chain	8,109
Mark1	MAP/microtubule affinity-regulating kinase 1	8,049
B4galnt4	beta-1,4-N-acetyl-galactosaminyl transferase 4	7,601
Tmem223	transmembrane protein 223	7,429
Slc5a7	solute carrier family 5 (choline transporter), member 7	7,331
F2rl1	coagulation factor II (thrombin) receptor-like 1	6,962
Mboat2	membrane bound O-acyltransferase domain containing 2	6,930
Lrp8	low density lipoprotein receptor-related protein 8, apolipoprotein e receptor	6,761
Ap1s3	adaptor-related protein complex AP-1, sigma 3	6,698
H2-Ab1	histocompatibility 2, class II antigen A, beta 1	6,341
Sulf2	sulfatase 2	6,105
Sorl1	sortilin-related receptor, LDLR class A repeats-containing	5,889
Cacna1c	calcium channel, voltage-dependent, L type, alpha 1C subunit	5,697
Eda	ectodysplasin-A	5,666
Ptch1	'patched homolog 1	5,664

## 9. Appendix

<b>MGI Symbol</b>	<b>Description</b>	<b>Fold Change: ATDC5 - C2C12</b>
Rnf182	ring finger protein 182	5,590
Kcnab2	potassium voltage-gated channel, shaker-related subfamily, beta member 2	5,583
Slc6a2	solute carrier family 6 (neurotransmitter transporter, noradrenalin), member 2	5,531
Adam23	a disintegrin and metallopeptidase domain 23	5,484
Cacna1g	calcium channel, voltage-dependent, T type, alpha 1G subunit	5,408
Scarb1	scavenger receptor class B, member 1	5,331
Cdc42ep5	CDC42 effector protein (Rho GTPase binding) 5	-19,520
Chrnbl	cholinergic receptor, nicotinic, beta polypeptide 1 (muscle)	-19,834
Gpm6b	glycoprotein m6b	-20,010
Anpep	alanyl (membrane) aminopeptidase	-21,229
Musk	muscle, skeletal, receptor tyrosine kinase	-21,507
Sema7a	sema domain, immunoglobulin domain (Ig), and GPI membrane anchor, (semaphorin) 7A	-21,762
Sytl5	synaptotagmin-like 5	-22,450
Sema5a	sema domain, seven thrombospondin repeats (type 1 and type 1-like), transmembrane domain (TM) and short cytoplasmic domain, (semaphorin) 5A	-22,455
Gfra1	glial cell line derived neurotrophic factor family receptor alpha 1	-22,761
Sgcd	sarcoglycan, delta (dystrophin-associated glycoprotein)	-22,796
Jph1	junctophilin 1	-23,926
Renbp	renin binding protein	-24,875
Cdh13	cadherin 13	-25,367
Tecrl	trans-2,3-enoyl-CoA reductase-like	-26,381
Enpp3	ectonucleotide pyrophosphatase/phosphodiesterase 3	-26,785
Chrng	cholinergic receptor, nicotinic, gamma polypeptide	-27,486
Csgalnact1	chondroitin sulfate N-acetylgalactosaminyltransferase 1	-28,382
Sulf1	sulfatase 1	-28,640
Lsp1	lymphocyte specific 1	-28,924
Ehd3	EH-domain containing 3	-30,166
Emb	embigin	-33,663
Ptgs1	prostaglandin-endoperoxide synthase 1	-33,773
Cacng1	calcium channel, voltage-dependent, gamma subunit 1	-34,602

<b>MGI Symbol</b>	<b>Description</b>	<b>Fold Change: ATDC5 - C2C12</b>
Thbd	thrombomodulin	-36,010
Cd53	CD53 antigen	-36,297
Cdh11	cadherin 11	-36,955
Itga7	integrin alpha 7	-41,087
Tmc3	transmembrane channel-like gene family 3	-45,265
Cacna2d1*	calcium channel, voltage-dependent, alpha2/delta subunit 1	-45,419
Cd200	CD200 antigen	-46,269
Tmem8c	transmembrane protein 8C	-46,344
Enpp1	ectonucleotide pyrophosphatase/phosphodiesterase 1	-46,973
Sgcg	sarcoglycan, gamma (dystrophin-associated glycoprotein)	-49,865
Hfe2	hemochromatosis type 2 (juvenile) (human homolog)	-53,511
Tmem182	transmembrane protein 182	-53,771
Popdc3	popeye domain containing 3	-54,243
Snx7	sorting nexin 7	-55,591
Pdpn	podoplanin	-58,999
Chrnd	cholinergic receptor, nicotinic, delta polypeptide	-61,219
Cd97	CD97 antigen	-62,166
Osmr	oncostatin M receptor	-66,662
Jam2	junction adhesion molecule 2	-74,523
Trdn*	triadin	-80,557
Gatm	glycine amidinotransferase	-86,470
Gpr126	G protein-coupled receptor 126	-88,978
Bves	blood vessel epicardial substance	-91,843
Cd34	CD34 antigen	-93,734
Chrna1	cholinergic receptor, nicotinic, alpha polypeptide 1 (muscle)	-97,205
Cd80*	CD80 antigen	-98,745
Tmem47	transmembrane protein 47	-134,210

\* these genes were listed more than once with different fold changes in the microarray data set. The entry with the highest fold change for each gene was included in this table.

*Table A1: The 100 most differentially expressed membrane-associated genes between ATDC5 and C2C12 cells.*

These data are included in Schliermann (2) 2018.

9.1.2. Overview of receptor-ligand pairings in the TGFβ growth factor family

Subfamily	TYPE I RECEPTORS					TYPE II RECEPTORS					Cripto		
	TSR-I	ActR-I (ALK2)	BMPR-IA (ALK3)	BMPR-IB (ALK6)	ActR-IB (ALK4)	TβR-I (ALK5)	ActR-IC	ActR-II	ActR-III	TβR-II		BMPR-II	AMHR-II
<b>BMPs</b>		BMP2/4 BMP5-8 BMP9/10	BMP2/4 BMP5-8 BMP15	BMP2/4 BMP5-8 BMP15	BMP3			BMP2/4 BMP3 BMP5-8	BMP2/4 BMP3 BMP5-8		BMP2/4 BMP5-8 BMP9/10 BMP15		
<b>GDFs</b>			GDF5/6/7	GDF5/6/7	GDF1/3 GDF8/11 GDF10			GDF1/3 GDF5/6/7 GDF8/11 GDF10	GDF1/3 GDF5/6/7 GDF8/11 GDF10		GDF5/6/7 GDF9		GDF1/3
<b>Activin/ Inhibin/ Nodal</b>					Nodal Activins			Nodal Activins Inhibins	Nodal Activins Inhibins				Nodal Lefty1/2
<b>TGFβs</b>	TGFβ1-3					TGFβ1-3					TGFβ1-3		
<b>others</b>		AMH	AMH	AMH	AMH							AMH	

Table A2: Pairings of TGFβ ligands and their receptors according to Müller 2012.



9.1.3. Overview of receptor-ligand pairings in the FGF growth factor family

Subfamily	FGFR1 IIIb IIIc	FGFR2 IIIb IIIc	FGFR3 IIIb IIIc	FGFR4	FGFRL1
1	FGF1 FGF2	FGF1 FGF2	FGF1 FGF2	FGF1 FGF2	FGF1 FGF2
4	FGF4 FGF5 FGF6	FGF4 FGF6	FGF4	FGF4 FGF6	
7	FGF3 FGF10	FGF3 FGF7 FGF10 FGF22			
8		FGF17 FGF18	FGF8 FGF17 FGF18	FGF8 FGF17 FGF18	
9		FGF9	FGF9	FGF9 FGF16	
secreted	FGF15 FGF21 FGF23	FGF15	FGF15 FGF21 FGF23	FGF15 FGF23	

Table A3: Pairings of FGF ligands and their receptors according to Ornitz 2015, Tiong 2013.

9.1.4. Overview of developmental stages and regulatory components of the cranial and appendicular skeleton

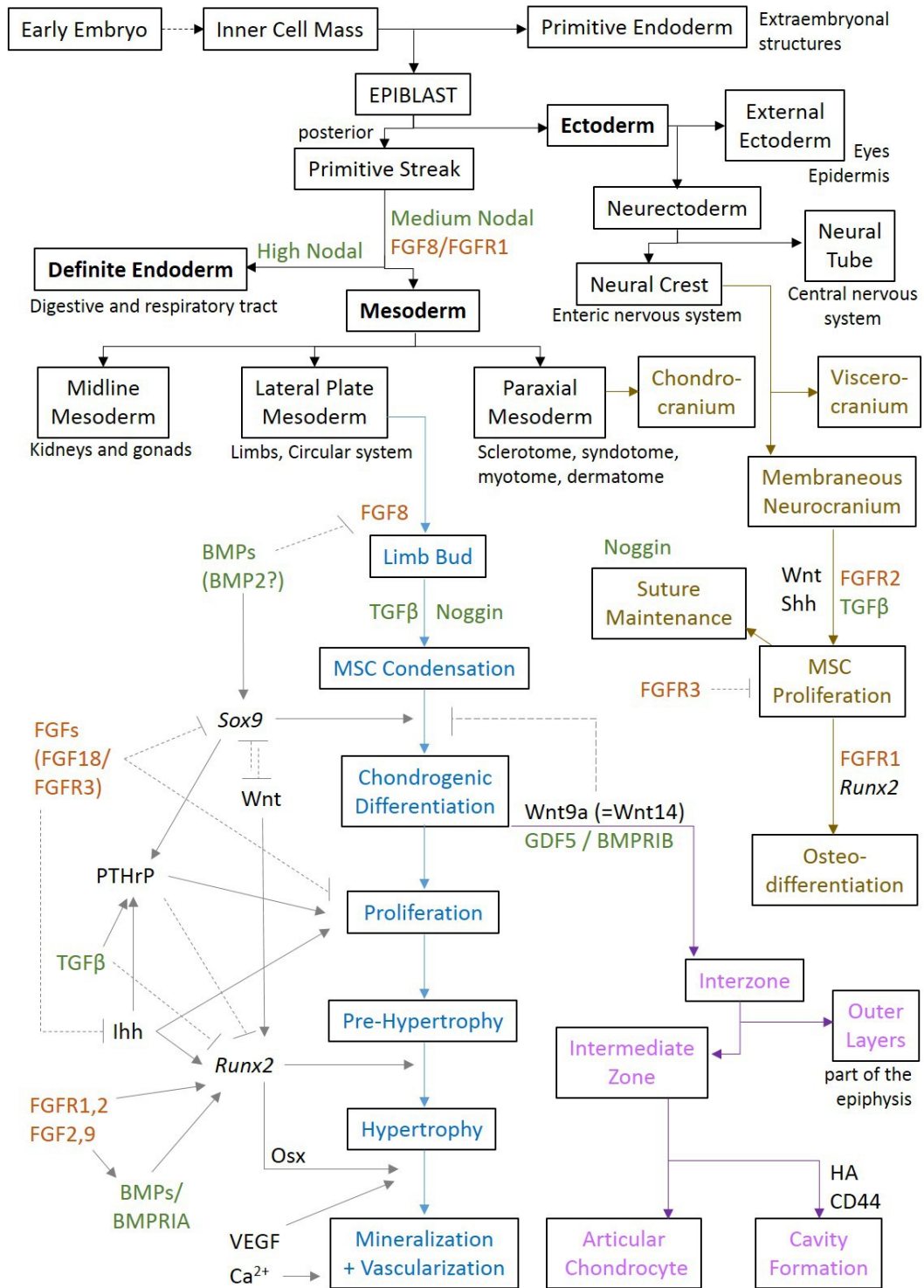


**Figure A21: Regulatory Components in the Development of the Cranial and Appendicular Skeleton**

The inner cell mass of the early embryo gives rise to all three germ layers, definite endoderm, mesoderm, and ectoderm. The appendicular skeleton (blue) and cartilage (purple) rise from lateral plate mesoderm, whereas the cranial skeleton (yellow) derives from structures of two different germ layers, paraxial mesoderm and neural crest. Key players in the specification of skeletal structures are specified, and members of the BMP family are marked green, whereas members of the FGF family are orange. Activating or enhancing connections are marked with a grey arrow, whereas inhibitory connections are specified with a dotted line. Factors grouped at an arrow between two stages have a promoting effect on the transition of these two stages. This information has been collected from the sources Ferguson 2000, Olsen 2000, Kishigami 2005, Pacifici 2005, Verheyden 2008, Dorey 2010, Basson 2012, Chen 2012, Nishimura 2012, Studer 2012, Tubbs 2012, van der Kraan 2012, Decker 2014, Norrie 2014, Berendsen 2015, Rivera-Perez 2015, Tuazon 2015, Wei 2016, Wu 2016.

9.1.5. Examples of BMP-FGF interactions in development

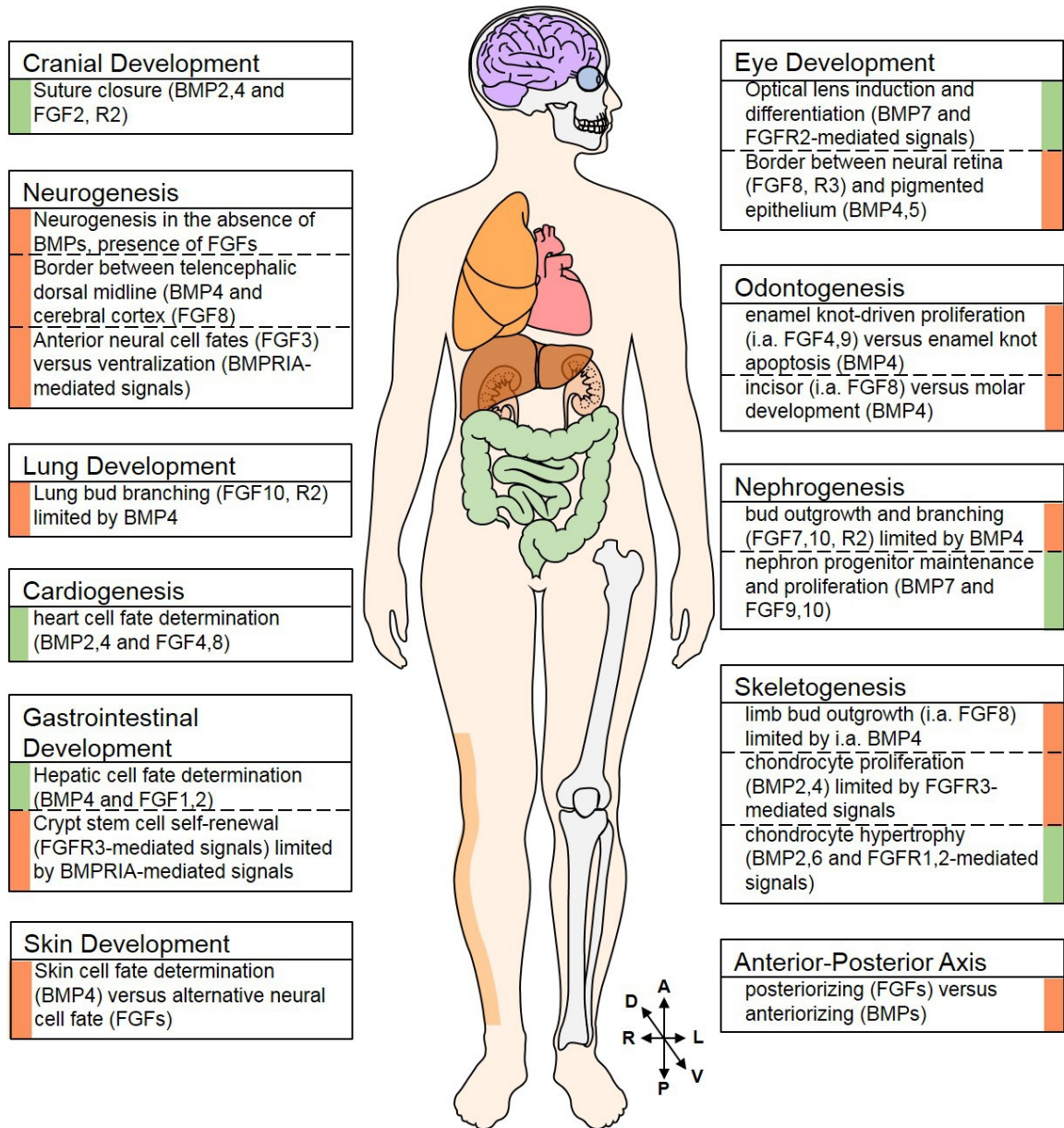


**Figure A22: Examples of BMP-FGF Interactions in Development**

BMPs and FGFs interact in the development of various tissues in the body. Examples of BMP-FGF synergy are flanked with a green bar, examples of BMP-FGF antagonism are flanked with a red bar. Graphical copyrights from ©motifolio.com. This figure is included in Schliermann (1) 2018.

## 9.2. Materials

### 9.2.1. Equipment

<i>Designation</i>	<i>Specification</i>	<i>Manufacturer</i>
Aspiration System	Vacunsafe	Integra Biosciences, Biebertal (Germany)
Autoclaves	Tecnoklav TableTop Autoclave Varioklav	Biomedis, Giessen (Germany) Systec, Wettenberg (Germany) H+P, Hackermos (Germany)
Bakterial Shaking Incubator	Multitron Standard	Infors HT, Einsbach (Germany)
Balances	SE2 Ultra	Sartorius Stedium Biotech, Göttingen (Germany)
Microbalance	EG 2200-2NM ABJ 220-4M	Kern, Balingen-Frommern (Germany) Kern, Balingen-Frommern (Germany)
Cell Culture Safety Cabinet	Safe2020	Thermo Fisher, Dreieich (Germany)
Cell Incubator: 37°C, 5 %CO <sub>2</sub>		Haraeus, Hanau (Germany)
Centrifuge	Multifuge X3R	Thermo Fisher, Dreieich (Germany)
Microcentrifuge	5417R	Eppendorf, Hamburg (Germany)
High-Speed Centrifuge	Avanti J-26 XP	Beckman Coulter, Krefeld (Germany)
Freezers	-20°C -80°C	Liebherr, Biberach (Germany) Kendro, Munich (Germany)
Fume Hood		Prutscher Laboratory Systems, Neudörfel (Austria)
Hand Tally Counter		NeoLab, Heidelberg (Germany)
Ice Machine	AF-80	Scotsman, Milan (Italy)
Immersion Thermostat for Water Bath		Lauda, Lauda-Königshofen (Germany)
Liquid Nitrogen Storage Tank	MVE 815 P-190	German-Cryo, Jüchen (Germany)
Magnetic Stirrer with integrated Heater	Type 720-HPS	VWR, Darmstadt (Germany)
Microscopes	Axiovert 40C confocal TCS SP8	Carl Zeiss, Jena (Germany) Leica Microsystems, Mannheim (Germany)
Microwave	NN-E205W	Panasonic, Hamburg (Germany)
PCR UV Cabinet	Captair Bio	Erlab, Cologne (Germany)
pH Meter		Mettler Toledo, Giessen (Germany)
Plate Reader	Infinite M200	Tecan, Maennedorf (Switzerland)
Power Supply	Gel Electrophoresis Blotting	Peqlab, Darmstadt (Germany)
Real-Time PCR Detection System	CFX96	Biorad, Munich (Germany)

<b>Designation</b>	<b>Specification</b>	<b>Manufacturer</b>
SDS Gel Imaging Station	FluorChemQ	Biozym Scientific GmbH, Hessisch Oldendorf (Germany)
Semi-Dry Blotting Chamber	PerfectBlue™ Sedec™	Peqlab, Darmstadt (Germany)
Shakers	Orbital: KM-2 Akku Rocking Platform Roller Mixer	Edmund Bühler, Hechingen (Germany) NeoLab, Heidelberg (Germany) Hartenstein, Wuerzburg (Germany)
Thermocycler		SensoQuest, Göttingen (Germany)
Ultrapure Water System		Millipore, Schwalbach (Germany)
Vortex Shaker	Vortex-Genie 2	Scientific Industries via Carl Roth, Karlsruhe (Germany)

Table A4: Equipment

### 9.2.2. Laboratory material and consumables

<b>Product Name</b>	<b>Manufacturer</b>
Adhesive Seals Microseal 'B'	Biorad, Munich (Germany)
Agarose Electrophoresis System PerfectBlue™	Peqlab, Darmstadt (Germany)
Amersham™ Protran™ 0.2 µm Nitrocellulose Membrane	GE Healthcare Life Sciences via Carl Roth, Karlsruhe (Germany)
Autoclaving Container	Fine Science Tools, Heidelberg (Germany)
Beakers	Schott, Mainz (Germany)
Bottles	Schott, Mainz (Germany)
Cell Culture Dishes	Thermo Scientific Nunc, Dreieich (Germany)
Cell Culture Dishes, Uncoated	Greiner Bio-One, Frickenhausen (Germany)
Cell Culture Flasks	TPP, Trasadingen (Germany)
Cell Culture Multiwell Plates	TPP, Trasadingen (Germany)
Cell Scraper	Sarstedt, Kleinstadt (Germany)
Cell Strainer EASYstrainer	Greiner Bio-One, Frickenhausen (Germany)
Centrifuge Tubes	Greiner Bio-One, Frickenhausen (Germany)
Combitips Plus	Eppendorf, Hamburg (Germany)
Cryo Tubes	Nunc, Wiesbaden (Germany)
Disposable Pipettes 5 ml, 10 ml, 25 ml, 50 ml	Greiner Bio-One, Frickenhausen (Germany)
Freezing Container: Mr Frosty	VWR, Darmstadt (Germany)
Glass Pipettes 5 ml, 10 ml	Brand, Wertheim (Germany)
Glass Platelets	Menzel-Glaeser, Braunschweig (Germany)

<b>Product Name</b>	<b>Manufacturer</b>
Glass Tube for Bacterial Culture	Scherf-Präzision Europa GmbH, Meiningen (Germany)
ILmABOR® Baffled Shake Flask for Bacterial Culture	Technische Glaswerke Ilmenau GmbH, Ilmenau (Germany)
Magnetic Stirring Bar	Hartenstein, Wuerzburg (Germany)
Microcentrifuge Tubes (PCR clean)	Eppendorf, Hamburg (Germany)
Microscopy Slides Polysine™	Langenbrinck, Emmerdingen (Germany)
Multichannel pipet	Eppendorf, Hamburg (Germany)
Multiplate for qPCR, 96well unskirted	Biorad, Munich (Germany)
Multistep Pipet	Brand, Wertheim (Germany)
NanoQuant Plate™	Tecan, Maennedorf (Switzerland)
Neubauer Cell Counting Chamber	Hartenstein, Wuerzburg (Germany)
Parafilm	Carl Roth, Karlsruhe (Germany)
Pasteur Pipettes	Brand, Wertheim (Germany)
Pipet Boy	Brand, Wertheim (Germany)
Pipet Filter Tips	Nerbe plus, Winsen/Luhe (Germany)
Pipet Tips	Eppendorf, Hamburg (Germany)
Pipets	Eppendorf, Hamburg (Germany)
Qiashredder Spin Columns	Biorad, Munich (Germany)
Scalpel Blades	Bayha, Tuttlingen (Germany)
Scalpel holder	Bayha, Tuttlingen (Germany)
SDS-PAGE Dual Chamber System PerfectBlue™ (M, S)	Peqlab, Darmstadt (Germany)
Spatula	Hartenstein, Wuerzburg (Germany)
Syringe	BD Biosciences, Heidelberg (Germany)
Syringe Filter Minisart NML 0.2 µm	Sartorius Stedium Biotech, Goettingen (Germany)
Water Bath Basin	Julabo Labortechnik, Seelbach (Germany)
Whatman paper	Hartenstein, Wuerzburg (Germany)

*Table A5: Laboratory Material and Consumables*

### 9.2.3. Chemicals

<b>Chemical</b>	<b>Manufacturer</b>
2-Propanol	Carl Roth, Karlsruhe (Germany)
4',6-Diamidino-2-phenylindoldihydrochlorid (DAPI)	Sigma-Aldrich, Munich (Germany)

<b>Chemical</b>	<b>Manufacturer</b>
Acetic Acid	Carl Roth, Karlsruhe (Germany)
Acrylamide (30 %)	Carl Roth, Karlsruhe (Germany)
Agarose	Biozym, Hessisch Oldendorf (Germany)
Albumin Fraction V (BSA)	Carl Roth, Karlsruhe (Germany)
Ammonium persulfate (APS)	Carl Roth, Karlsruhe (Germany)
Ampicillin Sodium Salt	Carl Roth, Karlsruhe (Germany)
Bromophenol Blue Sodium Salt	Carl Roth, Karlsruhe (Germany)
Chloroform	Sigma-Aldrich, Munich (Germany)
Crystal Violet	Carl Roth, Karlsruhe (Germany)
Descosept	Dr. Schumacher GmbH, Malsfeld (Germany)
Dimethyl Sulfide (DMSO)	Sigma-Aldrich, Munich (Germany)
DMEM GlutaMAX™ High Glucose	Gibco, Darmstadt (Germany)
DMEM/F-12, GlutaMAX™ Supplement	Gibco, Darmstadt (Germany)
Donkey Serum (D9663)	Sigma-Aldrich, Munich (Germany)
Ethanol, absolute	Sigma-Aldrich, Munich (Germany)
Ethanol, denatured, 96 %	Carl Roth, Karlsruhe (Germany)
Fetal Calf Serum (FCS) Lot 8SBO16 Lot BS210601.5 Lot BS226503	Lonza, Cologne (Germany) Bio&Sell, Feucht (Germany)
Gel Red	Genaxxon, Ulm (Germany)
Glycerol	Carl Roth, Karlsruhe (Germany)
Glycine	Carl Roth, Karlsruhe (Germany)
Hank's Balanced Salt Solution (HBSS)	Sigma-Aldrich, Munich (Germany)
HEPES (1M)	Life Technologies, Darmstadt (Germany)
Histofix (PFA 4 %)	AppliChem, Darmstadt (Germany)
Hydrochloric Acid (HCl)	Carl Roth, Karlsruhe (Germany)
Magnesium Chloride Hexahydrate (MgCl <sub>2</sub> *6 H <sub>2</sub> O)	Carl Roth, Karlsruhe (Germany)
Markers Protein (stained): ProSieve™ QuadColor 10 – 350 kD Protein (unstained): peqGold Marker I 14.4 – 116 kD DNA (100 – 3,000 bp): DNA Ladder Plus DNA (247 – 11,501 bp): Lamda DNA/PstI Marker	Lonza, Basel (Switzerland) Peqlab, Darmstadt (Germany) Peqlab, Darmstadt (Germany) Thermo Fisher Scientific, Darmstadt (Germany)
Methanol	Sigma-Aldrich, Munich (Germany)
Milk powder	Carl Roth, Karlsruhe (Germany)
Mowiol Mounting Medium	Carl Roth, Karlsruhe (Germany)
N, N, N', N'-Tetramethylethylenediamin (TEMED)	Carl Roth, Karlsruhe (Germany)



<b>Chemical</b>	<b>Manufacturer</b>
Na <sub>2</sub> /EDTA (pH 8.0)	Sigma-Aldrich, Munich (Germany)
Nonidet p40 (NP40)	AppliChem, Darmstadt (Germany)
Paranitrophenyl-Phosphate Disodium Hexahydrate	Sigma-Aldrich, Munich (Germany)
Penicillin-Streptomycin (100x)	Sigma-Aldrich, Munich (Germany)
Phosphate Buffered Saline (PBS)	Sigma-Aldrich, Munich (Germany)
Polybrene	Sigma-Aldrich, Munich (Germany)
Potassium Chloride (KCl)	Sigma-Aldrich, Munich (Germany)
Puromycin	InvivoGen, Toulouse (France)
Sodium Acetate (NaAc)	Sigma-Aldrich, Munich (Germany)
Sodium Chloride (NaCl)	Sigma-Aldrich, Munich (Germany)
Sodium Deoxycholate	Sigma-Aldrich, Munich (Germany)
Sodium Dodecyl Sulfate (SDS)	Carl Roth, Karlsruhe (Germany)
Sodium Fluoride (NaF)	Sigma-Aldrich, Munich (Germany)
Sodium Hydroxide (NaOH)	Carl Roth, Karlsruhe (Germany)
Sodium Orthovanadate	Sigma-Aldrich, Munich (Germany)
Sodium Pyruvate (100 mM)	Life Technologies, Darmstadt (Germany)
TRIS (Trizma Base)	Carl Roth, Karlsruhe (Germany)
Triton-X 100	Carl Roth, Karlsruhe (Germany)
Trypan Blue	Sigma-Aldrich, Munich (Germany)
Trypsine (10x)	Invitrogen, Darmstadt (Germany)
Tryptone	Carl Roth, Karlsruhe (Germany)
Tween 20	VWR, Darmstadt (Germany)
X-tremeGENE 9 Transfection Reagent	Sigma-Aldrich, Munich (Germany)
Yeast Extract	Carl Roth, Karlsruhe (Germany)
Zinc Chloride (ZnCl <sub>2</sub> )	Sigma-Aldrich, Munich (Germany)
β-Mercaptoethanol	Sigma-Aldrich, Munich (Germany)

Table A6: Chemicals

#### 9.2.4. Solutions

<b>Solution</b>	<b>Constitution</b>
Agarose Gel (DNA)	2 % TAE (50x Stock) 0.5 – 0.8 % agarose in Deionized Water

## 9. Appendix

<b>Solution</b>	<b>Constitution</b>
ALP buffer 1	0.1 M Glycine 1mM MgCl <sub>2</sub> 1mM ZnCl <sub>2</sub> in Ultrapure Water pH 9.6 1 % (v/v) Triton X100 Stored at 4 °C
ALP buffer 2	0.1 M Glycine 1mM MgCl <sub>2</sub> 1mM ZnCl <sub>2</sub> in Ultrapure Water pH 9.6 Stored at 4°C 2 mg / ml Paranitrophenyl-phosphate (added fresh)
Crystal Violet (Working Solution)	0.5 % (w/v) Cristal Violet 20 % Methanol in Deionized Water Stored at RT
Laemmli (SDS Page Sample Buffer)	1.25 ml 0.5 M Tris-HCl, pH 6.8 2.5 ml Glycerol 2 ml 10 % (w/v) SDS 0.2 ml 0.5% (w/v) Bromophenol Blue 5 % (v/v) β-Mercaptoethanol ad 10 ml Ultrapure Water Stored at -20 °C
LB medium	50 g Tryptone 25 g Yeast Extract 50 g NaCl ad 5 l Ultrapure Water pH 7.5 Autoclaved and stored at RT
Lower Tris (4x Stock)	15 M Tris 0.4 % SDS in Ultrapure Water pH 8.8 Stored at RT
Lysis buffer	20 mM Tris Hcl (pH 8) 137 mM NaCl 10 % (v/v) Glycerol 1% (v/v) NP40 2 mM EDTA 0.5 % (w/v) Sodium Deoxycholate 0.1 % (w/v) SDS 50 mM NaF in Ultrapure Water Stored at 4 °C. Added fresh: 1 mM Sodium Orthovanadate 1 tbl / 10 ml cOmplete Proteinase Inhibitor Cocktail

## 9. Appendix

<b>Solution</b>	<b>Constitution</b>
Plating Agar	15 % (w/v) Agar in LB Medium Plates stored at 4 °C
Running buffer (10x Stock)	250 mM Trizma Base 1.92 M Glycine 1 % (w/v) SDS in Ultrapure Water Stored at RT
Separation Gel (10 %)	2.5 ml Lower Tris 3.3 ml Acrylamide 2 ml Glycerol 14 µl APS 40 % 14 µl TEMED 3.2 ml Ultrapure Water Stored at RT
Stacking Gel (4 %)	1.25 ml Upper Tris 0.5 ml Acrylamide 12 µl APS 40 % 12 µl TEMED 3.2 ml Ultrapure Water Stored at RT
TAE Buffer (50x Stock)	242 g Trizma Base 57.1 ml Acetic Acid (100 %) 100 ml 0.5 M Na <sub>2</sub> /EDTA (pH 8.0) ad 1 l Ultrapure Water Stored at RT
TBS (10x Stock)	0.5 M Trizma Base 150 mM NaCl in Ultrapure Water pH 7.5 Autoclaved and stored at RT
TBST	10 % (v/v) TBS (10x Stock) 0.1 % (v/v) Tween 20 in Deionized Water Stored at RT
Transfer Buffer (10x Stock)	250 mM Trizma Base 1.92 M Glycine 0.37 % SDS in Ultrapure Water Stored at 4 °C
Transfer Buffer (Working Solution)	10 % Transfer Buffer (10x Stock) 20 % Methanol in Deionized Water Stored at RT

<b>Solution</b>	<b>Constitution</b>
Upper Tris (4x Stock)	0.5 M Tris 0.4 % SDS pH 6.8 Stored at RT

Table A7: Solutions

## 9.2.5. Cell lines

<b>Cell Line</b>	<b>Properties</b>	<b>Source</b>
ATDC5	Mouse Chondrogenic Cell Line Osteoinducible Upon BMP Ligand Stimulation	RIKEN #RCB0565
C2C12	Mouse Myoblast Cell Line Osteoinducible Upon BMP Ligand Stimulation When Undifferentiated Differentiable Into Myofibres	ATCC #CRL-172
C3040 bacteria	Competent Bacteria Ideally Suited for High Efficiency Transformation of Lentiviral Vectors and Large Plasmids	NEB, Frankfurt am Main (Germany)
HEK293AD	Variation of HEK293T Cells Easily Transfectable With Enhanced Adherence to Plastic Surfaces No Virus Particle Production Competence	In Collaboration Prof. Dr. Thomas Müller
HEK293T	Human Embryonic Kidney Cell Line Easily Transfectable and Competent to Produce Virus Particles Upon Lentiviral Transfection	ATCC #CRL-1573
NovaBlue bacteria	Competent Bacteria Ideally Suited as an Initial Cloning Host	Novagen via Merck, Darmstadt (Germany)

Table A8: Cell Lines

## 9.2.6. Enzymes and other proteins

<b>Protein</b>	<b>Manufacturer</b>
Antarctic Phosphatase	NEB, Frankfurt am Main (Germany)
BMP2 and Variants Thereof	In House
Complete Protein Inhibitor Cocktail Tablet, EDTA- free	Sigma-Aldrich, Munich (Germany)
FastDigest EcoRV Restriction Enzyme	Thermo Fisher Scientific, Dreieich (Germany)
FastDigest NotI Restriction Enzyme	Thermo Fisher Scientific, Dreieich (Germany)

<b>Protein</b>	<b>Manufacturer</b>
FastDigest XbaI Restriction Enzyme	Thermo Fisher Scientific, Dreieich (Germany)
GDF5 and Variants Thereof	In House
KAPA HiFi PCR Polymerase	KAPA Biosystems via Roche, Basel (Switzerland)
Q5(R) High-Fidelity DNA Polymerase	NEB, Frankfurt am Main (Germany)
Quick Ligation™ DNA Ligase	NEB, Frankfurt am Main (Germany)
Trypsin-EDTA	Life Technologies, Darmstadt (Germany)

Table A9: Proteins

### 9.2.7. Antibodies

<b>Antibody</b>	<b>Clone</b>	<b>Manufacturer</b>
Donkey αMouse Alexa Fluor 488	polyclonal	Invitrogen via Thermo Fisher Scientific, Dreieich (Germany)
Goat αMouse HRP	polyclonal	Abcam, Cambridge (United Kingdom)
Goat αRabbit HRP	polyclonal	Abcam, Cambridge (United Kingdom)
Mouse αHuman BMP RIA	#1564	BioRad, Munich (Germany)
Mouse αHuman FGF R2	#98739	R&D Systems, Wiesbaden-Nordenstadt (Germany)
Rabbit αAkt	polyclonal	Cell Signaling Technology, Leiden (Netherlands)
Rabbit αHA Tag DyLight®650	polyclonal	Abcam, Cambridge (United Kingdom)
Rabbit αp38 MAP Kinase	polyclonal	Cell Signaling Technology, Leiden (Netherlands)
Rabbit αp44/42 (Erk1/2)	#137F5	Cell Signaling Technology, Leiden (Netherlands)
Rabbit αPhospho-Akt (Ser473)	polyc	Cell Signaling Technology, Leiden (Netherlands)
Rabbit αPhospho-p38 MAP Kinase (Thr180/Tyr182)	polyclonal	Cell Signaling Technology, Leiden (Netherlands)
Rabbit αPhospho-p44/42 MAPK (Erk1/2) (Thr202/Tyr204)	#D13.14.4E	Cell Signaling Technology, Leiden (Netherlands)
Rabbit αPhospho-Smad1 (Ser463/465)/ Smad5 (Ser463/465)/ Smad9 (Ser465/467)	#D5B10	Cell Signaling Technology, Leiden (Netherlands)
Rabbit αSmad1	polyclonal	Cell Signaling Technology, Leiden (Netherlands)
αHA Tag (Rabbit)		

Table A10: Antibodies

## 9.2.8. Plasmids

<b>Plasmid</b>	<b>Manufacturer</b>
pBlue Skript II SK (+)	Agilent Technologies, Waldbronn (Germany)
pCDH-CMV-MCS-EF1-Puro	System Biosciences, Heidelberg (Germany)
pcDNA3_BMPRIA_HA	In House
pMD2.G	AddGene, Teddington (United Kingdom)
psPax	AddGene, Teddington (United Kingdom)
pTurboGFP-C	Evrogen, Heidelberg (Germany)

Table A11: Plasmids

## 9.2.9. Kits

<b>Kit Name</b>	<b>Components</b>	<b>Manufacturer</b>
DC Protein Assay	Alkaline Copper Tartrate Solution Dilute Folin Reagent Surfactant Solution Bovine Serum Albumin Standard	BioRad, Munich (Germany)
iScript cDNA Synthesis Kit	iScript Reverse Transcriptase 5x iScript Reaction Mix Nuclease-Free Water	BioRad, Munich (Germany)
JetPrime® Transfection Reagent	JetPrime™ JetPrime Buffer	Polyplus Transfection via VWR, Darmstadt (Germany)
Pierce® ECL Western Blotting Kit	Detection Reagent 1 Detection Reagent 2	Thermo Fisher Scientific, Dreieich (Germany)
Pierce® HA Tag IP/Co-IP Kit	HA-tagged Positive Control Anti-HA Agarose BupH™ Tris Buffered Saline Pack Elution Buffer Lane Marker Non-Reducing Sample Buffer (5x) Pierce Spin Columns Collection Tubes and Caps	Thermo Fisher Scientific, Dreieich (Germany)
Plasmid Mini / Maxi Kit	Qiagen Tip 20 / 500 Buffer P1 Buffer P2 Buffer P3 Buffer QBT Buffer QC Buffer QF Rnase A LyseBlue®	Qiagen, Hilden (Germany)

<b>Kit Name</b>	<b>Components</b>	<b>Manufacturer</b>
Rnase-free DNase Set	Buffer RDD DNase I RNase-free H <sub>2</sub> O	Qiagen, Hilden (Germany)
RNeasy® Mini Kit	Rneasy Mini Spin Columns Buffer RLT Buffer RW1 Buffer RPE RNase-Free Water	Qiagen, Hilden (Germany)
RT <sup>2</sup> SYBR Green PCR Master Mix	HotStart DNA Taq Polymerase PCR Buffer dNTP Mix SYBR Green Dye	Qiagen, Hilden (Germany)
SsoFast™ EvaGreen® Supermix	SsoFast EvaGreen Supermix	Biodad, Munich (Germany)
Wizard® Plus SV Minipreps DNA Purification System	Wizard® SV Minicolumns Cell Resuspension Solution Cell Lysis Solution Neutralization Solution Column Wash Solution Alkaline Protease Solution Nuclease-Free Water	Promega, Mannheim (Germany)
Wizard® SV Gel and PCR Clean-Up System	Wizard® SV Minicolumns Membrane Binding Solution Membrane Wash Solution Nuclease-Free Water	Promega, Mannheim (Germany)
Zymoclean™ Gel DNA Recovery Kit	ADB Buffer DNA Wash Buffer DNA Elution Buffer Zymo-Spin™ I Columns Collection Tubes	Zymo Research, Freiburg (Germany)
Zyppy™ Plasmid Miniprep Kit	7x Lysis Buffer (Blue) Neutralization Buffer (Yellow) Endo-Wash Buffer Zyppy™ Wash Buffer Concentrate Zyppy™ Elution Buffer Zymo-Spin™ IIN Columns Collection Tubes	Zymo Research, Freiburg (Germany)

Table A12: Kits

### 9.2.10. Software

<b>Software Name</b>	<b>Purpose</b>
ApE (A Plasmid Editor) 8.5.2.0	Handling DNA Sequences
CFX Manager (Biorad)	Analyzing Quantitative Real-Time PCR Data

<b>Software Name</b>	<b>Purpose</b>
Chromas Lite MFC Application 2.1.1.0	Visualization of Sequencing Data
Citavi 4.4.0.28 (Swiss Academic)	Reference Management
Fiji (Fiji Is Just ImageJ)	Edit and Compilation of Immunofluorescence and Westernblot Images, as well as Determination of the Co-localization Index
LAS AF (Leica)	Confocal Microscopy Image Generation and Management
MegaCapt (Vilber)	Gel Documentation
Microsoft Word 2013	
Microsoft Excel 15.0.4420.1017	Basic Calculations
Microsoft PowerPoint 15.0.4420.1017	Data Compilation and Presentation
OpenOffice Portable 1.4.1.1	Thesis Preparation / Compilation
Origin 8.6	Generation of ALP Graphs Statistical Data Analysis
Prism 5.00.288 (GraphPad )	Visualization of Data (Bar Graphs and Line Graphs) Statistical Data Analysis
SnapGene Viewer	Generation of Plasmid Maps

*Table A13: Software*



### 9.3. Figure References to the Laboratory Notebook

<i>Fig.</i>	<i>Description</i>	<i>Repeats</i>	<i>Reference/Experiment No.</i>
7	ALP on ATDC5: GDF5 vs. FGFR2-ECD	### I	367, 440, 472, 496, <b>504</b> , 560
7	ALP on ATDC5: BMP2 vs. FGFR2-ECD	### I	367, 440, 496, <b>504</b> , 507, 560
7	ALP on C2C12: BMP2 vs. FGFR2-ECD	### I	381, 496, <b>504</b> , 560, 565, 583
8	qPCR on ATDC5 $\pm$ FR2 shRNA	### I	<b>385, 395, 417</b> , 430, <b>432, 446</b>
8	Crystal Violet on ATDC5 $\pm$ FR2 shRNA	III	570, <b>574</b> , 577
8	ALP on ATDC5 $\pm$ FR2 shRNA: GDF5	### IIII	380, 393, 396, 415, 418, 426, 431, <b>440</b> , 441
8	ALP on ATDC5 $\pm$ FR2 shRNA: BMP2	### III	380, 393, 396, 415, 418, 426, 431, <b>440</b> , 441
9	qPCR on C2C12 $\pm$ FGFR2	### I	612, <b>680, 682</b>
9	Crystal Violet on C2C12 $\pm$ FGFR2	III	544, 570, 574, <b>577</b>
9	ALP on C2C12 $\pm$ FGFR2: GDF5	### II	448, 449, 457, 463, 543, <b>569</b> , 575, 576, 579, 659, 660, 670, 673, 678
9	ALP on C2C12 $\pm$ FGFR2: BMP2	### II	448, 449, 457, 460, 463, 543, 569, 575, 576, 579, 659, 660, <b>670</b> , 673, 678
11	WB on C2C12: GDF5 vs. FGFs	II	<b>600</b> , 629, 641
11	WB on C2C12: BMP2 vs. FGFs	II	533, 539, 555, <b>584, 588, 589, 641</b>
12	WB on ATDC5: GDF5 vs. FGFs	I	<b>600</b>
12	WB on ATDC5: BMP2 vs. FGFs	II	479, 481, 482, 483, 486, 487, 489, 491, <b>539</b> , 554B, <b>585, 588, 589</b>
13	WB Erk Inhibitors	I	<b>601</b>
13	ALP on ATDC5: BMP2/GDF5 vs Erk Inhibitors	II	602, <b>605</b>
13	ALP on C2C12: BMP2 vs. Erk Inhibitors	II	602, <b>605</b>
14	Crystal Violet on C2C12 $\pm$ FGFR2 <sup>KD</sup>	III	570, 574, 577
14	WB FGFR2 <sup>KD</sup>	I	607, <b>685</b>
14	ALP on C2C12 $\pm$ FGFR2 <sup>KD</sup> : GDF5	### II	543, 569, 575, 576, 579, 659, 660, <b>670</b> , 673, 678
14	ALP on C2C12 $\pm$ FGFR2 <sup>KD</sup> : BMP2	### II	543, 569, 575, 576, 579, 659, 660, 670, <b>673</b> , 678
14	qPCR on C2C12 $\pm$ FGFR2	### I	612, <b>680, 682</b>
17	ALP on ATDC5: GDF5 vs. FR2-AB	III	412, 433, <b>561</b>
17	ALP on ATDC5: BMP2 vs. FR2-AB	III	412, 433, <b>561</b>
17	ALP on C2C12: BMP2 vs. FR2-AB	IIII	412, 433, <b>561</b> , 633

<b>Fig.</b>	<b>Description</b>	<b>Repeats</b>	<b>Reference/Experiment No.</b>
17	ALP on ATDC5: GDF5 vs. FGFR2-ECD	### I	367, 440, 472, 496, <b>504</b> , 560
17	ALP on ATDC5: BMP2 vs. FGFR2-ECD	### I	367, 440, 496, 504, <b>507</b> , 560
17	ALP on C2C12: BMP2 vs. FGFR2-ECD	### I	381, 796, 504, 560, 565, <b>583</b>
17	ALP on ATDC5: GDF5 vs. BRIA-AB	I	<b>623</b> , 633
17	ALP on ATDC5: BMP2 vs. BRIA-AB	I	<b>623</b> , 633
17	ALP on ATDC5: GDF5 vs. BRIA-ECD	I	<b>625</b>
17	ALP on ATDC5: BMP2 vs. BRIA-ECD	I	<b>625</b>
17	ALP on C2C12: BMP2 vs. BRIA-AB	I	<b>623</b> , 633
17	ALP on C2C12: BMP2 vs. BRIA-ECD	II	<b>625</b>
18	ALP on ATDC5: BMP2/L51P	II	595, 604
18	ALP on C2C12: BMP2/L51P	IIII	595, 604, 614, 617
19	Co-Localization Staining FGFR2/BRIA	III	541, 549, <b>563</b>
20	ALP on C2C12 $\pm$ FGFR2 <sup>KD</sup> : GDF5-R57A	### II	543, 569, 575, 576, 579, 660, 670, <b>673</b> , 678
20	ALP on C2C12 $\pm$ FGFR2: GDF5-R57A	### II	448, 449, 547, 460, 463, 543, 569, 575, <b>576</b> , 579, 670, 673, 678
20	ALP on ATDC5: GDF5 mutants	IIII	473, <b>484</b> , 488, 505
20	ALP on C2C12: GDF5 mutants	III	<b>484</b> , 488, <b>505</b>
20	ALP on ATDC5 $\pm$ FR2 shRNA: GDF5-R57A	### IIII	380, 393, 396, 415, 418, 426, 431, 440, 441

*Table A14: Figure References to the Laboratory Notebook*

Each shown experiment is referenced to the laboratory notebook by its respective experiment numbers. The number of the experiment that is shown in the indicated figure is marked in **bold**.

#### 9.4. Supplemental References

- Basson** MA. Signaling in cell differentiation and morphogenesis. Cold Spring Harbor perspectives in biology. 2012;4(6).
- Berendsen** AD, Olsen BR. Bone development. Bone. 2015;80:14-8.
- Chen** CG, Thuillier D, Chin EN, Alliston T. Chondrocyte-intrinsic Smad3 represses Runx2-inducible matrix metalloproteinase 13 expression to maintain articular cartilage and prevent osteoarthritis. Arthritis and rheumatism. 2012;64(10):3278-89.
- Decker** RS, Koyama E, Pacifici M. Genesis and morphogenesis of limb synovial joints and articular cartilage. Matrix biology : journal of the International Society for Matrix Biology. 2014;39:5-10.
- Dorey** K, Amaya E. FGF signalling: diverse roles during early vertebrate embryogenesis. Development. 2010;137(22):3731-42.
- Ferguson** CM, Schwarz EM, Reynolds PR, Puzas JE, Rosier RN, O'Keefe RJ. Smad2 and 3 mediate transforming growth factor-beta1-induced inhibition of chondrocyte maturation. Endocrinology. 2000;141(12):4728-35.
- Kishigami** S, Mishina Y. BMP signaling and early embryonic patterning. Cytokine Growth Factor Reviews. 2005;16(3):265-78.
- Mueller** TD, Nickel J. Promiscuity and specificity in BMP receptor activation. FEBS letters. 2012;586(14):1846-59.
- Nishimura** R, Hata K, Matsubara T, Wakabayashi M, Yoneda T. Regulation of bone and cartilage development by network between BMP signalling and transcription factors. Journal of biochemistry. 2012;151(3):247-54.
- Norrie** JL, Lewandowski JP, Bouldin CM, Amarnath S, Li Q, Vokes MS, Ehrlich LIR, Harfe BD, Vokes SA. Dynamics of BMP signaling in limb bud mesenchyme and polydactyly. Developmental biology. 2014;393(2):270-81.
- Olsen** BR, Reginato AM, Wang W. Bone development. Annual review of cell and developmental biology. 2000;16:191-220.
- Ornitz** DM, Itoh N. The Fibroblast Growth Factor signaling pathway. Wiley interdisciplinary reviews Developmental biology. 2015;4(3):215-66.
- Pacifici** M, Koyama E, Iwamoto M. Mechanisms of synovial joint and articular cartilage formation: recent advances, but many lingering mysteries. Birth defects research Part C, Embryo today : reviews. 2005;75(3):237-48.
- Rivera-Pérez** JA, Hadjantonakis AK. The Dynamics of Morphogenesis in the Early Mouse Embryo. Cold Spring Harbor Perspectives in Biology. 2014;7(11).
- Schliermann** AT (1), Nickel J. Unraveling the Connection between Fibroblast Growth Factor and Bone Morphogenetic Protein Signaling. International journal of molecular sciences. 2018;19(10).

- Schliermann AT (2)**; Seher, A; Prenzlau, F; Siverino, C; Sasse, F; Kneitz, S; Mueller, TD; Nickel, J. A Receptor with Identity Crisis: Fibroblast Growth Factor Receptor 2 Directly Binds BMPs to modulate their signaling outcome. In: PNAS (submitted).
- Studer D**, Millan C, Ozturk E, Maniura-Weber K, Zenobi-Wong M. Molecular and biophysical mechanisms regulating hypertrophic differentiation in chondrocytes and mesenchymal stem cells. *European cells & materials*. 2012;24:118-35; discussion 35.
- Tiong KH**, Mah LY, Leong CO. Functional roles of fibroblast growth factor receptors (FGFRs) signaling in human cancers. *Apoptosis : an international journal on programmed cell death*. 2013;18(12):1447-68.
- Tuazon FB**, Mullins MC. Temporally coordinated signals progressively pattern the anteroposterior and dorsoventral body axes. *Seminars in cell & developmental biology*. 2015;42:118-33.
- Tubbs RS**, Bosmia AN, Cohen-Gadol AA. The human calvaria: a review of embryology, anatomy, pathology, and molecular development. *Child's nervous system : ChNS : official journal of the International Society for Pediatric Neurosurgery*. 2012;28(1):23-31.
- van der Kraan PM**, van den Berg WB. Chondrocyte hypertrophy and osteoarthritis: role in initiation and progression of cartilage degeneration? *Osteoarthritis and cartilage*. 2012;20(3):223-32.
- Verheyden JM**, Sun X. An Fgf/Gremlin inhibitory feedback loop triggers termination of limb bud outgrowth. *Nature*. 2008;454(7204):638-41.
- Wei X**, Hu M, Mishina Y, Liu F. Developmental Regulation of the Growth Plate and Cranial Synchronosis. *Journal of dental research*. 2016;95(11):1221-9.
- Wu M**, Chen G, Li YP. TGF-beta and BMP signaling in osteoblast, skeletal development, and bone formation, homeostasis and disease. *Bone research*. 2016;4:16009.